DYMAT Winter School 2023

Jan. 29th - Feb. 3rd 2023, AUSSOIS, France

Program and proceedings

Organised by Pr. P. Forquin
Université Grenoble Alpes, 3SR Lab.

DYMAT Winter School 2023 - Jan. 29th - Feb. 3rd

Experimental testing and modelling of materials at high-strain rates

As chairman of this 2nd DYMAT Winter-School, it is my great pleasure to welcome you to Centre Paul Langevin belonging to CNRS (The French National Centre for Scientific Research), a world's leading research institutions, in a such beautiful location, Aussois, a typical Savoyard village facing south at the gates of the Vanoise National Park.

On behalf of the Scientific Committee and DYMAT Governing Board, I want to express my deep gratitude to the Centre Paul Langevin who gave us this opportunity, and especially to Mrs. Christina BALZER, Hosting/Conferences Manager.

I am also grateful to our 5 invited lecturers:

- *Pr. Michel Arrigoni, ENSTA Bretagne,*

- *Dr. Cyril Bolis, CEA-DIF,*

- *Pr. Gérard Gary, Ecole Polytechnique,*

- *Pr. Amos Gilat, The Ohio State University,*

- *Pr. Dirk Mohr, ETH Zürich.*

I want to express my deep gratitude to our 5 sponsors for supporting this event:

- **AMOtronics**, **Hadland**, **iX-Cameras**, **ScandiFlash** and **Shimadzu** *companies.*

I also want to express my special thanks to all the staff involved in the local organization (ExperDYN team, 3SR) and especially to Dr. Charles FRANCART, Julia GENEVOIS and Mushfiqullah SAPAY for their tremendous help.

We hope you will enjoy this Winter School. This event is a great opportunity, especially for PhD students, to discover emerging approaches, to exchange with young and senior researchers and to glimpse opportunities for the rest of their career.

We are wishing you an unforgettable stay in AUSSOIS!
Yours sincerely,

Pascal FORQUIN

HIGH-SPEED CAMERAS FOR RESEARCH AND ENGINEERING

i-SPEED® 7 Series

8,512 fps @ 2072 x 1536

27+ GPixels/s throughput

Up to 288 GB RAM

2.45 M fps

Touchscreen CDUe tablet control

External SSD

1 hour battery life

i-SPEED® 5 Series

6,382 fps @ 1920 x 1080

13 GPixels/s throughput

Up to 8 TB Internal SSD

1 M fps

Touchscreen CDUe tablet control

External SSD

Innovative cooling system

Applications

Ballistics, PIV/DIC, Fluid Dynamics, Shock and Vibration, Material Science, Aerodynamics

iX Cameras

ix-cameras.com | info@ix-cameras.com

SHIMADZU

Excellence in Science

Cyberspeed reality X2

The ultra-high-speed video camera HPV-X2

With its improved blooming-free FTCMOS2 sensor, the ultra-high-speed video camera HPV-X2 gives insights into phenomena which have been invisible to the human eye before now. The HPV-X2 enables extreme applications, e.g. in aerospace, explosion and shockwave visualization, cavitation, electrical discharge, advanced medical such as microbubbles, material testing of CFRPs and more.

Cyberspeed recording
of up to 10 million frames per second

Extreme sensitivity
over 10 times higher than other cameras in its class

Longer recording times
through extended frame capacity

3D perspectives
based on synchronized recording using two cameras simultaneously from different angles

Lecture 1: _In-depth Analysis of a Hopkinson Bar Experiment_

Pr. Gérard GARY, _Ecole Polytechnique_

The presentation will be student-oriented. The objective is to propose a critical approach to that of Kolsky, almost systematically quoted in all the articles presenting results of tests on Hopkinson bars. We will first recall the hypotheses, in particular those which are not stated. For this, a reminder of the basic knowledge necessary for understanding will be given. Various subtleties can then be approached through examples of test analyzes. Interventions and questions from the public will be welcome and even desired.

Lecture 2: _An Introduction to Machine-learning for Modeling the Dynamic Behavior of Materials and Structures_

Pr. Dirk MOHR, _Dep. of Mechanical and Process Eng., ETH Zürich_

Machine learning is a powerful computational modeling tool whose application is currently pursued in many branches of engineering science. In this lecture, we introduce basic deep learning techniques such as fully-connected neural networks (FCNNs), graph-neural networks (GNNs), convolutional neural networks (CNNs) and recurrent neural networks (RNNs). We then ask the question about their potential application in the field of dynamic behavior of materials. It is demonstrated that FCCNs provide a very useful tool for modeling the rate- and temperature dependent hardening of both metals and polymers. The merits of FCCNs for predicting the dynamic crushing response of thin-walled structures is also shown. We proceed to the application of GNNs to facilitate the design of optimal lightweight structures such as truss- and shell-lattices. And finally, the development of new RNNs is discussed that address the mechanics-specific challenges of modeling history dependent behavior. The outcome is universal material model which can capture the large deformation response of a wide spectrum of engineering material.

Lecture 3: _The Addition of DIC measurement to the Split Hopkinson Bar Experiment_

Pr. Amos GILAT, _The Ohio State University_

The Digital Image Correlation (DIC) technique for full field measurement of deformation is probably the most significant advance in experimental mechanics in recent years. When applied to the SHB experiment it provides means for examining the validity of the strain measurement from the recorded waves that assumes uniform deformation in the specimen during the test, and it provide means for conducting tests where the deformation is intentionally not uniform. Both issues are addressed, and several experimental setups where DIC has a crucial role are presented.

Lecture 4: _Metal Response to Shock Loading: From Microscale to Applications_

Dr. Cyril BOLIS, _CEA-DIF_

Equation of state, strength and damage models are the main components needed when you want to perform shock simulations. If some part of these models can easily be adjusted by simple experiments and considerations, it is always difficult to obtain some data along all thermo-mechanical paths encountered during our simulations. It is also difficult to understand some effects using only macroscopic considerations such as phase changes, kinetics. That's why some multi-scales approaches have been developed in the last decades, in particular with the extensive use of supercomputers. In our speech, we will present a quick overview of what can be done with these methods.

Lecture 5: *Composite Materials and Multi-material Assemblies under Dynamic Stresses at High Strain-rates*

Pr. Michel Arrigoni, *ENSTA Bretagne*

The requirements for the service life of some high value-added structures in the aeronautics or aerospace fields, as well as for defense applications, are becoming higher and higher. The expected mechanical performances are increased to resist to severe shocks and impacts for lower and lower expected structural weigh. This antagonism gives birth to the paradigm of physical protection by advanced materials. Among these materials, composite materials remain a preferred choice but cannot be sufficient on their own in some situations involving extreme loads such as detonation waves or shock waves resulting from ballistic impacts or hypervelocity fragments. In these cases, the dynamic behaviour must be revisited to consider the supersonicity related to shock waves propagating in the target material. This presentation aims at presenting experimental methods allowing the establishment of numerical models dedicated to this kind of events. These models are used in predictive tools of numerical modelling in order to limit the number of experiments, generally dangerous, expensive and where some key parameters cannot be easily tuned. The numerical tool also allows optimization steps. A few examples taken from the research work carried out at the Dupuy de Lôme Research Institute illustrate the modeling approach. These examples highlight the progress of the experimental and numerical methods used to study the mechanical effects of impacts and explosions.

Special talk: The Space Shuttle Columbia Last Mission

Pr. Amos GILAT, *The Ohio State University*

The 28th and last mission of the space shuttle Columbia started on January 18, 2003. The mission tragically ended on February 1st as Columbia was traveling back to Earth at an altitude of about 70 km and a speed of about Mach 24. The presentation describes the space shuttle operation, the details of the last mission, and the investigation after the accident that has determined the exact technical cause of the accident.

LAST NAME	First name	Institution	City	Country	email
AGIRRE	Julen	Mondragon Unibertsitatea	Arrasate	Spain	jagirreb@mondragon.edu
ARRIGONI	Michel	ENSTA Bretagne	Brest	France	michel.arrigoni@ensta-bretagne.fr
BADIKA	Menes	3SR - Univ. Grenoble Alpes	Grenoble	France	menesbadika01@gmail.com
BEERLI	Thomas	ETH Zürich	Zurich	Switzerland	beerlit@ethz.ch
BEGAUD	Marie-Amélie	Institut Saint-Louis	Saint-Louis	France	marieamelie.begaud68@gmail.com
BOLIS	Cyril	CEA-DIF	Bruyères-Le-Châtel	France	cyril.bolis@cea.fr
BRACQ	Anthony	Institut Saint-Louis	Saint-Louis	France	anthony.bracq@isl.eu
BREMAUD	Luc	I2M-Arts et Métiers	Talence	France	luc.bremaud@ensam.eu
BUZAUD	Eric	CEA-CESTA	Le Barp	France	eric.buzaud@cea.fr
CADET	Clément	CEA-DIF	Bruyères-Le-Châtel	France	clement.cadet@cea.fr
CARASSUS	Hugo	Safran	Villaroche	France	hugo.carassus@safrangroup.com
COLON	Xavier	IRDL-Univ. De Bretagne sud	Lorient	France	xavier.colon@univ-ubs.fr
COGET	Yann	CEA-DIF	Bruyères-Le-Châtel	France	Yann.Coget@CEA.fr
COSCULLUELA	Antonio	CEA-CESTA	Le Barp	France	antonio.cosculluela@cea.fr
DEPIERRE	Sébastien	Safran	Issoudun	France	sebastien.depierre@safrangroup.com
FALTA	Jan	Czech Technical University	Prague	Czech Republic	falta@fd.cvut.cz
FORQUIN	Pascal	3SR - Univ. Grenoble Alpes	Grenoble	France	pascal.forquin@univ-grenoble-alpes.fr
FRANCART	Charles	3SR - Univ. Grenoble Alpes	Grenoble	France	charles.francart@univ-grenoble-alpes.fr
GARY	Gérard	Ecole Polytechnique	Palaiseau	France	gary.lms@orange.fr
GENEVOIS	Julia	3SR - Univ. Grenoble Alpes	Grenoble	France	julia.genevois@3sr-grenoble.fr
GILAT	Amos	The Ohio State University	Columbus	USA	gilat.1@osu.edu
GOUR	Govind	University of Oxford	Oxford	UK	govind.gour@linacre.ox.ac.uk
GROLLEAU	Vincent	IRDL-Univ. De Bretagne sud	Lorient	France	vincent.grolleau@univ-ubs.fr
GUSTAFSSON	Pär	Scandiflash AB	Uppsala	Sweden	par.gustafsson@scandiflash.com
HENRY	Quentin	I2M - Arts et Métiers	Talence	France	quentin.henry@ensam.eu
HESPER	Johannes	Shimadzu	Duisburg	Germany	jhe@shimadzu.eu
HESSING	Martin	AMOtronics	Aachen	Germany	Hessing@amotronics.de
HOKKA	Mikko	Tampere University	Tampere	Finland	mikko.hokka@tut.fi
HU	Wanrui	Monash University	Melbourne	Australia	wanrui.hu@monash.edu
JORDAN	Benoit	ETH Zürich	Zurich	Switzerland	jordanb@ethz.ch
KAMBLE	Arun	Indian Institute of technology	Mumbai	India	arun15@iitb.ac.in
KARATHANASOPOULOS	Nikolaos	New York University	Abu Dhabi	United Arab Emirates	n.karathanasopoulos@nyu.edu

KRCMAROVA	Nela	Czech Technical University	Prague	Czech Republic	krcmarova@fd.cvut.cz
LANGE	Christopher	Institut Saint-Louis	Saint-Louis	France	christopher.lange@isl.eu
LE MOUROUX	Solenn	Nexter	Versailles	France	S.LEMOUROUX@nexter-group.fr
LI	Xueyang	ETH Zürich	Zurich	Switzerland	lixue@ethz.ch
LONGCHAMP	Vincent	I2M - Arts et Métiers	Talence	France	vincent.longchamp@ensam.eu
MENDIGUREN	Joseba	Mondragon Unibertsitatea	Arrasate	Spain	jmendiguren@mondragon.edu
MEYER	Paul	ETH Zürich	Zurich	Switzerland	paumeyer@ethz.ch
MEYNARD	Joane	CEA-CESTA	Le Barp	France	joane.meynard@gmail.com
MOHR	Dirk	ETH Zürich	Zurich	Switzerland	dmohr@ethz.ch
MORENA	Alberto	Politecnico di Torino	Torino	Italy	alberto.morena@polito.it
NIKOLAKOPOULOS	Konstantinos	Safran Aircraft Engines	Paris	France	konstantinos.nikolakopoulos@safrangroup.com
OPITZ	Raphael	Shimadzu	Duisburg	Germany	rop@shimadzu.eu
PARIS	Nick	iX-Cameras	London	UK	nick.paris@ix-cameras.com
RAMAKRISHNAN	Karthik	Bristol Composites institute	Bristol	UK	karthik.ramakrishnan@bristol.ac.uk
REYNIER	Baptiste	CEA-CESTA	Le Barp	France	baptiste.reynier@ensta-bretagne.org
ROTH	Christian	ETH Zürich	Zurich	Switzerland	ccroth@ethz.ch
RUBIO RUIZ	Rafael Arturo	Tampere University	Tampere	Finland	arturo.rubioruiz@tuni.fi
RUMBAUGH	Todd	Hadland	Santa Cruz	Usa	trumbaugh@hadlandimaging.com
SAKARIDIS	Emmanouil	ETH Zürich	Zurich	Switzerland	esakaridis@ethz.ch
SAPAY	Mushfiqullah	3SR - Univ. Grenoble Alpes	Grenoble	France	mushfiqullah.sapay@univ-grenoble-alpes.fr
TANCOGNE	Thomas	ETH Zürich	Zurich	Switzerland	thomatan@ethz.ch
TAWFIK	Ahmed	Technische Universität Dresden	Dresden	Germany	ahmed.tawfik@tu-dresden.de
TOMASZEWSKI	Piotr	TenCate Advanced Armour	Vissenbjerg	Denmark	Piotr.Tomaszewski@tencatearmour.com
UTZERI	Mattia	Università Politecnica delle Marche	Ancona	Italy	m.utzeri@pm.univpm.it
VICAUD	Alexandre	I2M-Arts et Métiers	Talence	France	alexandre.vicaud@outlook.fr
WALLEY	Stephen	University of Cambridge	Cambridge	UK	smw14ster@googlemail.com
WANG	Huachuan	Monash University	Melbourne	Australia	huachuan.wang@monash.edu
ZINSNER	Jean-Luc	CEA-GRAMAT	Gramat	France	Jean-Luc.ZINSZNER@cea.fr

Program

Sunday, January 29th, Centre Paul-Langevin, 24, rue du Coin, 73500 Aussois, France

15h00	**Opening of the centre**
18h00	**Opening of the WS desk**
19h20	**Dinner**

Monday, January 30th, Centre Paul-Langevin, 24, rue du Coin, 73500 Aussois, France

Time	TITLE	SPEAKER	INSTITUTIONS
7h50	**Opening of the WS desk**		
8h10	**Monday morning – Opening ceremony** **Pascal Forquin**, Univ. Grenoble Alpes, 3SR Lab. (France)		
	Monday morning – Invited Lecture 1 *Chairmen: Dr. S. Walley and Pr. P. Forquin*		
8h20	In-depth Analysis of a Hopkinson Bar Experiment	**Pr. Gérard Gary**	Ecole Polytechnique
9h50	**Coffee break**		
	Monday morning, session 1 - Dynamic behavior of metals *Chairmen: Dr. S. Walley and Pr. P. Forquin*		
10h15	An experimental and modelling investigation of Al 6061-T6 response under intense impulsive X-ray radiation	**Eric Buzaud**	CEA-CESTA
10h40	A laboratory-scale instrumented hammer for intermediate strain rate testing: Application to hot forging of nickel-based superalloys	**Julen Agirre**, Joseba Mendiguren, Borja Erice, Nagore Otegi, Lander Galdos	Mondragon Unibertsitatea, Basque Foundation for Science
11h05	Static and dynamic in-plane torsion testing of sheet metal	**Xavier Colon**, **Vincent Grolleau**, Bertrand Galpin, Christian Roth, Dirk Mohr	ETH Zürich IRDL Ecoles de St-Cyr Coëtquidan
11h30	Multiaxial rate dependent behavior of Titanium alloys	**Govind Gour**, Yuan Xu, Julian Reed, Nik Petrinic, Antonio Pellegrino	University of Oxford
11h55	Statistical characterization of mechanical behavior of Ti6Al4V and Bayesian calibration of a constitutive model	**Charles Francart**	3SR - Univ. Grenoble Alpes
12h20	**End of the session**		
12h25	**Lunch**		
13h30	**Private Time**		
	Monday afternoon, session 2 - Dynamic behavior of metals *Chairmen: Dr. C. Bolis, Dr. C. Francart*		
17h50	On the Mechanical Properties of Tungsten Heavy Alloys used in Kinetic Energy Impactors	**Christian Roth**, Teresa Fras, Dirk Mohr	ETH Zürich Institut Saint-Louis
18h15		**Nick Paris**	iX-Cameras
18h30		**Martin Hessing**	Amotronics
18h45	**End of the session**		
18h50	**Cocktail**		
19h30	**Dinner**		
20h30	**Special talk**: The Space Shuttle Columbia Last Mission	**Pr. Amos Gilat**	The Ohio State University

Tuesday, January 31st, Centre Paul-Langevin, 24, rue du Coin, 73500 Aussois, France

Time	TITLE	SPEAKER	INSTITUTIONS
Tuesday morning – Invited Lecture 2 *Chairmen: Pr. A. Gilat, Pr. V. Grolleau*			
8h20	An Introduction to Machine-learning for Modeling the Dynamic Behavior of Materials and Structures	**Pr. Dirk Mohr**	ETH Zürich
9h50	Coffee break		
Tuesday morning, session 3 - Plasticity and Fracture *Chairmen: Pr. A. Gilat, Pr. V. Grolleau*			
10h15	Rate-Dependent Stress-Strain Response of Polypropylene: Robot-Assisted Testing and Neural Network Modeling	**Benoit Jordan**, Dirk Mohr	ETH Zürich
10h35	Neural Network Model Describing the Response of Tubular Structures Subject to Impact Loading	**Emmanouil Sakaridis**, Dirk Mohr	ETH Zürich
10h55	Neural Network Based Temperature and Strain Rate Dependent Plasticity and Fracture Modelling	**Xueyang Li**, Christian Roth, Dirk Mohr	ETH Zürich
11h15	SHPB experiments on plate-lattice materials made through selective laser melting: experiments & analysis	**Paul Meyer**, Thomas Tancogne-Dejean, Li Xueyang, Christian C. Roth, Dirk Mohr	ETH Zürich
11h35	Micro-tensile experiments of metals covering a wide range of stress-states	**Thomas Beerli**, Christian Roth, Dirk Mohr, Vincent Grolleau	ETH Zürich IRDL
11h55	Enhance crashworthiness of 3D printed cellular materials (poster introduction)	**Mattia Utzeri**, Martina Scapin, Marco Sasso, Lorenzo Peroni	Polytechnic University of Marche Polytechnic of Turin
12h20	End of the session		
12h25	Lunch		
13h30	Social event		
Tuesday afternoon, session 4 - Dynamic testing of materials *Chairmen: Pr. M. Hokka, Dr. C. Roth*			
17h50	The high-rate mechanical properties of wood	**Stephen Walley**, Philippe Viot	University of Cambridge I2M - Arts et Métiers
18h15	Dynamic Indentation Response of Lithium-ion Batteries: Experiments and Modeling	**Thomas Tancogne-Dejean**, Vincent Grolleau, Dirk Mohr	ETH Zürich IRDL
18h40	Finite element simulations of dynamic compression of bulk metallic glasses at elevated temperatures using split Hopkinson pressure bar setup	**Arun Kamble**, Parag Tandaiya	Indian Institute of Technology
19h05		**Todd Rumbaugh**	Hadland
19h20	End of the session		
19h30	Dinner		

Wednesday, February 1ˢᵗ, Centre Paul-Langevin, 24, rue du Coin, 73500 Aussois, France

Time	TITLE	SPEAKER	INSTITUTIONS
	Wednesday morning – Invited Lecture 3 *Chairmen: Pr. G. Gary, Dr. C. Bolis*		
8h20	The Addition of DIC measurement to the Split Hopkinson Bar Experiment	**Pr. Amos Gilat**	The Ohio State University
9h50	**Coffee break**		
	Wednesday morning, session 5 - Experimental techniques *Chairmen: Pr. G. Gary, Dr. C. Bolis*		
10h15	Taylor impact	**Stephen Walley**, Hervé Couque	University of Cambridge Nexter Munitions
11h40	Laser-shock dynamic loading of innovative materials for beam intercepting devices of particle accelerators	**Alberto Morena**, Lorenzo Peroni, Martina Scapin	Politecnico di Torino
11h05	Synchrotron X-Ray Diffraction for Investigating High Strain Rate Material Behavior	Matti Isakov, Veera Langi, Lalit Pun, Guilherme Soares, **Mikko Hokka**	Tampere University
11h30	The dynamic loading stage for the instrumented testing at intermediate strain rates with real-time control of the experiment parameters	**Jan Falta**, Tomáš Fíla	Czech Technical University, Prague
11h50	Dynamic testing of the UHPC reinforced by steel fibres using SHPB	**Krčmářová Nela**, Fíla Tomáš, Falta Jan, Šleichrt Jan	Czech Technical University, Prague
12h10	**End of the session**		
12h15	**Lunch**		
13h30	**Private Time**		
	Wednesday afternoon, session 6 - Dynamic behavior of geomaterials *Chairmen: Pr. M. Hokka, Dr. C. Roth*		
17h50	Experimental and numerical study of dynamic behaviour of geomaterials under multiaxial confinements	**Wanrui Hu**, **Huachuan Wang**, Qianbing Zhang	Monash University
18h15	Considerations on the shear behavior of concrete-rock interfaces under dynamic loading	**Menes Badika**, Sophie Capdevielle, Matthieu Briffaut, Dominique Saletti	3SR - Univ. Grenoble Alpes Univ. de Lille
18h40	Identification of the dynamic tensile strength and fracture energy of five geomaterials subjected to spalling tests	**Mushfiqullah SAPAY**, Pascal Forquin	3SR - Univ. Grenoble Alpes
19h05		**Pär Gustafsson**	Scandiflash AB
19h20	**End of the session**		
19h30	**Dinner**		

Thursday, February 2ⁿᵈ, Centre Paul-Langevin, 24, rue du Coin, 73500 Aussois, France

Time	TITLE	SPEAKER	INSTITUTIONS
	Thursday morning – Invited Lecture 4 *Chairmen: Dr. E. Buzaud, Dr. J.-L. Zinszner*		
8h20	Metal Response to Shock Loading: From Microscale to Applications	**Dr. Cyril Bolis**	CEA-DIF
9h50	**Coffee break**		
	Thursday morning, session 7 - Dynamic behavior of ceramics *Chairmen: Dr. E. Buzaud, Dr. J.-L. Zinszner*		
10h15	Effects of microstructure on mechanical behavior of multiscale porous alumina stressed up to high strain rates	**Quentin Henry**, Jean-Benoit Kopp, Louise Le Barbenchon, Philipe Viot, Antonio Cosculluela	I2M - Arts et Métiers CNRS
10h40	Wavy flyer plate test for shockless plate-impact application	**Julia Genevois**, Pascal Forquin, Jean-Luc Zinszner	3SR - Univ. Grenoble Alpes CEA Gramat
11h05	Dynamic characterisation of two spinel ceramics	**Jean-Luc Zinszner**, Christophe Coureau, David Lebaillif	CEA Gramat SOLCERA Nexter Systems
11h30	Numerical simulations of the dynamic behavior of porous alumina ceramics	**Joane Meynard**, Pierre Pradel, Antonio Cosculluela	CEA-CESTA Arts et Métiers - Bordeaux
11h55	Microscopic modeling of plasma sprayed ceramics under dynamic loading with the discrete element method	**Vincent Longchamp**, Jérémie Girardot, Damien André, Frédéric Malaise, Ivan Iordanoff	CEA-CESTA I2M - Arts et Métiers Univ. de Limoges
12h20	**End of the session**		
12h25	**Lunch**		
13h30	**Private Time**		
	Thursday afternoon, session 8 - Numerical modelling *Chairmen: Dr. A. Cosculluela, Dr. J.-L. Zinszner*		
17h50	Numerical modelling of spalling tests using Discrete Element Method (DEM)	**Luc Bremaud**, Jérémie Girardot, Frédéric Malaise, Pascal Forquin, Ivan Iordanoff	Institut polytechnique de Bordeaux CEA-CESTA 3SR - Univ. Grenoble Alpes I2M - Arts et Métiers
18h15	Advanced numerical methods for the characterization of materials loaded under extreme conditions	**Rafael Arturo Rubio Ruiz**, Mikko Hokka, Guilherme C. Soares	Tampere University
18h40	Analysis of damage and deformation processes in hailstones under impact loading: dynamic testing and numerical simulation	**Pascal Forquin**	3SR - Univ. Grenoble Alpes
19h05		**Johannes Hesper, Raphael Opitz**	Shimadzu
19h20	**End of the session**		
19h30	**Dinner**		

Friday, February 3rd, Centre Paul-Langevin, 24, rue du Coin, 73500 Aussois, France

Time	TITLE	SPEAKER	INSTITUTIONS
Friday morning – Invited Lecture 5			
Chairmen: Dr. A. Bracq			
8h20	Composite materials and multi-material assemblies under dynamic stresses at high strain rates	**Pr. Michel Arrigoni**	ENSTA Bretagne IRDL
9h50	**Coffee break**		
Friday morning, session 9 - Dynamic behavior of composites			
Chairmen: Pr. M. Arrigoni, Dr. A. Bracq			
10h15	Mechanical characterisation and constitutive modelling of single layer UHMWPE composite: application to low-velocity impact loading	Thibault Poulet, **Anthony Bracq**, Yaël Demarty, Pauline Respaud, Jean Beugels, Bruno Bennani, Nadia Bahlouli, Franck Lauro	Institut Saint-Louis University Polytechnique Hauts de France ICube
10h40	Effect of carbon nanotube interlayers on the low velocity impact damage resistance of CFRP composites	**Karthik Ram Ramakrishnan**, Zhifang Zhang	Bristol Composites Institute
11h05	Response of polymer-based interpenetrating phase composites in impact loads	**Nikolaos Karathanasopoulos**	New York University
11h30	A novel shear device for testing mineral-bonded composites under high strain-rates	**Ahmed Tawfik**, Cesare Signorini, Viktor Mechtcherine	Technische Universität Dresden
11h55	**End of the session**		
12h00	**Lunch**		
13h00	**End of Winter School**		

Table of contents

Experimental and numerical study of dynamic behaviour of geomaterials under multiaxail confinements

Wanrui Hu * [1], Huachuan Wang , Qianbing Zhang

[1] Wanrui Hu – Australia

Dynamic fracturing and fragmentation of geomaterials play a significant role in mining and underground engineering (e.g., occurrence of rockburst and the efficiency of block caving mining). The triaxial Hopkinson bar is adopted to conduct combined static-dynamic tests on rock samples. A couple continuum-discrete model of the full-scale triaxial Hopkinson bar is correspondingly established. The steel bars are simulated by continuous zones while the sample is represented by discrete bonded particle model. The fracturing process, deformation fields and the fracturing properties are quantified and identified by high-speed cameras, 3D-DIC and synchrotron-based micro-CT techniques. Combined with the experimental studies, the rationality of the numerical model is verified and the micromechanical damage characteristics are revealed. The influences of confinement, strain rate and structure of geomaterial on the fracturing and fragmentation characteristics are further explored and discussed.

Keywords: Dynamic load, Tiaxial Hopkinson bar, Coupled continuum, discrete model, fracturing and fragmentation

---

*Speaker

The high-rate mechanical properties of wood

Stephen M. Walley[1*], Philippe Viot[2]

[1] *Cavendish Laboratory, J.J. Thomson Avenue, Cambridge CB3 0HE, United Kingdom*
[2] *Arts et Métiers, Talence 33400, France*

Keywords: wood, Kolsky bar, high strain rate

Abstract: Like any other material used in the construction of buildings, wood may be subject to ballistic impact or blast loading in the event of military conflict or terrorist attack. However, it has been a long time (the 1860s) since such studies were carried out and at that time instrumentation did not exist for determining what occurs during high rate deformation: all it was possible to do was perform a test and see what happened. Although the Kolsky bar was developed in the 1940s, there are only about 80 published studies where it has been used to obtain the high rate mechanical properties of wood. And most of these have been conducted in the last 25 years. Other circumstances where wood may be subjected to impact include (i) the entrainment of debris by strong winds and flowing water, (ii) impact limiters in the nuclear industry, and (iii) lightning damage to wind turbines whose blades may include a wooden core.

1. Introduction

Although wood has always been important to the building industry, there is increasing interest in its use in the construction of modern buildings due to its perceived green credentials [1-3]. And any building, whether green or not, can be subject to military or terrorist attack [4]. However, the last previous time that the response of wood to blast and ballistic impact was seriously studied was the 1860s (Figure 1), the decade in which the transition was made from wooden to steel naval ships [5].
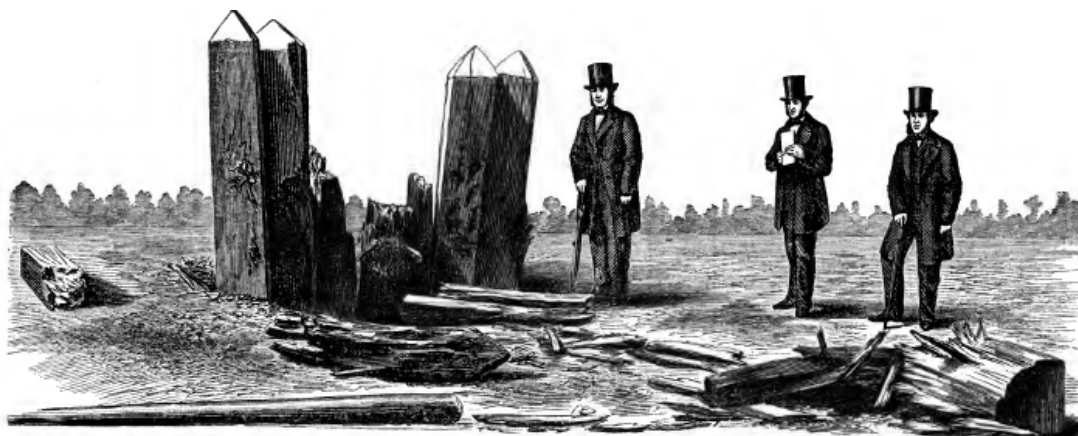
Figure 1: Engraving made from a photograph showing the damage done to a test wooden palisade caused by the close-in explosion of a box of gun-cotton. Experiment reported in 1865. From [6].

Despite this, there have been relatively few studies performed of the high-rate properties of wood. For example, we know of 80 such studies performed using the Kolsky bar. The first paper in which results were reported for wood at strain rates of up to 10^3 s^{-1} (Figure 2) was published in 1977 [7]. Although the authors did not state in this paper what experimental techniques they used, many years later the first-named author published an article on rate effects in wood obtained using a Kolsky bar and in which he also referred back to the earlier paper [8]. What is impressive about the 1977 study on wood is that results were presented for six

out of the eight decades of strain rate range investigated, something that was rare for many materials until relatively recently [9].
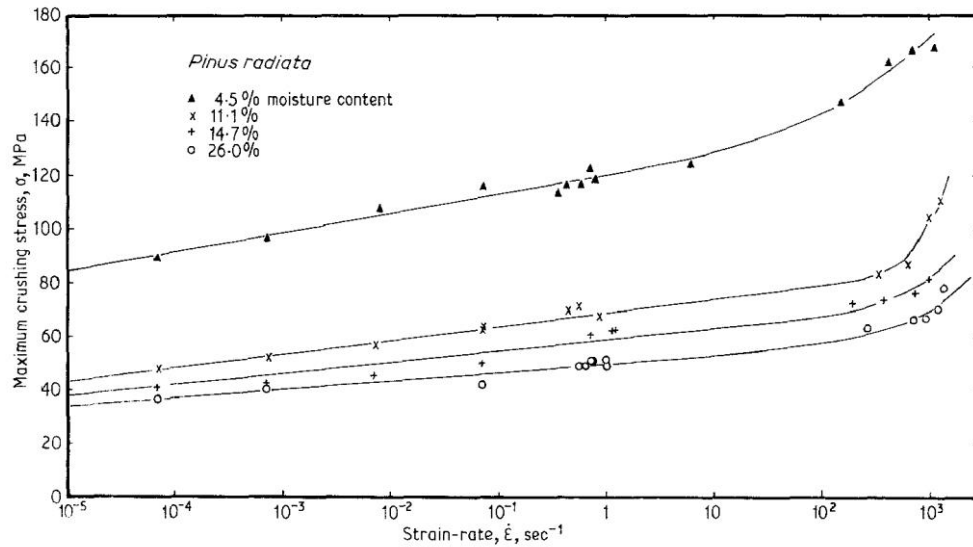
Figure 2: Plot of the crushing strength of *Pinus radiata* as a function of strain rate for various moisture content. From [7].

In this present article, we will very briefly consider: (i) dynamic fracture; (ii) high-rate Kolsky bar studies; (iii) damage to buildings caused by wooden debris hurled at them by wind and water; and (iv) industrial applications where wood may be subjected to impact. The problems associated with applying data obtained using small specimens of wood in the modelling of large wooden structures are also discussed. This problem is called the size effect. It is an issue for all classes of materials but is particularly severe for wood due to the large scale of its mesostructure [10]. A longer version of this review is in preparation for submission to *Journal of Dynamic Behavior of Materials.*

2. High-rate studies of wood

At low rates of deformation, there is a monotonic relationship between the size of a wood specimen and its fracture strength i.e. long beams are always weaker than short ones [10]. The reason for this is connected to the statistical distribution of defects such as knots [11, 12]. However, a recent paper by Bal about Poplar and Pine wood showed that matters may be more complicated in dynamic fracture (Figure 3b) [13].

(a)
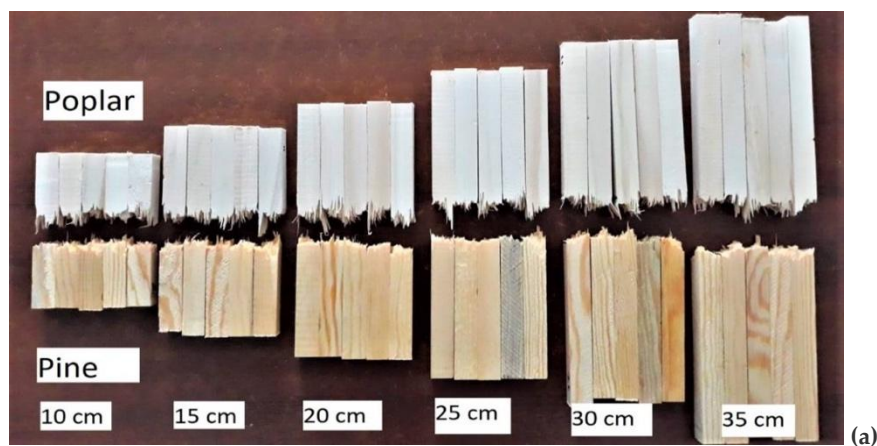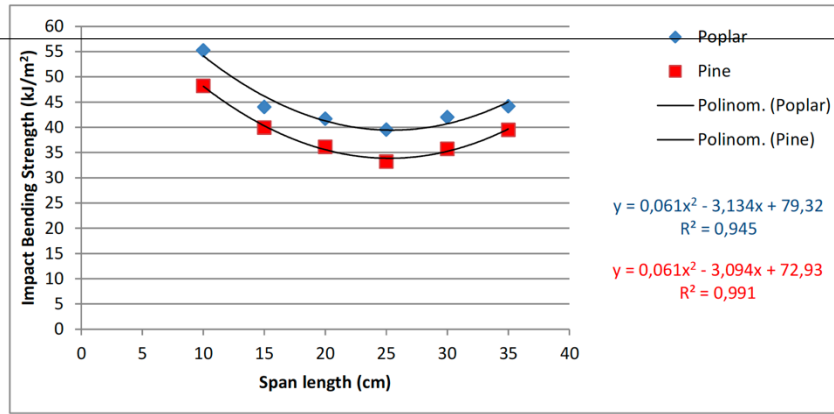
(b)

Figure 3. (a) Photographs of groups of five test specimens of Poplar and Pine wood that had been subjected to an impact bending strength test. The labels give the lengths of the original specimens in each group. (b) Plots of the impact bending strengths of Poplar and Pine specimens as a function of the span length. From [13].

Figures 2 and 4 suggest that the effect of strain rate on the mechanical properties of wood is similar to that of metals [14] and polymers [9], namely that the effect of deformation rate is bilinear with a weak rate effect up to a strain rate of about 10^3 s^{-1} and a strong rate effect above that value. What neither figure shows, however, is the effect of strain. For since wood has a tubular structure [15], like an anisotropic cellular material or a polymeric foam, its mechanical behaviour consists of three phases: (i) elastic deformation to (ii) a stress plateau (where large strains are imposed on the tubular cells), and finally (iii) densification of the structure from a certain critical value. From these high values of strain, its resistance to deformation increases rapidly up towards that of the fully-dense macromolecules it consists of (mostly cellulose and lignin) [16].
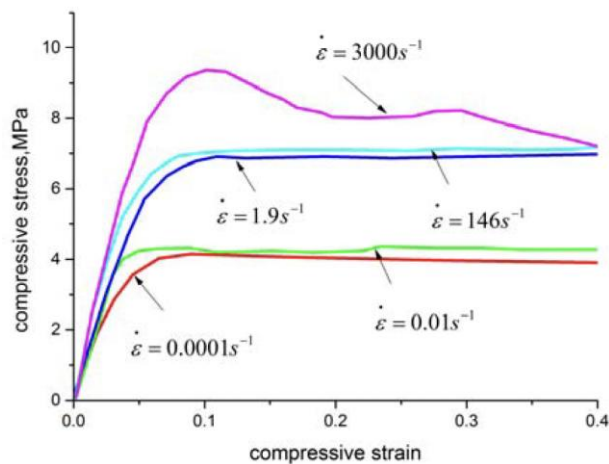
Figure 4. Comparison of the compressive stress-strain curves of balsa wood at quasistatic, intermediate, and high strain rates. From [16].

Another feature of wood that is not shown in Figures 2 and 4 is its anisotropy. Due to the way that trees grow, the mechanical behaviour is anisotropic with a preferred direction corresponding to the axis of the trunk of the tree. If the behaviour is often considered as orthotropic, studies show that the high-rate mechanical properties of the resulting wood have values that depend on the angle between the loading and growth directions (Figure 5) [17].
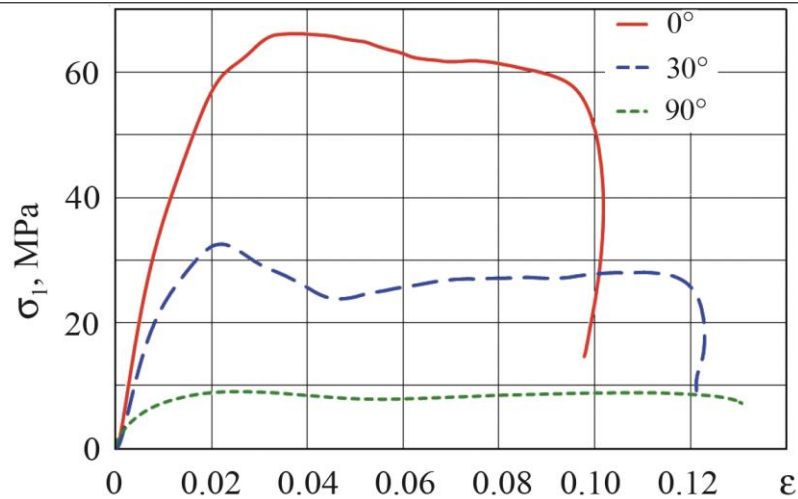
Figure 5. Compression Kolsky bar stress-strain curves for Sequoia wood deformed in 1D strain (specimens were constrained using a metal jacket) at various angles to the fibre direction. From [17].

Because of the uses to which it is put, there is also interest in the high rate properties of wood at temperatures both below and above ambient [18-21].

Wood's anisotropy has to be taken into account when designing experiments to study, for example, ballistic impact on wooden plates. The optical technique used to take the images presented in Figure 6 shows that the effect of an impact propagates about three times faster parallel to the fibre direction as compared to perpendicular.
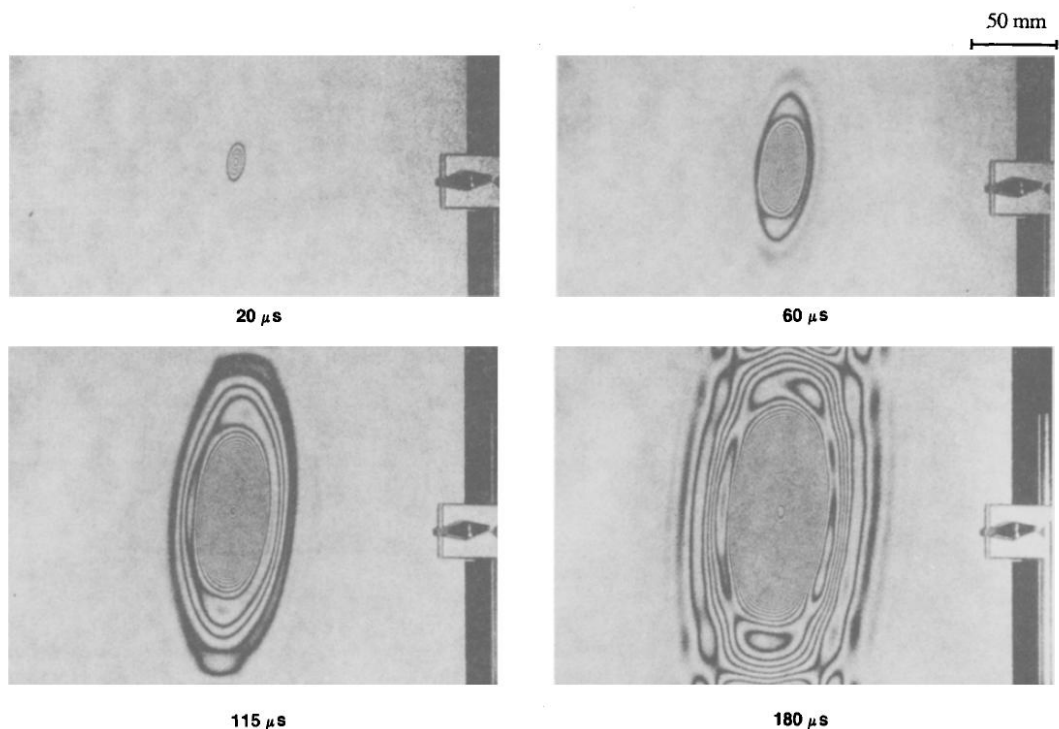
Figure 6. Interferograms showing the propagation of transverse waves in a 5mm thick plate of pine wood that was struck by a ballistic pendulum. The fibres of the wooden plate are parallel to the major axis of the ellipse and almost parallel with the shorter side of the plate (vertical in this figure). Total duration of impact was 500 μs. From [22].

At the time that it became possible to measure the velocity of cannonballs and shells [23], wood was still highly important in military applications such as warships [5]. Thus it was one of the first substances to have its penetration-velocity relationship investigated [24, 25]. By the 1830s, military researchers working in Metz, France had determined that the resistance of substances to ballistic penetration scaled as the square of the

impact velocity [26]. In 1856 in a summary of terminal ballistics experiments performed in the United States, Dahlgren showed that the formulae developed in Metz gave very good agreement for results obtained for wood [27].

3. Industrial applications

Applications where wood may be subjected to dynamic loading include the nuclear industry where it is used in the impact limiters in the base of spent nuclear fuel flasks (Figure 7) [28] and the blades of electricity-generating wind turbines which are subject to lightning strikes [29] and hailstorms [30]. Trees themselves can also, of course, be severely damaged in this way [31].
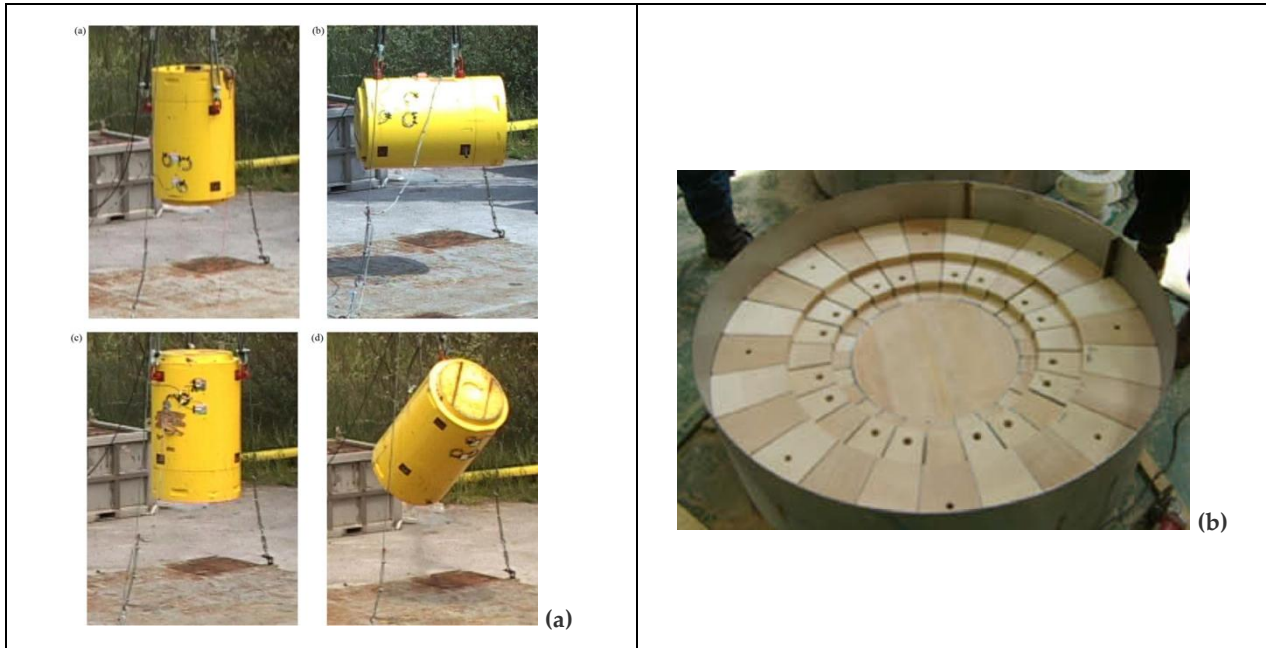
Figure 7. (a) Drop test configurations for spent nuclear fuel (SNF) flask. From [32]. (b) Photograph of wooden blocks in place in an impact limiter for an SNF flask. From [33].

Wood may not only be subject to impact, but can itself be a projectile when debris is picked up by strong winds or by moving water [34, 35]. Although in these scenarios the impact velocities are usually at least one order of magnitude lower than in ballistic impact, the damage inflicted on structures can be severe due to the large mass of the wooden objects involved (Figure 8).
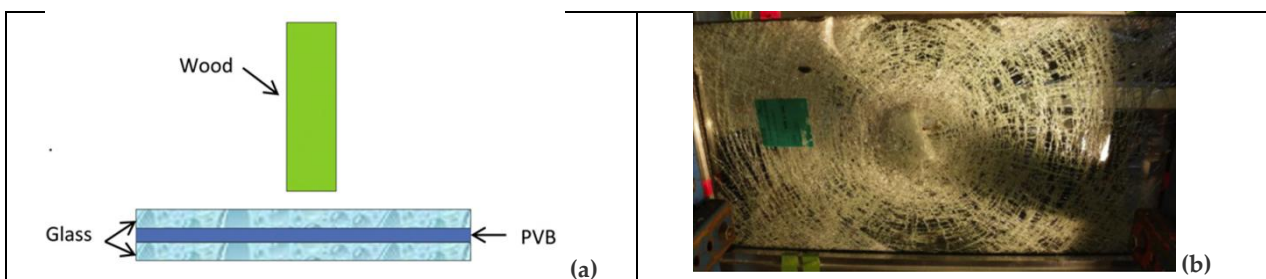
Figure 8. (a) Schematic diagram of experiment in which a 4 kg cylindrical wood projectile (100mm long 50mm diameter) impacts a 2m × 0.6m × 3mm laminated glass specimen. (b) Glass specimen after impact at 15 m/s. From [34].

References:
1. Wang L., Toppinen A., Juslin H. 2014. *J Cleaner Production* **65**, 350-361. (10.1016/j.jclepro.2013.08.023)
2. De Luca P., Carbone I., Nagy J.B. 2017. *J Green Building* **12**(4), 141-161. (10.3992/1943-4618.12.4.141)
3. Hurmekoski E., Pykalainen J., Hetemaki L. 2018. *J Cleaner Production* **172**, 3644-3654. (1016/j.jclepro.2017.08.031)
4. Huang Z.H., Wang X., Cai L.P., Tao Y., Tolone W.J., El-Shambakey M., Bhattacharjee S.D., Cho I. 2020. *J Performance Constructed Facilities* **34**, 04020022. (10.1061/(ASCE)CF.1943-5509.0001414)

5. Walley S.M. 2018. The beginnings of the use of iron and steel in heavy armour. In: Kaufman B., Briant C.L. (eds) Metallurgical Design and Industry. New York: Springer. pp. 71-153. (10.1007/978-3-319-93755-7_2)

6. Holley A.L. 1865. Gun-cotton: Manufacture and experiments in England. In: A Treatise on Ordnance and Armor. New York: van Nostrand. pp. 828-831.

7. Ferguson W.G., Yew F.K. 1977. *J Mater Sci* **12**, 264-272. (10.1007/BF00566266)

8. Ferguson W.G. 2009. *IOP Conf Ser: Mater Sci Engng* **4**, 012004. (10.1088/1757-899X/4/1/012004)

9. Walley S.M., Field J.E. 1994. *DYMAT Journal* **1**, 211-228.

10. Walley S.M., Rogers S.J. 2022. *Materials* **15**, doi: 10.3390/ma15155403.

11. Madsen B., Tomoi M. 1991. *Canad J Civil Engng* **18**, 637-643. (10.1139/l91-078)

12. Kohler J., Brandner R., Thiel A.B., Schickhofer G. 2013. *Engng Struct* **56**, 691-697. (10.1016/j.engstruct.2013.05.048)

13. Bal B.C. 2021. *BioResources* **16**, 4021-4026.

14. Follansbee P.S., Regazzoni G., Kocks U.F. 1984. *Inst Phys Conf Ser* **70**, 71-80.

15. Gibson L.J., Ashby M.F. 2014. Wood. In: Cellular Solids: Structure and Properties (Second Edition). Cambridge: Cambridge University Press. pp. 387-428. (10.1017/CBO9781139878326.012)

16. Zhao S., Zhao J.X., Han G.Z. 2016. *IOP Conf Ser: Mater Sci Engng* **137**, 012036. (10.1088/1757-899X/137/1/012036)

17. Konstantinov A.Y., Lomunov A.K., Iuzhina T.N., Gray III G.T. 2018. *Problems Strength Plasticity* **80**, 555-565. (10.32326/1814-9146-2018-80-4-555-565)

18. Holmgren S.E., Svensson B.A., Gradin P.A., Lundberg B. 2008. *Exper Techniq* **32**(5), 44-50. (10.1111/j.1747-1567.2008.00318.x)

19. Caetano L., Grolleau V., Galpin B., Penin A., Capdeville J.-D. 2018. *Strain* **54**, doi: 10.1111/str.12264.

20. Bragov A.M., Iuzhina T.N., Lomunov A.K., Igumnov L.A., Belov A.A., Eremeyev V.A. 2022. *J Applied Computational Mechanics* **8**, 298-305. (10.22055/JACM.2021.38486.3239)

21. Le Barbenchon L., Viot P., Girardot J., Kopp J.-B. 2022. *J Dyn Behav Mater* **8**, 39-56. (10.1007/s40870-021-00316-5)

22. Fällström K.-E., Gustavsson H., Molin N.-E., Wåhlin A. 1989. *Exper Mech* **29**, 378-387. (10.1007/BF02323854)

23. Prony M. 1805. *J Natural Philosophy Chemistry Arts* **12**, 41-46.

24. Johnson W. 1986. *Int J Impact Engng* **4**, 161-174. (10.1016/0734-743X(86)90003-5)

25. Johnson W. 1986. *Int J Impact Engng* **4**, 175-183. (10.1016/0734-743X(86)90004-7)

26. Piobert G., Morin A.J., Didion I. 1837. *Mémorial Artillerie* **4**, 299-383.

27. Dahlgren J.A. 1856. Penetration. In: Shells and Shell-Guns. Philadelphia, PA: King & Baird. pp. 173-203.

28. Lee E.H., Ra C.W., Roh H.Y., Lee S.J., Park N.C. 2022. *Nuclear Engng Technology* **54**, 3766-3777. (10.1016/j.net.2022.05.028)

29. Yan J.Y., Wang G.Z., Ma Y.F., Guo Z.X., Ren H.W., Zhang L., Li Q.M., Yan J.D. 2019. *Wind Energy* **22**, 1603-1621. (10.1002/we.2392)

30. Macdonald H., Nash D., Stack M.M. 2019. *Wear* **432**, 102926. (10.1016/j.wear.2019.06.001)

31. Yanoviak S.P., Gora E.M., Bitzer P.M., Burchfield J.C., Muller-Landau H.C., Detto M., Paton S., Hubbell S.P. 2020. *New Phytologist* **225**, 1936-1944. (10.1111/nph.16260)

32. Lo Frano P., Pugliese G., Nasta M. 2014. *Nuclear Engng Design* **280**, 634-643. (10.1016/j.nucengdes.2014.09.034)

33. Kim K.S., Kim J.S., Choi K.S., Shim T.M., Yun H.D. 2010. *Annals Nuclear Energy* **37**, 546-559. (10.1016/j.anucene.2009.12.023)

34. Zhang X., Hao H., Ma G. 2013. *Int J Impact Engng* **55**, 49-62. (10.1016/j.ijimpeng.2013.01.002)

35. Kim M.I., Kwak J.H. 2020. *Water* **12**, doi: 10.3390/w12072021.

Taylor impact

Stephen M. WALLEY[1*], Hervé COUQUE[2]

[1] Cavendish Laboratory, J.J. Thomson Avenue, Cambridge CB3 0HE, United Kingdom
[2] Nexter Munitions, 18023 Bourges Cedex, France

Keywords: Taylor impact, constitutive relations, dynamic plasticity

Abstract: During the Second World War, G.I. Taylor developed a technique that enabled the compressive strengths of materials at strain rates of tens of thousands per second to be estimated. The method simply involved measuring the change of length and shape of a short cylinder of the material of interest that had been fired at a known velocity against a hard massive anvil. This technique was not often subsequently used for its original purpose because a more accurate technique of measuring dynamic compressive strengths of materials was developed during the same conflict, namely the split Hopkinson pressure bar. The test was revived in the mid 1970s after developments in high-speed photography meant that it had become possible to obtain information about intermediate deformation states. This allowed the test to be used for materials such as polymers, ceramics and glasses for which the final specimen state cannot be determined. The Taylor test is now primarily used for validating constitutive models whose parameters are determined using other techniques.

1. Introduction

In a lecture he gave in 1946, Professor Sir Geoffrey Ingram Taylor reviewed the techniques that were available during World War 2 for measuring the mechanical properties of materials at high rates of deformation [1]. One of these techniques involved firing short right circular cylinders against hard steel plates. This method became known a few years later as Taylor impact [2]. Upon impact, Taylor found that plastic deformation occurred within a limited region at the front end of the rod, resulting in an increase in the cross-sectional area and a decrease in the length (Figure 1). Note that some of the historic figures used in this paper quote velocities in feet per second and specimen dimensions in inches: 1 foot (= 12 inches) is about 0.3m.

Figure 1: Shadowgraph images of cylindrical mild steel specimens (originally 1 inch long and 0.3 inches diameter) after impact on 'heavy armour' plates at various speeds. From [1].

This was not the first time that results had been published on the deformation produced in short metal rods due to their impact on a hard anvil, for as early as 1902, Gilles Louis de Maupeou d'Ableiges had published the photograph shown in Figure 2 in a general review of the mechanics of materials. However, although it is clear

from the article that de Maupeou had good physical insight into this experiment, he did not perform an analysis which would have allowed him to estimate the dynamic strength of the cylinders.
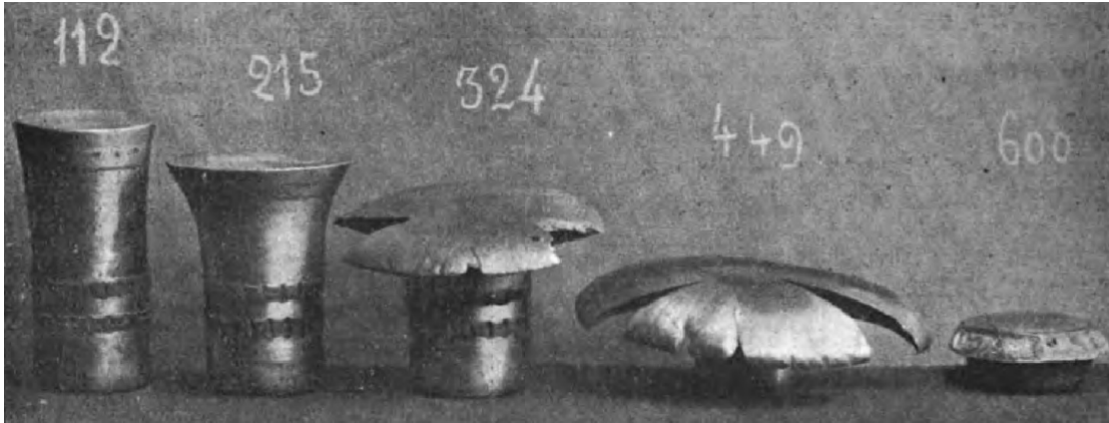
Figure 2: Photograph of 43mm diameter steel rods after impact on a rigid anvil. The impact speeds (m/s) for each specimen are written on the photograph. From [3, 4].

2. What information did Taylor obtain from this test?

Taylor's insight was that in order to use the final shape of the impacted cylinder to estimate the dynamic compressive yield stress, σ, it is necessary to work out how the final position of the elastic-plastic boundary depends on that stress. His analysis and the assumptions that he made may be found in [5, 6]. The expression that Taylor derived is given in Equation (1):

$$\sigma = \frac{\rho V^2 (L-X)}{2(L-L_1)\ln(L/X)} \qquad , \qquad (1)$$

where L is the original length, L_1 is the final overall length, X is the length of the undeformed section after impact, and V is the impact velocity. Note that Taylor assumed the materials he investigated were rigid up to yield and then deformed perfectly plastically at constant stress.

Taylor was well aware of the limitations of the test. The advantage of the technique as he saw it was that elaborate and expensive dynamic measurement apparatus was not needed in order to obtain an estimate of the dynamic compressive flow stresses of the alloys being used for projectiles and armour [7]. All that was required were measurements of the cylinder dimensions before and after impact. It should be noted that at the start of World War 2 there were no techniques under development for obtaining the high-rate properties of materials in compression [8].

3. Revival of the Taylor impact test

It can be seen from the histogram presented in Figure 3 that Taylor impact was not often used until about 30 years after Taylor and his colleagues published papers about it. The main reason was that alternative techniques were available that gave more accurate data. These included the split Hopkinson pressure bar [9] and instrumented long rod impact [10, 11].
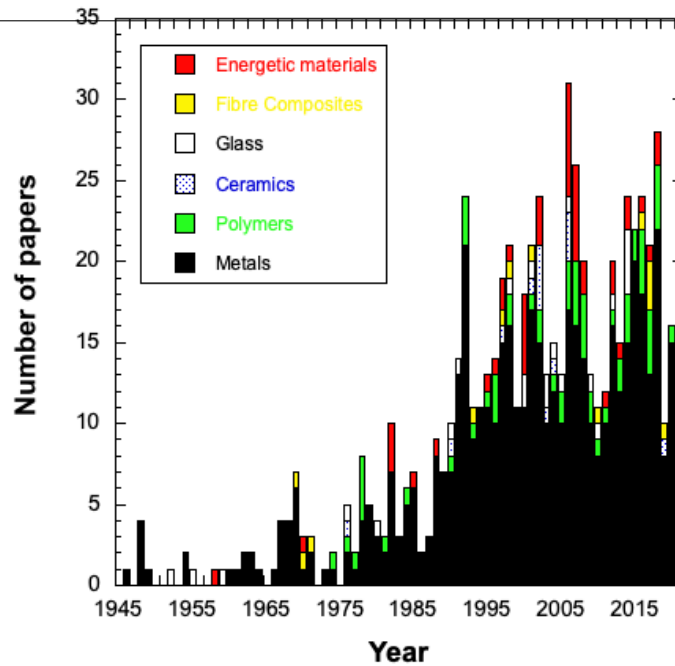
Figure 3: Histogram of the number of papers published about Taylor impact between 1946 and 2021 for six different types of material.

The short rod Taylor impact test was revived in the 1970s by a number of researchers [12, 13]. Wilkins & Guinan also performed the first numerical analysis of the technique using classical plasticity models [12]. Briscoe & Hutchings chose this test because they wished to study the effect of temperature on the flow stress of high-density polyethylene at a high rate of strain. However, the values they obtained for the dynamic yield stress using Equation (1) (Taylor's theory) were much higher than they were expecting. This is because polymers are not rigid-perfectly plastic. Hutchings therefore reanalysed the problem making the assumption that polymers are elastic perfectly-plastic [14]. Something else that needs to be considered for polymers is the large amount of viscoelastic recovery that takes place after impact even on a timescale of tens of microseconds (Figure 4). This means that measuring the final dimensions of polymer rods recovered after impact gives results for their dynamic yield stress that are seriously in error. Thus recording the impact using high-speed framing photography is essential for this class of materials, as indeed it is for brittle materials such as glasses and ceramics [15-17].
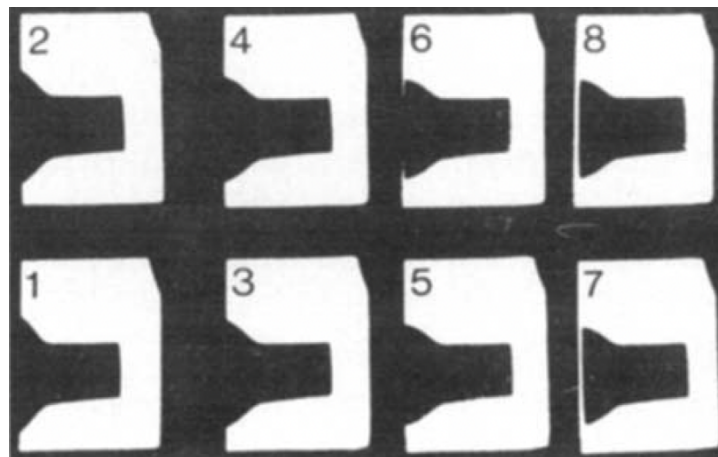
Figure 4: High-speed photographic sequence of the rebound of a 16mm diameter high-density polyethylene rod after normal impact at 170 m s⁻¹. Temperature 100 °C, interframe time 19 µs. From [13].

4. Symmetric Taylor test (or rod-on-rod impact)

It was clear from the original studies by Taylor and colleagues that friction between the rod and the anvil strongly affected the deformation [18]. A method of eliminating friction in this test was later developed by researchers studying the dynamic propagation of plasticity in long rods [19, 20]. The technique involves

impacting two rods of the same diameter coaxially and collinearly. The symmetric test is experimentally much more difficult to perform than the classic Taylor test. However, rod-on-rod impact ensures that the two ends of the rods deform together without slipping. This 'no-slip' condition means that friction, no matter how large, will have no effect on the deformation, and if the rods are made from the same material, neither will indent the other. Thus rod-on-rod impact can thus be considered equivalent to the impact of a single rod at half the speed with an ideally rigid anvil. This technique later became known as symmetric Taylor impact [21]. The combination of this technique with high-speed photography allows intermediate deformation states to be compared with predictive numerical modelling [22] (Figure 5). It should be emphasised that the red simulation curve in Figure 5 is not a fit to the experiment but rather a prediction based on a constitutive model for copper: the student who carried out this simulation was not shown the experimental result before performing the calculation.
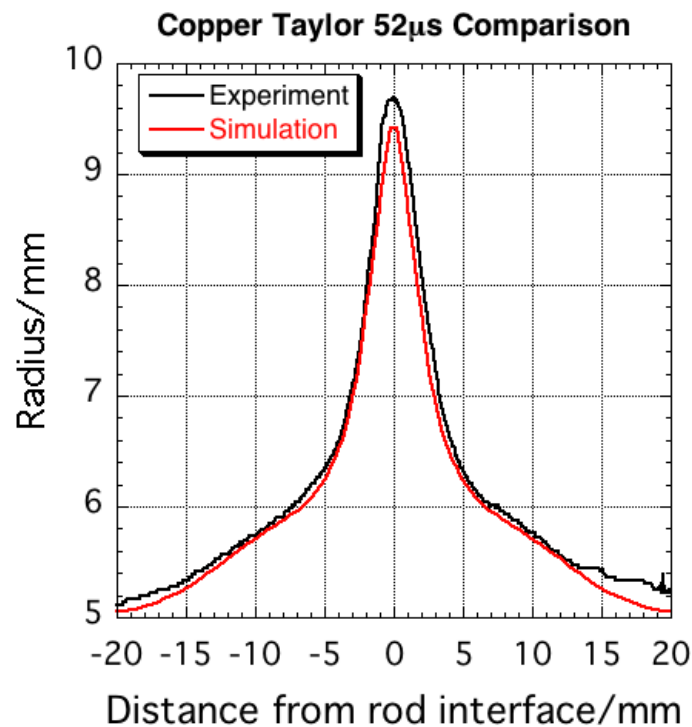
Figure 5: Comparison of experimental and predictive simulation profiles for a symmetric Taylor impact test performed at 395 m/s using copper rods. From [22].

For the rod-on-rod test to be strictly symmetric, the two rods would both have to be travelling at the same speed in opposite directions at impact. But the experimental difficulties are great enough that it is unlikely such an experiment will ever be carried out. So the test is normally performed by coaxially firing a rod at a stationary rod made of the same material and of identical dimensions (Figure 6) [23, 24]. As in Figure 6, the impacting rod is usually carried to the target rod using a light-weight polymer sabot [22, 24, 25].
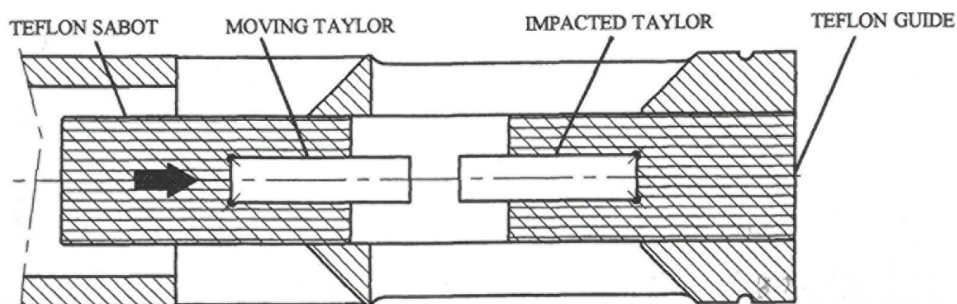
Figure 6: Schematic diagram of apparatus for performing symmetric Taylor impact inside a gun barrel for high-strength materials. The target rod is held in place using a Teflon sabot. From [23].

Figure 7 shows an X-radiograph obtained for symmetric Taylor impact of a high-strength tungsten alloy using the system presented in Figure 6. The polymer sabot holding the target rod appears as a light grey shadow in the right-hand section of the X-ray image.

Figure 7: Flash X-radiograph taken 20 μs after symmetric Taylor impact at 127 m/s of 9mm diameter 35mm long tungsten alloy rods. From [23].

Although polymer sabots have been observed to have no measurable effect on the plastic deformation of target materials that have strengths greater than 800 MPa, in an ideal rod-on-rod impact there would be no external constraint at all on the lateral deformation of the rods i.e. the impacting rod would be in free flight and the target rod would be levitated. A method that comes close to this ideal was proposed in 2015 in which the target rod is held in place using a spring-tensioned wire cradle (Figure 8) [26]. This mount is sufficiently rigid to stabilise the rod against airblast from the gun as long as the experiment is performed in a vacuum. It also puts very little mechanical constraint on the dynamic plastic expansion of the target rod.
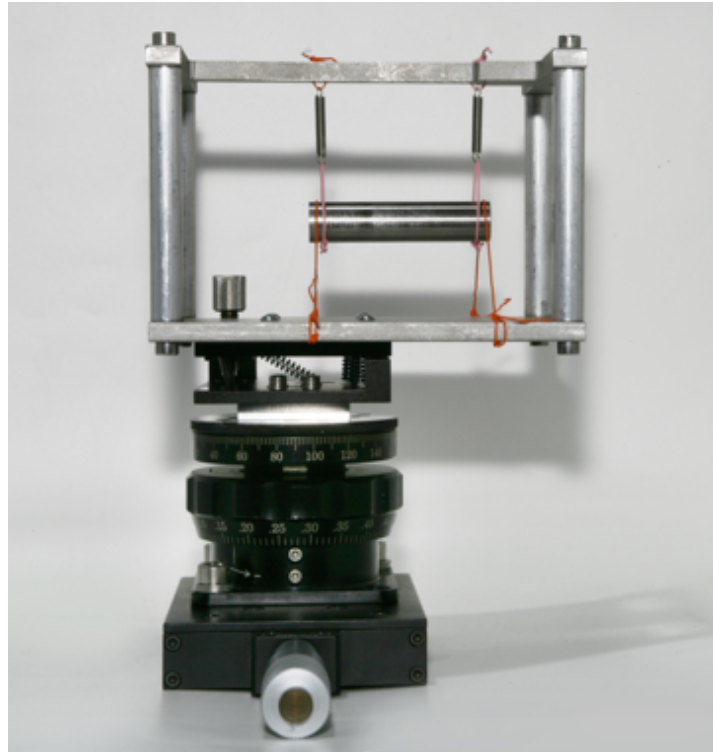
Figure 8: Spring-tensioned wire cradle for holding the target rod for symmetric Taylor impact experiment. From [26].

Some frames from a high-speed photographic sequence of symmetric Taylor impact performed on pure aluminium are presented in Figure 9. It can be seen from Figure 9*b* that a sabot was not used in this experiment.

(a)

(b)
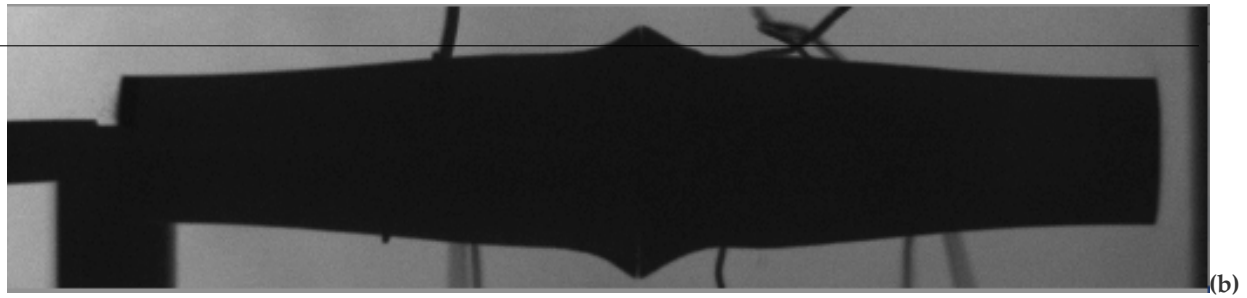
Figure 9: Two frames from the high-speed photographic sequence of the impact of a 63.3 mm long, 12.66 mm diameter pure aluminium rod by another pure aluminium rod of the same dimensions at 334 m/s. (a) 2.8 μs after impact. (b) 202.8 μs after impact. From [26].

5. Summary and conclusions

A simple-to-perform, but difficult-to-analyse, short-rod impact technique was developed during the Second World War by G.I. Taylor and colleagues to estimate the high strain rate compressive mechanical properties of strong metal alloys. As the stress state, strain, strain rate and temperature vary significantly with distance from the impact face, it has been realised in the last 20 years or so that Taylor impact is a severe test of the constitutive models that are being developed to describe the response of materials to dynamic loading. Excellent agreement has been found between prediction and experiment for those fcc and bcc metals whose mechanical parameters have been measured using a wide range of other experimental techniques.

References:
1. Taylor G.I. 1946. *J Inst Civil Engrs* **26,** 486-519. (10.1680/ijoti.1946.13699)
2. Lee E.H., Tupper S.J. 1954. *J Appl Mech* **21,** 63-70. (10.1115/1.4010820)
3. de Maupeou G.L. 1902. *Bull Assoc Technique Maritime* **13,** LVIII-LIX, 271-365.
4. Régnauld P. 1927. *Rev Métall Mémoires* **24,** 509-515. (10.1051/metal/192724090509)
5. Taylor G.I. 1948. *Proc R Soc Lond A* **194,** 289-299. (10.1098/rspa.1948.0081)
6. Chapman D.J., Radford D.D., Walley S.M. 2005. A history of the Taylor test and its present use in the study of lightweight materials. In: Teixeira-Dias F., Dodd B., Lach E., Schultz P. (eds) Design and Use of Light-Weight Materials. Aveiro, Portugal: University of Aveiro. pp. 12-24
7. Hawkyard J.B., Eaton D., Johnson W. 1968. *Int J Mech Sci* **10,** 929-948. (10.1016/0020-7403(68)90048-9)
8. Walley S.M. 2020. *J Dyn Behav Mater* **6,** 113-158. (10.1007/s40870-020-00237-9)
9. Kolsky H. 1949. *Proc Phys Soc Lond B* **62,** 676-700. (10.1088/0370-1301/62/11/302)
10. Duwez P.E., Clark D.S. 1947. *Proc Amer Soc Testing Materials* **47,** 502-532.
11. Bell J.F. 1956. *J Appl Phys* **27,** 1109-1113. (10.1063/1.1722212)
12. Wilkins M.L., Guinan M.W. 1973. *J Appl Phys* **44,** 1200-1206. (10.1063/1.1662328)
13. Briscoe B.J., Hutchings I.M. 1976. *Polymer* **17,** 1099-1102. (10.1016/0032-3861(76)90013-6)
14. Hutchings I.M. 1978. *J Mech Phys Solids* **26,** 289-301. (10.1016/0022-5096(78)90001-7)
15. Brar N.S., Bless S.J., Rosenberg Z. 1988. *J Phys France Colloq* **49**(C3)**,** 607-612. (10.1051/jphyscol:1988385)
16. Murray N.H., Bourne N.K., Field J.E., Rosenberg Z. 1998. *AIP Conf Proc* **429,** 533-536. (10.1063/1.55560)
17. Willmott G.R., Radford D.D. 2005. *J Appl Phys* **97,** 093522. (10.1063/1.1889249)
18. Carrington W.E., Gayler M.L.V. 1948. *Proc R Soc Lond A* **194,** 323-331. (10.1098/rspa.1948.0083)
19. Raftopoulos D. 1969. *Int J Solids Structures* **5,** 399-412. (10.1016/0020-7683(69)90021-3)
20. Critescu N. 1970. *Int J Mech Sci* **12,** 723-738. (10.1016/0020-7403(70)90071-8)
21. Erlich D.C. 1985. Rod impact (Taylor) test. In: Metals Handbook Vol 8 (9th edn). Metals Park, OH: American Society of Metals. pp. 203-207
22. Forde L.C., Walley S.M., Peyton-Jones M., Proud W.G., Cullis I.G., Church P.D. 2009. The use of symmetric Taylor impact to validate constitutive models for an fcc metal (copper) and a bcc alloy (RHA steel). In: Dyckmans G. (Ed.) Proc 9th Int Conf on the Mechanical and Physical Behaviour of Materials under Dynamic Loading (DYMAT 2009). Les Ulis, France: EDP Sciences. pp. 1245-1250. (10.1051/dymat/2009175)
23. Couque H. 2000. *J Phys IV France* **10**(Pr. 9)**,** 179-184. (10.1051/jp4:2000930)
24. Forde L.C., Proud W.G., Walley S.M. 2009. *Proc R Soc A* **465,** 769-790. (10.1098/rspa.2008.0205)
25. Couque H., Nicolas G., Altmayer C. 2007. *Int J Impact Engng* **34,** 412-423. (10.1016/j.ijimpeng.2005.12.003)
26. Walley S.M., Taylor N.E., Williamson D.M., Jardine A.P. 2015. *EPJ Web Conferences* **94** 01029, (10.1051/epjconf/20159401029)

Statistical characterization of mechanical behavior of Ti6Al4V and bayesian calibration of a constitutive model

Charles Francart[1*]

[1]: *Laboratoire sols, solides, structures-risques, CNRS : UMR5521, Université de Grenoble-Alpes, Institut polytechnique de Grenoble – Grenoble institute of Technology*

Keywords: constitutive model, experimental uncertainties, titanium alloy, Bayesian calibration, dynamic testing

Abstract

Mechanical characterizations of materials are a very common research projects and impact all industrial fields from aeronautic to medicine. However, quantification of experimental uncertainties are generally overlooked in most works even if they can change the interpretation of the results by themselves such as explaining data dispersion or help to improve efficiently the experimental setup accuracy.

Furthermore, the quantification of uncertainties can be used to improve the calibration of constitutive laws using the Bayesian inference method. Indeed, model parameters obtained through such method consists into a probabilistic distribution of their values and can then be adjusted according to the suitable application. It can also greatly helps in failure risks calculations by providing reliable material data to feed in a numerical model. Finally, in addition to help to understand the experiments better and to improve the versatility of the results, uncertainties quantification also removes all doubts about results credibility.

1. Introduction

Results uncertainties has always been a major issue in all science fields. Indeed, being able to estimate them gives a better understanding of the data and also grants more credibility in the research results. However, very few works have been carried out around that topic in mechanical testing and especially in experimental dynamic [1, 2]. The work presented here aims to illustrate a procedure to characterize the mechanical behaviour of any material characterized over wide ranges of temperatures and strain rates while determining precisely the experimental uncertainty on each test. Then those experimental data are used to calibrate a probabilistic Johnson-Cook model [3] using the Bayesian inference method [1, 2]. This work can be transposed to any kind of material experimental characterization even if only quasi-static and dynamic compression are analysed in this paper.

2. Experimental procedure

The Ti6Al4V titanium alloy ($\rho = 4340\ kg.m^{-3}$) is used in a lot of different application fields such as military protection, aircraft or medical prosthesis for instance. The material tested for this study has been chosen for its already wide database of test results that can be found in the literature such as [4-8]. Therefore, the results can be easily compared with several references.

For this study, quasi-static and dynamic tests have been carried out from 0.001 /s up to 5000 /s and a wide range of temperature has also been investigated from 213K up to 893K. The aim of such wide experimental condition domains is to study the limit of the Bayesian calibration. A total of 51 tests have been performed under those various conditions of temperature and strain rates.

Tests have been carried out on compression sample of Ø=6mm and h=6mm for the quasi-static conditions with an INSTRON uniaxial testing machine and Ø=6mm and h=3mm for the Hopkinson bar tests in order to reduce the duration of the transitory phase. The Hopkinson bars [9] details are reported in Table 1.

Table 1 : Hopkinson bar setup characteristics

BAR	INPUT BAR	OUTPUT BAR	STRIKER
LENGTH (M)	1.9	1.3	0.4
DIAMETER (MM)	20	20	20
MATERIAL	Steel	Steel	Steel

The tests at high temperature have been performed with a climatic chamber for quasi-static tests and a pulsated hot air device for dynamic tests (temperature monitored on surface with infrared method). Tests at low temperature have only been done for dynamic tests using a bath of liquid nitrogen and ethanol to adjust temperature.

3. Uncertainties estimation

The estimation of the results uncertainties are calculated with the propagation of the different setup parameters uncertainties through the standard data processing [1, 2]. The procedure consists into determining the uncertainty of each of the M setup and sample parameters required to perform the data processing of the raw data from the experiment to get information about the mechanical behaviour of the material. Then, N sets of the M parameters are generated using distribution laws such as the normal law and a standard determinist data processing is performed for each of those parameters set (Fig.1.a). Finally, statistical analysis is performed over the N set of results and probabilistic curves can be plotted (Fig.1.b). This method allows also understand the influence of each parameter on the results uncertainties and then to improve the experimental setup more efficiently. This method can be applied to any kind of experiment and in any scientific domain.

(a)

(b)
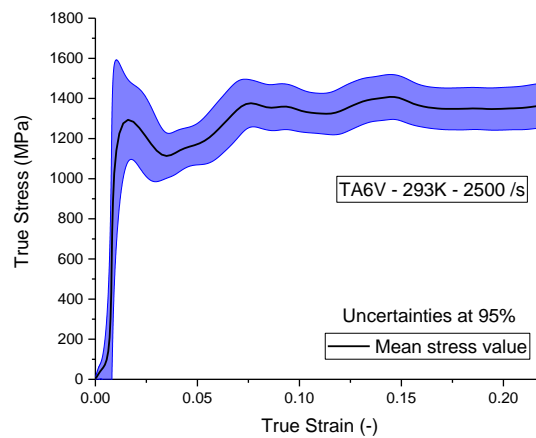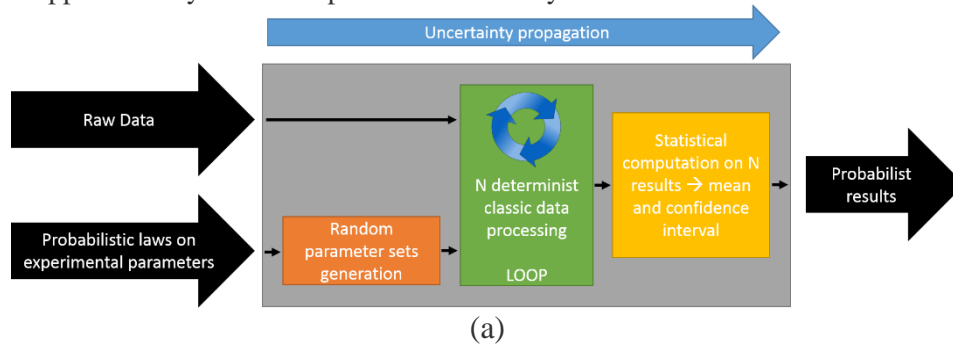
Figure 1 : (a) Schematic representation of the probabilistic data processing using uncertainties propagation and (b) strain/stress probabilistic curves (uncertainties at 95%)

4. Bayesian model calibration

Bayesian model calibration allows to obtain probabilistic repartition of each model parameter instead of one unique value. This approach is very useful to model material with very high dispersion in their behaviour such has biomaterials, highly heterogeneous materials or material stock providing from numerous suppliers. Furthermore, it allows to readjust parameters values with a controlled method. The calibration procedure follows a complex mathematical method which has been used in [2] for another model. The model chosen for this study is the most widely used Johnson-Cook model [3] (Eq.1). The calibration is performed on 26 test results and 25 are kept for model validation. The calibration is performed using the free Python library PYMC3.

$$\sigma\left(\varepsilon_p, \dot{\varepsilon}_p, T\right) = \left(A + B\varepsilon_p{}^n\right)\left(1 + C \ln\left(\frac{\dot{\varepsilon}_p}{\dot{\varepsilon}_0}\right)\right)\left(1 - \frac{T - T_0}{T_m - T_0}\right)^m \qquad (1)$$

With ε_p the plastic strain, $\dot{\varepsilon}_p$ the plastic strain rate and T the temperature. A, B, n, C and m are the 5 parameters to calibrate. The reference strain rate is $\dot{\varepsilon}_0 = 0.001\ /s$, the reference temperature is $T_0 = 293\ K$ and the melting point is $T_m = 1905\ K$.

The calibrated parameters are given in Fig.2. Their values are generally provided under the form of a normal distribution: mean value and standard deviation but other type of distribution can be used depending on the result.
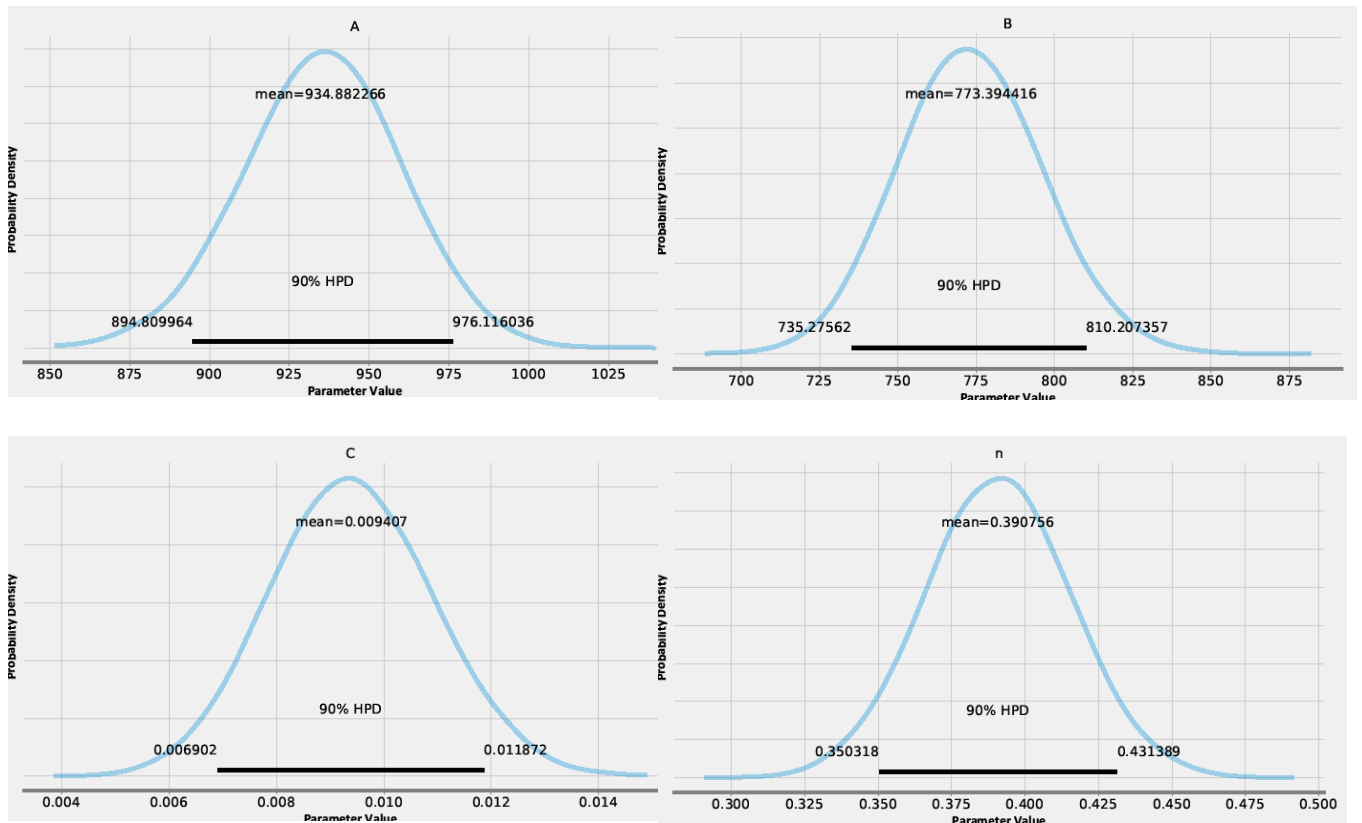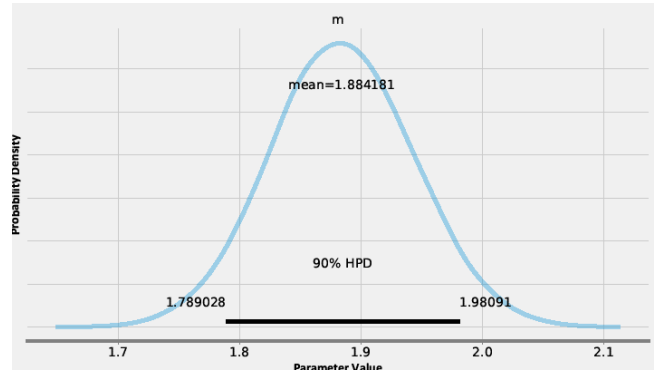
Figure 2 : Probabilistic repartition of calibrated parameters values of the Johnson-Cook law for a Ti-6Al-4V alloy

The Fig.3.a-d are several examples of comparison of the calibrated model with experimental data which have not been used for the calibration. It can be observed that the model has more issues to fit the mechanical behaviour at high strain rate and high temperature (Fig.3.c). It is due to the fact that the model does not have any form of coupling between temperature and strain rate (see Eq.1) and will necessarily have difficulty to grasp the full behaviour of a material over a wide ranges of experimental variables.
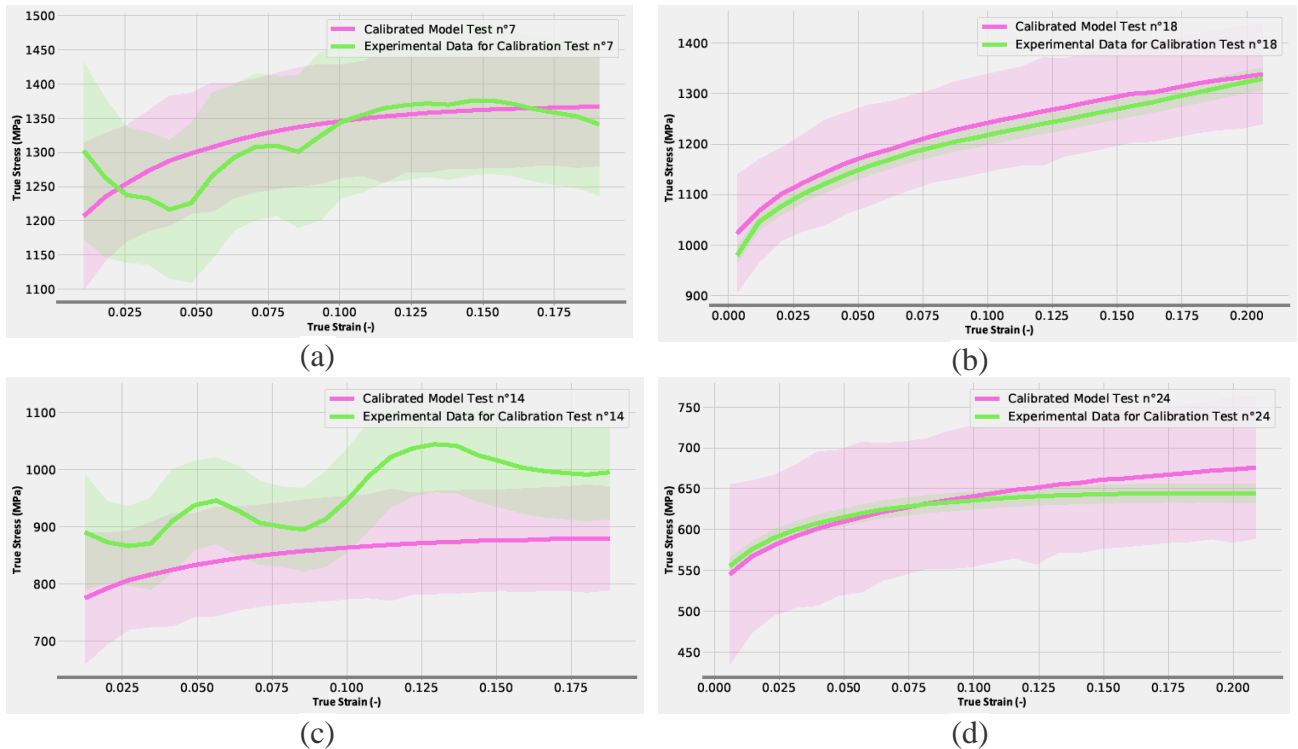
Figure 3 : comparison between calibrated model and experimental data at (a) $T_0 = 293\ K$ and $\langle \dot{\varepsilon}_p \rangle = 2700\ /s$, (b) $T_0 = 300\ K$ and $\langle \dot{\varepsilon}_p \rangle = 0.001\ /s$, (c) $T_0 = 623\ K$ and $\langle \dot{\varepsilon}_p \rangle = 2000\ /s$ and (d) $T_0 = 793\ K$ and $\langle \dot{\varepsilon}_p \rangle = 0.02\ /s$ (with $\langle \dot{\varepsilon}_p \rangle$ the mean plastic strain rate)

5. Conclusion

The presented work aimed to display the possibilities allowed from determining the experimental setup parameters uncertainties and by injecting them inside a probabilistic data processing in order to understand the reliability of the results. Those results can even be expended to perform a Bayesian model calibration to get parameters in a probabilistic forms. Those can be used with a better versatility than the unique values obtained through deterministic data processing and calibration. However, it the performance of the calibrated model will

always depends on its choice. Indeed, some models are more efficient than others to grasp the whole mechanical behaviour of the tested material.

References:

1. Seisson, G., et al. *Flow stress of beryllium: Attempt for a bayesian crossed-data analysis from hopkinson bars to Rayleigh-Taylor instabilities*. in *EPJ Web of Conferences*. 2018. EDP Sciences.
2. Weisz-Patrault, D., C. Francart, and G. Seisson, *Uncertainty estimation and hierarchical Bayesian analysis of mechanical dynamic tests.* Journal of Dynamic Behavior of Materials, 2021. **7**(3): p. 447-468.
3. Johnson, G.R. and W.H. Cook. *A constitutive model and data for metals subjected to large strains, high strain rates and high temperatures*. in *Proceedings of the 7th International Symposium on Ballistics*. 1983. The Netherlands.
4. Nemat-Nasser, S., et al., *Dynamic response of conventional and hot isostatically pressed Ti–6Al–4V alloys: experiments and modeling.* Mechanics of Materials, 2001. **33**(8): p. 425-439.
5. Zhou, T., et al., *Dynamic shear characteristics of titanium alloy Ti-6Al-4V at large strain rates by the split Hopkinson pressure bar test.* International Journal of Impact Engineering, 2017. **109**: p. 167-177.
6. Guo, X., et al. *Direct-impact Hopkinson tests on the Ti-6Al-4V alloy at very high strain rate and inverse identification of the Johnson-Cook constitutive model*. in *MECAMAT*. 2015.
7. Berkovic, L., et al. *Modeling of high temperature Hopkinson tests on AA5083 and Ti6Al4V*. in *Proceedings of DYMAT 2009-9th International Conference on the Mechanical and Physical Behaviour of Materials Under Dynamic Loading*. 2009.
8. Francart, C., et al., *Application of the Crystallo-Calorific Hardening approach to the constitutive modeling of the dynamic yield behavior of various metals with different crystalline structures.* International Journal of Impact Engineering, 2017. **109**: p. 52-66.
9. Jankowiak, T., A. Rusinek, and T. Lodygowski, *Validation of the Klepaczko–Malinowski model for friction correction and recommendations on Split Hopkinson Pressure Bar.* Finite Elements in Analysis and Design, 2011. **47**(10): p. 1191-1208.

Numerical modelling of spalling tests using Discrete Element Method (DEM)

Luc Bremaud * , Jérémie Girardot [1], Frédéric Malaise [2], Pascal Forquin [3], Ivan Iordanoff [4]

[1] Arts et Métiers Science et Technologie, Institut de Mécanique et d'Ingénierie (I2M) – Institut polytechnique de Bordeaux, Arts et Métiers ParisTech, CNRS : UMR5295, Université de Bordeaux – 33400 Talence, France
[2] Centre d'études scientifiques et techniques d'Aquitaine (CESTA) – CEA – BP 2 33114 Le Barp, France
[3] Sols, Solides, Structures-Risques (3SR) – Université Grenoble Alpes – BP 53, 38041 Grenoble Cedex 9, France
[4] Institut de Mécanique et d'Ingénierie -Durabilité Matériaux des Assemblages et des Structures (DUMAS) – Université Sciences et Technologies - Bordeaux I, CNRS : UMR5295, Arts et Métiers ParisTech, Institut polytechnique de Bordeaux – Arts et Métiers ParisTech - Centre de Bordeaux Talence Esplanade des Arts et Métiers 33405 TALENCE cedex, France

The Discrete Element Method (MED) has already proven its ability to model the behavior of fragile materials in quasi-static regime. The purpose of this study is to assess its potential to represent the behavior of brittle materials under dynamic loading. After calibration step of the parameters of the DEM model in order to represent an alumina ceramic, the model is then used to simulate the propagation and the interactions of waves generated during dynamic experiments. The relevance of DEM model is demonstrated by the comparisons between the calculated and experimentally measured speed profiles. The spalling phenomenon is simulated, highlighting the strain rate sensitivity of the DEM model.

Keywords: Discrete Element Method (DEM), spalling phenomenon, dynamics fragmentation, strain rate sensibility

---

*Speaker

Simplified Split Hopkinson Tension Bar with long pulse duration using Polyoxymethylene striker

Puneeth Jakkula [1,*], **Georg Ganzenmüller** [1,2] **and Stefan Hiermaier** [1,2]

[1] *Albert-Ludwigs-Universität Freiburg, Sustainable Systems Engineering, Emmy-Noether Str. 2, 79110 Freiburg, Germany.*
[2] *Fraunhofer Institute for High-Speed Dynamics, Ernst-Mach-Institut - EMI, Ernst-Zermelo Str. 4, 79104 Freiburg, Germany.*

Keywords: Impact, Split Hopkinson Tension Bar, Dynamic Material Testing, SS316L

Summary

The Kolsky bar, also commonly known as Split Hopkinson Pressure Bar (SHPB), is now one of the most important methods for testing the mechanical properties of materials undergoing deformation at a high rates of strain and for obtaining a constitutive relation for numerical modelling. It enables us to examine materials in the strain rate regime of 10^2 to 10^4 [1] . The classical SHPB can be utilised to test materials in compression loading [2, 3]. The SHPB later has been modified for tension and torsion conditions [4, 5, 6] . These modifications enable not only to specify the properties of materials in the field of high strain rate deformation, but also to examine the process of material fractures in various stress states.

The determination of stress–strain behaviour of the material being tested in a Hopkinson bar, whether it is loaded in compression or in a tensile bar configuration, is based on the same principles of one-dimensional elastic wave propagation within the pressure loading bars [7, 8] as shown in Fig. 1. A hollow striker which slides along the incident bar and impacts the transfer flange with a velocity V to produce the tensile load in the incident bar which is propagated into the transmitted bar via the specimen.
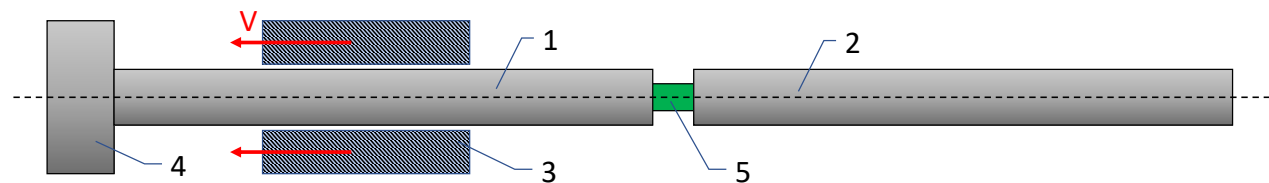
Figure 1: A design of the Split Hopkinson Tension Bar apparatus with a hollow striker based on the principle of one-dimensional wave propagation; 1 – the incident bar; 2 – the transmitted bar; 3 – the striker impacting on the transfer flange with a velocity equal to V; 4 – transfer flange; 5 - a specimen.

This paper provides a simpler design for a Split Hopkinson Tension Bar (SHTB) that allows for pulse durations greater than one millisecond with the use of a short Polyoxymethylene (POM) striker. Traditionally, Split Hopkinson techniques directly rely on wave propagation effects, achieving high strain rates call for long loading pulse durations which in turn require long striker (in meters scale). However, a practical problem appears when using long strikes: the striker needs to be guided in a concentric manner along the long axis of the incident bar to achieve the uni-axial stress state during loading. In this research we use only 750 mm long hollow POM striker to achieve a loading pulse of ≈ 1.15 ms, which otherwise is achieved by 3000 mm long aluminium hollow striker.

The duration of the pulse [9] is given by

$$\tau = \frac{2L}{C_0} \tag{1}$$

The Equation 1 shows that length L of the striker and pulse duration τ are directly proportional to each other and inversely proportional to the material wave velocity C_0. Having longer pulse duration ensures that

material yields and gives enough time to fully develop plastic deformation for material testing. Therefore, material wave velocity C_0 also plays a key role in deciding the pulse length which in our case has been modified.
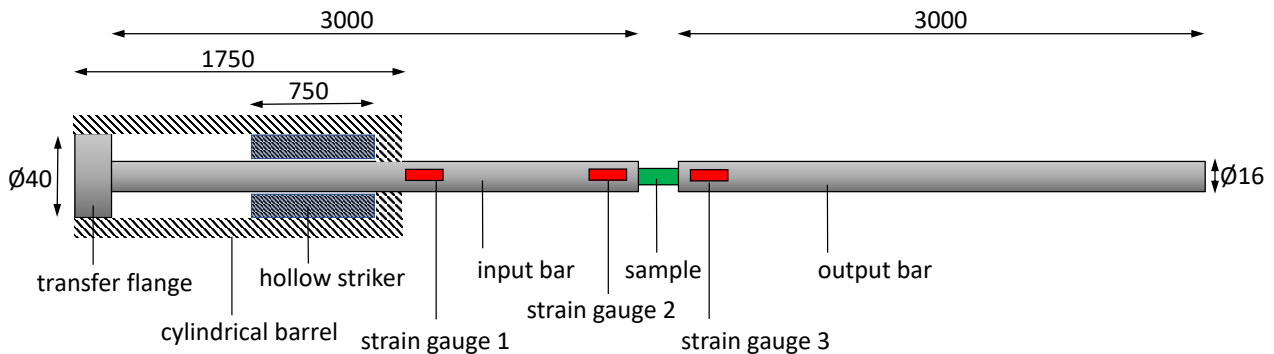
Figure 2: Sketch of the SHTB setup employed in this work. All dimensions are in mm. Input and output bars are 16 mm diameter and 3 meter long aluminium rods. The striker is a hollow POM tube of 40 mm outer diameter and 20 mm inner diameter. Two strain gauges on the input bar to measure the incident wave [ε_{inc}] and reflected wave [ε_{ref}] ,and one on output bar to measure the transmitted wave [ε_{tra}].

The new SHTB design employed in our work is sketched in Fig. 2 uses an 16 mm diameter EN 6060 Aluminium shafts of each 3 meter long for the input bar and output bar. The striker tube is a hollow POM shaft of length $L_s = 750$ mm with an outer diameter of 40 mm and an inner diameter of 16.1 mm. The striker rests of the shaft of the cylindrical barrel which also guides it axially along the long axis. The hollow striker which slides along the input bar and impacts the transfer flange to produce a tensile wave in to the input bar and propagates into the output bar via the specimen, resulting in the deformation of the specimen. To validate our new SHTB design we conducted a series of experiments on SS316L round notched metal specimens. The results of pulse optimisation using pulse shaping techniques, pressure-velocity plots *i.e.,* pressure supplied to the striker vs velocity gained by the striker, and example application of the setup with tension tests on SS316L will be given in the full article submission.

References

[1] H. Kolsky. "An Investigation of the Mechanical Properties of Materials at very High Rates of Loading". In: *Proceedings of the Physical Society. Section B* 62 (Oct. 1949), pp. 676–700.

[2] P. Baranowski, J. Janiszewski, and J Malachowski. "Study on computational methods applied to mod-ellingof pulse shaper in split-Hopkinson bar". In: *Arch. Mech.* 66.6 (2016), pp. 429–452.

[3] Leopold Kruszka, Mariusz Magier, and Mariusz Zielenkiewicz. "Experimental Analysis of Visco-Plastic Properties of the Aluminium and Tungsten Alloys by Means of Hopkinson Bars Technique". In: *Applied Mechanics and Materials* 566 (2014), pp. 110–115.

[4] Robert Gerlach, Christian Kettenbeil, and Nik Petrinic. "A new split Hopkinson tensile bar design". In: *Impact Engineering* 50 (Aug. 2012), pp. 63–67.

[5] D. Mohr and G. Gary. "M-shaped Specimen for the High-strain Rate Tensile TestingUsing a Split Hopkin-son Pressure Bar Apparatus". In: *Experimental Mechanics* 47 (Feb. 2007), pp. 681–692.

[6] Q. Xue, L. T. Shen, and Y. L. Bai. "A Review of the Torsional Split Hopkinson Bar". In: *Advances in Civil Engineering* 66 (Oct. 1995), pp. 5298–5304.

[7] George T. (Rusty) Gray. "Classic Split-Hopkinson Pressure Bar Testing". In: *ASM Handbook* 8 (2000). ISBN : 978-1-62708-176-4, pp. 462–476.

[8] Weinong Chen and Bo Song. "Split Hopkinson (Kolsky) Bar". In: *Mechanical Engineering Series (MES)* (2011).

[9] Marc Andre Meyers. *Dynamic behavior of materials*. John Wiley and Sons, New York, 1994.

Microscopic modeling of plasma sprayed ceramics under dynamic loading with the discrete element method

V. Longchamp[1,2,3*], J. Girardot[1], D. André[2], F. Malaise[3], I. Iordanoff[1]

[1]*Arts et Métiers Science et Technologie I2M UMR CNRS 5295, Esplanade Arts et Métiers , Talence, 33400, France*
[2]*Université de Limoges IRCER UMR CNRS 7315, 12 Rue Atlantis, Limoges, 87068, France*
[3]*CEA CESTA, 15 avenue des Sablières - CS60001, Le Barp cedex, 33116, France*

Keywords: Discrete Element Method, Microstructure, Air Plasma Spray, Ceramics, Shock

Absract

The macroscopic behavior of plasma sprayed ceramic coatings is greatly affected by their microstructure. A numerical model, based on the discrete element method, is proposed to perform high strain rate simulations in order to study the link between microsctrure and macroscopic properties. The real 3D microstructure of plasma sprayed ceramics, observed with a focused ion beam - scanning electron microscope, is used to generate digital twins. Dynamic compressive simulations are performed on these twins to identify their macroscopic response with respect to their microstructure.

Summary

Ceramic coatings are usually manufactured using an *Air Plasma Spray* (APS) process, which induces a specific porosity, in the form of voids and cracks. Their presence has a great influence on the final macroscopic properties of the coatings [1]. One noteworthy effects is their ability to mitigate mechanical shock waves [2]. However, the understanding of the link between microstructure and macroscopic properties remain limited, for instance homogeneized law used to their characterization still required a lot of complex experiments in order to be calibrated. The aim of this work is to predict the macroscopic properties of plasma sprayed coatings only from the observation of their microstructure. For this purpose, an approach based on the construction of digital twins of the ceramics at the scale of their microstructure is proposed. Dynamic compressive loadings are applied on these digital twins to study their macroscopic behavior.

To characterize the complex micro-cracks 3D network of APS ceramics, a *Focused Ion Beam - Scanning Electron Microscope* (FIB-SEM) [3] is used: this measuring instrument provides high-precision 3D visualizations (until 10^3nm^3 per voxel). From these visualizations, a methodology, derived from the work in [4], which is based on image processing and image analysis is proposed to identify and classify the microstructure components, namely the pores and the cracks. These components are reproduced exactly into a numerical model with a *Discrete Element Method* (DEM). This method is selected because it suits well to model heterogeneous media [5], to represent discontinuous phenomena such as multi-cracking damage that occurs in porous brittle materials [6] and perform dynamic simulation like shock wave propagation [7]. In DEM, a continuous medium is modeled with a compact set of spherical *discrete elements* (DE) that represent the bulk material in terms of volume and mass. These DE are linked together with mechanical bonds that transmit forces to represent the strength and mechanical properties of the media.

A modeling of the porosity according to its size facing the DE size is proposed: pores (bigger than the DE size) are modeled by suppressing DE, whereas cracks (smaller than the DE size) are modeled by suppressing bonds. This allows to get the best microstructure representation while limiting the number of elements required to have acceptable computation time. From this methodology, two kind of digital twins are created: i) 2D analogue of a full coating thickness and ii) 3D elementary volumes inside the coating. Dynamics simulations are performed on these twins: the mitigation of mechanical compressive wave (*cf.* Figure 1) and the creation of new cracks is studied. The 2D twins, although being an over simplification of reality, can be used to reproduce laser-induced shock waves experiments as it is able to model the full thickness of a coating

*Author for correspondence (vincent.longchamp@ensam.eu).
† Present address: Arts et Métiers Science et Technologie I2M UMR CNRS 5295, Esplanade Arts et Métiers , Talence, 33400, France

($> 500 \ \mu m$). For 3D twin, the total observable volume with FIB-SEM is limited (about $25 \times 25 \times 25 \ \mu m^3$) and only allow to represent a small part of the coating thickness. Nonetheless, dynamic compressions can be applied to study the local crack initiation and propagation induced by dynamic loadings. Quasi-static compressions are also used to identify macroscopic pressure-density relationship.
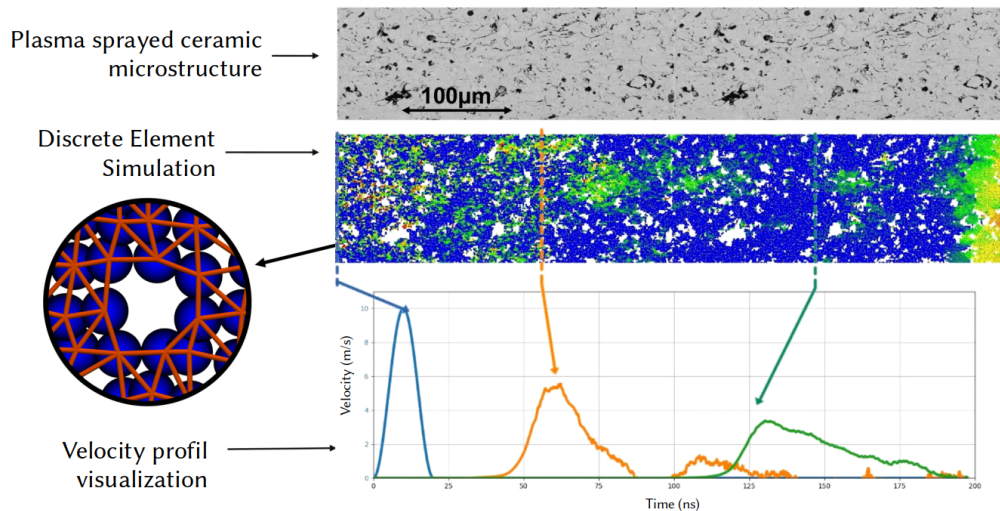
Figure 1: Illustration of the methodology: microsctructure modeling and dynamic compressive simulation with DEM

Overall, the first results demonstrate the suitability of the model to represent complex microstructure of plasma sprayed ceramics. Indeed, the simulations are able to reproduce macroscopic phenomena observed in the literature such as non-linear behaviors in compression and shock waves mitigation. Laser-induced shock waves experiments are planned to validate quantitatively these simulation. In addition, a particular attention will be paid to the representation of the local cracking to study its effect on macroscopic fracture and compaction.

References

[1] F. Kroupa *et al.*, 2002. "Nonlinear elastic behavior in compression of thermally sprayed materials," *Mater. Sci. Eng.*, vol. 328, no. 1-2, pp. 1–7

[2] D. Grady, 2004, "Analytic Solutions and Constitutive Relations for Shock Propagation in Porous Media," *AIP Conference Proceedings*, **vol. 706**, pp. 205–208

[3] J. A. Taillon *et al.*, 2018, "Improving microstructural quantification in FIB/SEM nanotomography," *Ultramicroscopy*, **vol. 184**, pp. 24–38

[4] S. Deshpande *et al.*, 2004, "Application of image analysis for characterization of porosity in thermal spray coatings and correlation with small angle neutron scattering," *Coatings Technology*, p. 11

[5] N. Ferguen *et al.*, 2019, "DEM model for simulation of crack propagation in plasma-sprayed alumina coatings," *Surf. Coat. Technol.*, **vol. 371**, pp. 287–297

[6] D. André *et al.*, 2013, "Using the discrete element method to simulate brittle fracture in the indentation of a silica glass with a blunt indenter," *Comput Methods Appl Mech Eng*, **vol. 265**, pp. 136–147

[7] Z. Jiang *et al.*, 2021,"Mechanical response and deformation mechanisms of porous PZT95/5 ceramics under shock-wave compression," *J. Eur. Ceram. Soc.*, p. 12

Effects of microstructure on mechanical behavior of multiscale porous alumina stressed up to high strain rates

Quentin HENRY[1], Jean-Benoît KOPP[1], Louise LE BARBENCHON[2], Antonio COSCULLUELA[3], Philippe VIOT [1]

[1]*Arts et Métiers Institut of Technology, Université de Bordeaux, CNRS, INRA, INP, I2M, HESAM Université, Esplanade des Arts et Métiers, 33400 Talence, France*
[2]*CNRS, INRA, INP, I2M, HESAM Université, Esplanade des Arts et Métiers, 33400 Talence, France*
[3]*CEA Cesta, CS 60001, Avenue des Sablières, 33116 Le Barp, France*

Keywords: Porous Alumina, Multiscale microstructure, X-ray Tomography, Mechanical behavior, Dynamic test.

Abstract: Within the framework of the development of protections for mobile structures (space transport systems, satellites, aeronautical transport systems, radomes, armored tanks, ...) or solutions for the protection of personnel against accidental or operational mechanical aggressions, manufacturers are seeking to improve the mechanical strength/mass ratio of onboard protections. Very often, this improvement of the mechanical strength/mass ratio leads to the search for the lowest possible densities of the constituent materials for these structures while maintaining sufficient mechanical performance [1]. Polycrystalline ceramics are of particular interest because they combine lightness and high mechanical performance in compression, allowing them to dissipate the mechanical energy accumulated during an impact, a shock or a blast [2]. The introduction of porosities in these materials allows considerable weight savings, while maintaining mechanical properties adapted to severe stresses [3]. The objective of this work is to evaluate the effects of the microstructure on the mechanical behavior of a quasi-brittle and heterogeneous material at small scales stressed up to high strain rates.

Heterogeneous aluminas were manufactured by a gel-casting process. Three shades of heterogeneous alumina have been manufactured: samples with a relative density of 80 % containing microporosities induced by sub-sintering but also samples with respectively a relative density of 80% and 40% containing mesoporosities induced by the addition of polymeric spheres (tab. 1). A dense one (98.5% of relative density) was also produced to serve as a reference (tab. 1). These alumina were finely characterized by different observation means in order to detect critical defects. The heterogeneous structure induced by the presence of porosities at different scales was observed by Scanning Electron Microscopy (SEM) in order to qualitatively analyze the morphology of porosities. These observations were coupled with X-ray microtomography in the case of samples with mesoporosities.

sample	sintering temperature	sintering time	relative density	type of porosity
dense	1530°C	9h	98.5 %	interstitial
80micro	1300°C	3h	79.8 %	microporosity
80meso	1530°C	3h	77.7 %	spherical mesoporosity
40meso	1530°C	3h	´39.2 %	spherical mesoporosity

Table 1: Manufacturing parameters and caracteristics of heterogeneous alumina sample.

Characterization tests were carried out over a wide range of strain rates (10^{-4} to 10^3 s^{-1}) to understand the effects of strain rate on mechanical properties on these heterogeneous alumina. Quasi-static uniaxial compression tests were be performed on a standard 250 kN tension/compression Zwick Roell experimental set-up coupled with a high speed camera (Phantom TMX 6410, 100 kHz) to observe fracture processes during testing. Dynamic compression tests were performed using steel Split Hopkinson Pressure Bar (SHPB) instrumented with a high speed camera (Phantom TMX 6410, 100 kHz). The test configuration (sample clamped between two half-diabolo shaped tungsten carbide compression plates) developed according to ASTM recommendations was used for both quasi-static and dynamic compression tests.

The observations show that the microstructure is strongly dependent on the manufacturing process. Depending on the type and amount of porosities introduced into the ceramic, it can be interconnected or not. Sub-sintering leads to a tortuous and interconnected microporosity observable at the grain scale (lower than 3 μm) qualified as "microporosity" (fig. 1.a). The addition of polymer spheres introduces quasi-spherical

*quentin.henry@ensam.eu
† Present address: DuMas, I2M, Esplanade des Arts et Métiers, Talence, 33400, France

mesopores with the majority of the pores diameter between 10 and 50 µm. These pores are qualified as "mesporosity". Some porosities can reach a diameter greater than 100 µm. For alumina with a relative density of 80 %, the pores are mainly isolated but some of them show interconnection which leads to non-spherical pores. For alumina with a relative density of 40 %, the pores are strongly interconnected by the presence of holes in the walls (fig. 1.b and c). Preliminary results in quasi-static regime ($\dot{\varepsilon} \approx 10^{-4} \ s^{-1}$) show that stress/strain curve is linear for all relative density. A small non-linearity just before fracture is observed for the sample with the lowest relative density (40%). This shows a quasi-brittle behavior rather than a brittle behavior like higher relative density samples (fig. 1.d). This change in mechanical behavior has been observed in the literature by Meille et *al.* [6]. In addition, results show the increase of porosity rate leads to a decrease of elastic modulus and compression strength. For a 40 % decrease in relative density (80 to 40 %), the compressive strength decreases by a factor of 5. For the same realtive density (≈ 80 %), the compression strength is higher for alumina with microporosites than for the one with mesoporosities. Pore morphology and/or size has an influence on the elastic properties. For low density alumina (relative density of 40 %), one main crack is observed thank to the high speed camera. On the contrary, porous aluminas with a relative density of 80% (micro and mesoporous samples) demonstrate multicracking mechanisms. All the identified parameters will allow to define and feed a behavioral law which will be integrated in a numerical model [7].
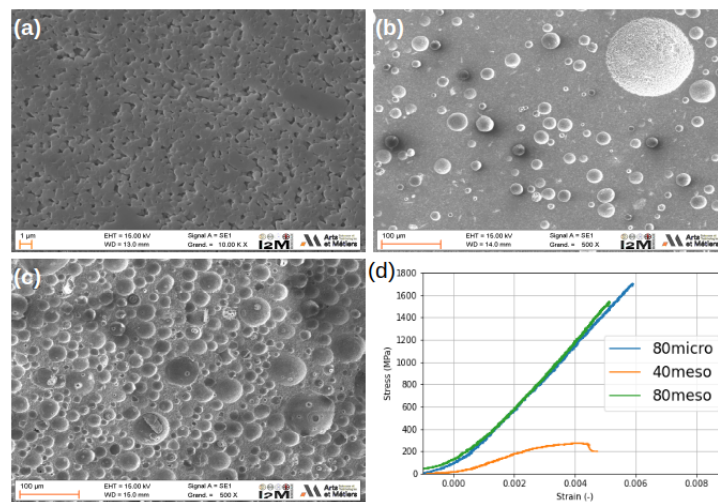

Figure 1: SEM observation of alumina with respectively a relative density 80% containing micropores (a), 80% containing mesopores (b), 40% containing mesopores (c) and stress/strain curves of these three heterogeneous aluminas (d).

References

1. M. Ashby and K. Johnson, Materials and Design. 2010 (doi)

2. E. Medvedovski. 2010. Ballistic performance of armour ceramics: Influence of design and structure. Part 1. *Ceramics International*. **vol 36**. 2103–2115. (10.1016/j.ceramint.2010.05.021)

3. B. S. M. Seeber. 2013. Mechanical properties of highly porous alumina foams. *Journal of Materials Research*. **vol 28**. 2281–2287. (10.1557/jmr.2013.102)

4. J. J. Swab. 2021. Dynamic Compression Strength of Ceramics: What was Learned from an Interlaboratory Round Robin Exercise? *Journal of Dynamic Behavior of Materials*. **vol 7**. 34–47.(10.1007/s40870-020-00264-6)

5. J. Lankford. 1998. The role of plasticity as a limiting factor in the compressive failure of high strength ceramics. *Mechanics of Materials*. **vol 29**. 205-218. (10.1016/S0167-6636(98)00023-4)

6. S. Meille. 2012. Mechanical properties of porous ceramics in compression: On the transition between elastic, brittle, and cellular behavior. *Journal of the European Ceramic Society*. **vol 32**. 3959–3967.(10.1016/j.jeurceramsoc.2012.05.006)

7. J. Meynard, A. Cosculluela, P. Pradel. 2023. Numerical simulations of the dynamic behavior of porous alumina ceramics. *In DYMAT Winter School 2023.* Aussois. France.

Considerations on the shear behavior of concrete-rock interfaces under dynamic loading

Badika Menes[1], Sophie Capdevielle[1], Matthieu Briffaut[2], and Dominique Saletti[1]

[1]*Grenoble INP (Institute of Engineering University of Grenoble Alpes), CNRS, Université Grenoble Alpes, 3SR,38000 Grenoble, France*
[2]*Laboratoire de Mécanique, Multiphysique, Multiéchelle-LaMcube-UMR 9013, CNRS, Centrale Lille,University Lille, 59000 Lille, France*

Abstract

To investigate the shear behavior of concrete-rock interfaces under dynamic loading, a modified punch through shear test designed with concepts similar to the direct shear test was introduced. This test uses a confinement system adapted to produce confinement stress representative of the low normal stresses encountered in concrete gravity dams. The shear loading is applied using the Split Hopkinson Pressure Bar to simulate high strain rate events. Furthermore, a static version of this test was also adapted to compare the shear behavior under static and dynamic loading. Preliminary results show that the confinement system is suitable to produce low confinement stress.

Introduction

Most recommendations on the design and stability assessment of concrete gravity dams are based on the literature on the shear behavior of rock-rock interfaces (rock joints) and do not consider the peculiarities of the concrete-rock interfaces. For example, they do not usually take into account the influence of bond strength, which is shown to be very influential on the shear resistance of the concrete-rock interfaces [1, 2, 3]. Another aspect not properly addressed is the resistance of these structures to a dynamic loading.

Geotechnical structures such as concrete gravity dams might experience in their lifetime dynamic loading, caused by explosions, impacts, or seism. This way, it is important to understand how these high strain rate events influence the sliding resistance of the concrete-rock interface as these structures usually experience failure by sliding at the interface. For this reason, an experimental campaign is underway to investigate the shear behavior of bonded concrete-rock interfaces under dynamic loading. This study is perhaps one of the first in the literature to investigate the shear behavior of bonded concrete-rock interfaces under dynamic loading.

In this paper, we present the preview of this experimental study designed to investigate the shear behavior of bonded concrete-rock interfaces submitted to low confinement stresses similar to those experienced by concrete gravity dams and under static and dynamic loading.

Methods and materials

Experimental setup

The investigation of the shear behavior of bonded concrete-rock interface stems from the literature on the shear behavior of rock-rock interface (rock joints), which is usually carried out using the direct shear test. The direct shear test is performed in two steps; the first one consists of applying a loading normal to the

interface and maintaining this loading throughout the test, and the second step consists of applying the shear loading parallel to the interface. Here the interface is the region formed by the superposition of two slabs located one above the other.

The experimental approach devised to investigate the shear behavior of bonded concrete-rock interfaces under dynamic loading maintains the concepts of the direct shear test. In the first step, the confinement loading is applied using a confinement ring, this initial confinement is maintained throughout the test. In the second step, to apply the shear loading with strain rates representative of seismic or blasting events the Split Hopkinson Pressure Bar (SHPB) is selected. The SHPB can apply shear loading with strain rates varying from 10^1 - $10^4/s$. The SHPB setup used is composed of one input bar and two output bars (**Figure 1**). This setup is adapted to the two configurations of the sample used which is either a rock slab with concrete cast in the two extremities or two rock slabs at the extremities with concrete cast in between. This way the incident bar impacts the sample (middle part) generating a pulse wave that shears the two concrete-rock interfaces and is recorded in the output bars. This test is a version of the Punch through shear test (PTS).
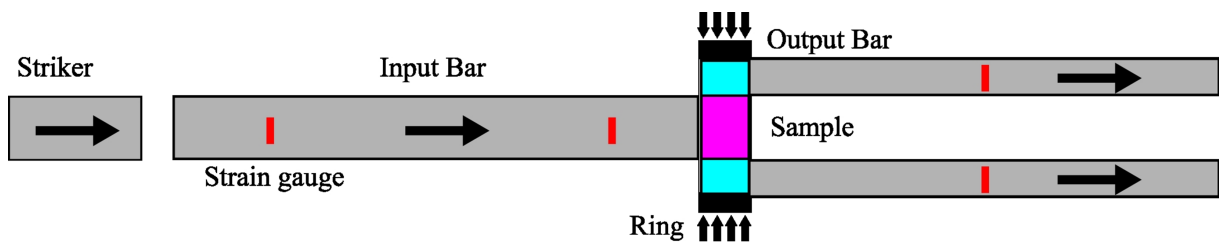

Figure 1: Punch through shear test - Dynamic

The ring used in the PTS test is a modified version of the ring presented in [4, 5]. The first modification consisted of changing based on numerical modeling (finite element method) the geometry of the ring reducing its thickness to accommodate more elastic deformation when compressed with a lower magnitude loading (below 1.5 MPa). And the second modification of the ring consisted of changing the material used in the manufacture of the ring from steel to aluminum to enhance further the ability to deform elastically when submitted to lower compression loading. These modifications are crucial to apply lower confinement stress to the specimen and to generate significant elastic deformation to the ring such that it can be continuously recorded by the strain gauges.

The ring is instrumented by four strain gauges wired in quarter bridges that record the variation of strain during the confinement step and during the shearing step. The record of the strain is later converted to the confinement stress applied to the specimen thanks to a calibration process. The confinement of the sample using the ring is carried out in three steps. First, the ring is compressed within its elastic limit, second, the sample is introduced to the deformed ring, and last the compressive load applied to the ring is released, which causes the ring to deform elastically back to its initial state, unable to do so it confines the sample (**Figure 2**).
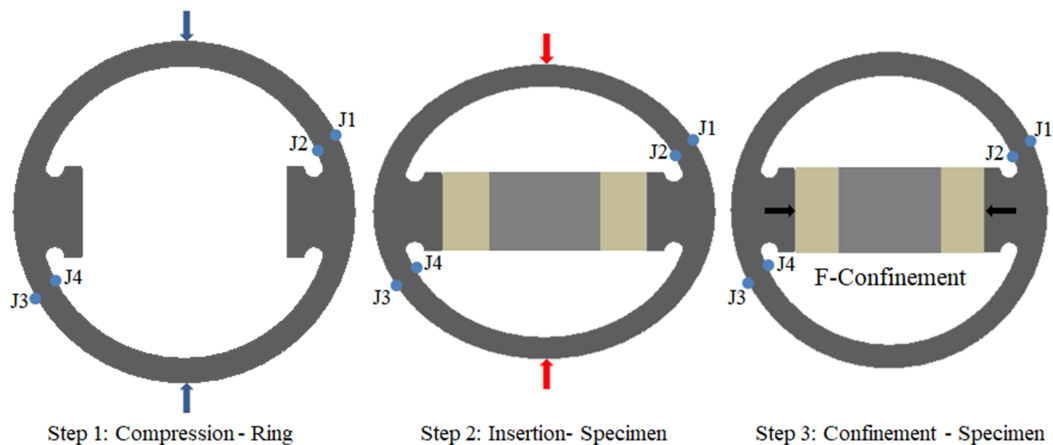

Figure 2: Confinement system

*Author for correspondence (badikakm@univ-grenoble-alpes.fr).
† Present address: Laboratoire 3SR, Université Grenoble Alpes, Grenoble, 38400, France.

To assess the influence of the dynamic loading on the shear behavior of concrete-rock interfaces, it is reasonable to compare the results of these tests with the one obtained using a similar PTS test but with a static shear loading. For this reason, the Punch through shear test presented above was modified replacing the SHPB with a static shear loading applied using a hydraulic press (**Figure 3**).
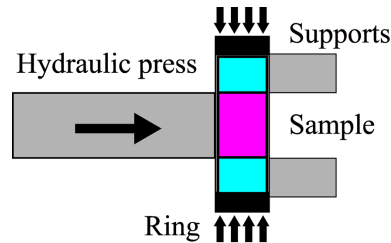

Figure 3: Punch through shear test - Static

Materials

The geometry of the sample used in these tests is 70x30x30 mm^3 , with the middle part of 40x30x30 mm^3 and the extremities of 15x30x30 mm^3 each.

In the large experimental campaign that this paper is part of and which is in progress, two types of rocks are used; Granite (UCS: 130 MPa) representing hard rocks and Limestone representing soft rocks. The surfaces of the rock slabs forming the concrete-rock interface are selected such that they represent different classes of roughness, which are smooth interfaces, bush-hammered interfaces, and naturally rough interfaces. This is to appraise the influence of the roughness on the shear strength of interfaces under dynamic loading.

The concrete used to form the sample is the R30A7, which has a uniaxial compressive strength of approximately 30 MPa after 28 days of healing.

Preliminary results

The qualitative assessment of the two tests performed is hereby presented. The tests consist of a PTS test under static and dynamic loading. Each sample used is composed of a granite slab with two opposite sides naturally rough allowing the formation of two naturally rough concrete-granite interfaces. The concrete cast on both extremities is the R30A7.

Static test

The results of the static test are displayed in **Figure 4**. During the test, the shear behavior increases almost linearly in time, reaches a first peak shear strength, and then drops rapidly, thereafter there is an increase in the shear stress until the completion of the test. In terms of the confinement stress, the confinement load has remained constant until the drop of the shear stress after the first peak, thereafter the shear stress increases throughout the rest of the test.

From this test, it is possible to verify that the confinement system performs well in the PTS test under static loading. This means the initial confinement load applied to the interfaces by the ring remains constant throughout the transfer from the confinement setup to the setup to apply static shear load. Furthermore, the ring is capable to apply very low confinement stress.

The increase of the stresses after the sequence of the first peak and the first drop of the shear stress could be related to the combination of different aspects of the tests. First, during shear loading the interfaces tend to dilate to overcome the asperities of the rough surfaces of granite, this dilation is resisted by the ring, increasing the confinement stress. Second, the result of the PTS test using static shear loading is an expression of the average shear evolution at both interfaces, which makes it difficult to separate the influence of each and the interaction between them.

*Author for correspondence (badikakm@univ-grenoble-alpes.fr).
† Present address: Laboratoire 3SR, Université Grenoble Alpes, Grenoble, 38400, France.
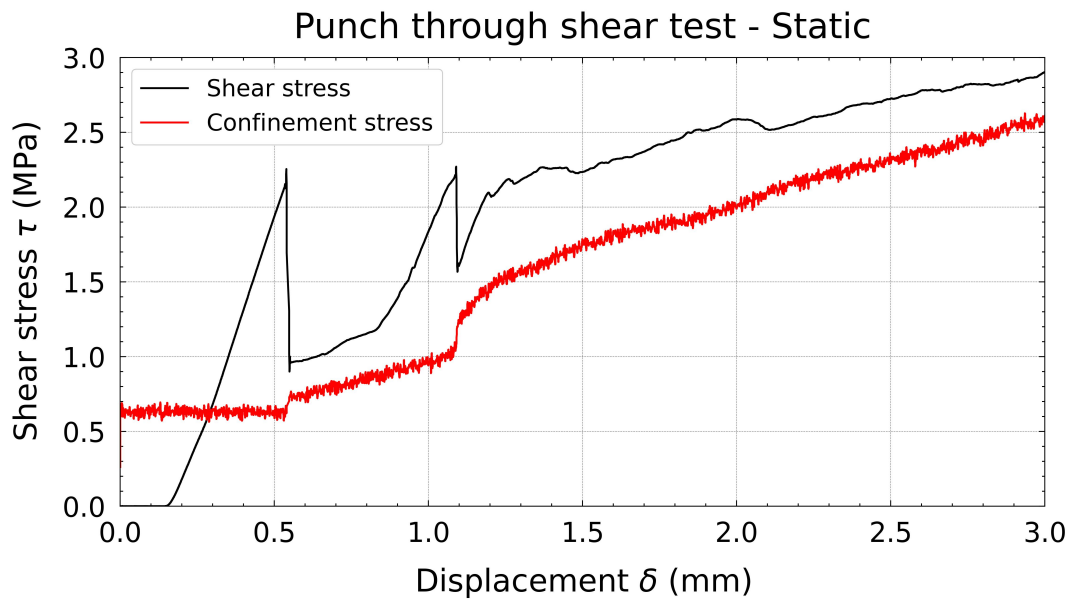
Figure 4: Shear evolution - Static

Dynamic test

The results of the dynamic test are presented in **Figure 5**. Unlike the PTS static test, the pulse wave recorded in the two output bars helps discriminate globally the shear stress evolution in both interfaces. In these interfaces, the shear stresses increase in time to reach a peak and then drop to zero. Visual assessment of the sample in the post-mortem shows that both interfaces failed mostly along the interfaces with less damage in either concrete or granite.

In terms of the confinement stress, unlike the static test, the confinement stress increases almost immediately after the beginning of the shear loading. By the instant, the shear stress reaches its peak, the confinement stress had approximately tripled its initial magnitude. The increase of the confinement stress could be related to the same combination of interdependent events identified in the static test; resistance to dilation and the influence of shear evolution of one interface to the other.

Figure 5: Shear evolution - dynamic

*Author for correspondence (badikakm@univ-grenoble-alpes.fr).
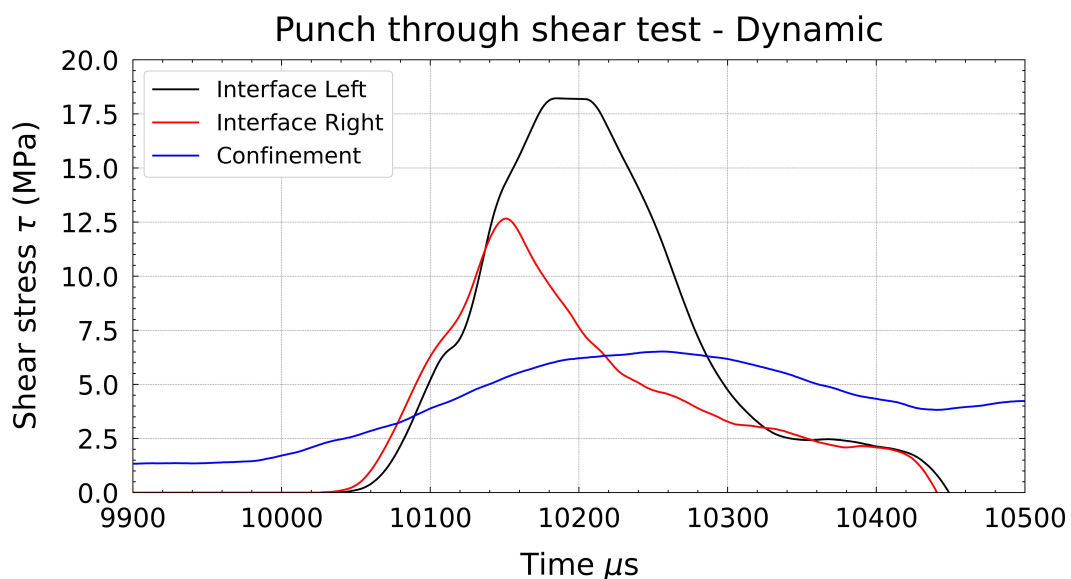† Present address: Laboratoire 3SR, Université Grenoble Alpes, Grenoble, 38400, France.

Summary and perspectives

To investigate the shear behavior of concrete-rock interfaces under dynamic loading, a modified version of the Punch through shear test was presented. This test maintains the concept of the direct shear test, with the normal loading, applied using a confinement ring designed to reproduce lower confinement stress representative of confinement stress encountered in concrete gravity dams, and the shear loading applied using the SHPB to reproduce high strain rate events. An equivalent test with static shear loading was used to compare the shear behavior of concrete-rock interfaces under static and dynamic loading. Two preliminary tests were presented, one in static and one in dynamic. These tests help fine-tune the large experimental campaign underway by confirming that the confinement system designed is suitable to reproduce low confinement stress. Furthermore, these tests help shift the focus of the type of the interfaces tested, encouraging a gradual increase in complexity of the roughness of the interfaces; smooth interfaces, bush-hammered interfaces, and naturally rough interfaces.

References

1. Saiang, David and Malmgren, Lars and Nordlund, Erling. 2005. Laboratory Tests on Shotcrete-Rock Joints in Direct Shear, Tension and Compression. *Rock Mech. Rock Engng* **38**, 275–297. (https://doi.org/10.1007/s00603-005-0055-6).
2. Krounis, Alexandra and Johansson, Fredrik and Larsson, Stefan. 2016. Shear Strength of Partially Bonded Concrete-Rock Interfaces for Application in Dam Stability Analyses. *Rock Mech Rock Eng* **49**, 27112722. (https://doi.org/10.1007/s00603-016-0962-8).
3. Badika, Menes and El Merabi, Bassel and Capdevielle, Sophie and Dufour, Frederic and Saletti, Dominique and Briffaut, Matthieu. 2022. Influence of Concrete–Rock Bonds and Roughness on the Shear Behavior of Concrete–Rock Interfaces under Low Normal Loading, Experimental and Numerical Analysis. *Appl. Sci.* **12**, 5643. (https://doi.org/10.3390/app12115643).
4. Abdul-Rahman, Reem and Saletti, Dominique and Forquin, Pascal. 2021. Experimental study of the static and dynamic behavior of pre-stressed concrete subjected to shear loading. *Engineering Structures* **Volume 234**, 111865. (. https://doi.org/10.1016/j.engstruct.2021.111865).
5. Forquin, Pascal and Abdul-Rahman, Reem and Saletti, Dominique. 2022. A novel experimental method to characterise the shear strength of concrete based on pre-stressed samples. *Strain***12**, 58(2), e12407. (. https://doi.org/10.1111/str.12407).

Wavy flyer plate test for shockless plate-impact application.

J. Genevois[1a], P. Forquin[1b], J.-L. Zinszner[2]

1Univ. Grenoble Alpes, Grenoble INP, CNRS, 3SR laboratory, BP 53, 38041 Grenoble Cedex 9, France
2CEA, DAM, GRAMAT, F-46500 Gramat, France
[a]*julia.genevois@univ-grenoble-alpes.fr,*[b]*pascal.forquin@univ-grenoble-alpes.fr,* [c]*Jean-Luc.zinszner@cea.fr*

Keywords: Compression, High loading-rates, Plate-impact, Ceramic, Lagrangian analysis

Abstract: In the present work, wavy-machined flyer plate produced by chip-forming were designed to be used in shockless plate-impact and compared to planar plate-impact. According to the velocity profiles measured on the rear face, whereas a sharp rising edge is noted in case of flat contact (planar plate-impact), a smooth rising edge is obtained in the case of shockless plate-impact test. Considering a target made up of two ceramic plates of different thicknesses this kind of test provides the possibility to conduct a Lagrangian analysis of data.

1. Introduction

Ceramic materials are widely used in armour or protective structures. In these conditions they experience extreme damage, micro-plasticity and fragmentation mechanisms. To fully understand these behaviours, characterization under high-strain-rate compression needs to be conducted. Several experimental techniques are used to investigate the dynamic behaviour of ceramic under high compressive loading and one of them is the plate-impact testing technique. During this test, a metallic flyer plate hits the desired target, and some mechanical properties such as the HEL (Hugoniot Elastic Limit) as well as the Hugoniot curve of the material can be deduced thanks to the velocity profile measured at the back of the target. Nevertheless, this test has the inconvenient of not providing a controllable loading-rate in the target and the hardening behaviour cannot be directly deduced. The high-pulsed-power technology, such as the GEPI machine, provides the possibility to perform Lagrangian analysis, which gives access to the whole loading path of the material whereas only one point on this loading path can be obtained from one plate impact experiment [1-2]. This method, based on the integration of the equations of conservation of mass, momentum and energy does not need any assumption on the behaviour of the material. The principle is based on a comparison of velocity signals obtained considering two plates of different thicknesses.

An alternative to the GEPI machine in order to apply a Lagrangian analysis is the use of a wavy-machined flyer plate (Fig. 1) impacting a buffer plate taped to two ceramic plates of different thicknesses as it is proposed in [3]. However, such test requires the different parts to be well-sized and the flyer and buffer materials to be carefully selected. Indeed, the yield strength of both plates needs to be high enough. Steel being easy machined and providing high yield strength, it was decided to use this kind of metal. Given the very high impact speed required to test ceramics in compression (over 800 m/s), steel without phase transformation needs to be considered.
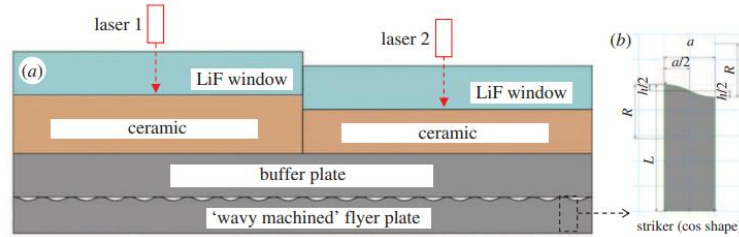
Figure 1: Experimental technique based on a wavy-machined flyer plate that produces a pulse-shaping effect in order to perform Lagrangian analysis [3].

2. Experimental work

For these purpose, planar plate-impact and shockless plate-impact experiments were first conducted considering only a buffer plate made of steel as target. "Classical" planar plate-impact tests with flyer and buffer plates made of the same steel were conducted at various impact speeds up to about 900 m/s. The experiment performed with 316L steel reveals that this steel does not exhibit any phase transformation in such loading conditions (Fig. 2a, planar curve). It is the reason why this steel was used to make flyer and buffer plates in the experiments conducted with ceramic target.. Next, a plate impact test was conducted considering a 316L wavy-machined plate as flyer plate. The wavy-machined surface is characterised by a wave period of 2 mm and a height of wavy surface of 0.5 mm. A flat plate made of the same steel was used as target. The velocity profile measured on the target rear face shows a rising time about 0.4 µs as illustrated in Fig. 2a (wavy flyer curve).

In the next experiment, a SiC ceramic called Forceram was used as target material. First, a planar plate-impact was used by using a flat 316L plate as flyer plate directly projected against the ceramic plate. The velocity profile measured on the ceramic rear face shows a rising time about 0.45 µs as illustrated in Fig. 2b (planar curve). In the next experiment, a wavy-machined flyer plate was launched against a target made of 316L buffer plate taped on a SiC ceramic plate. . A rising time about 1.2 µs is noted in the velocity profile measured on the ceramic rear face (Wavy flyer, Fig. 2b).
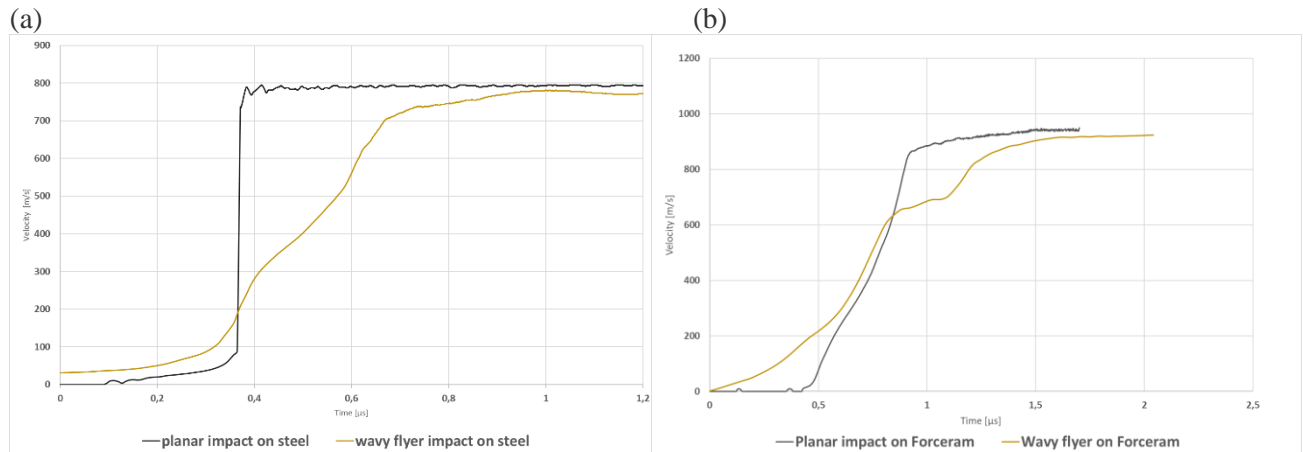
Figure 2: Comparison of the velocity profiles measured on 316L steel (a) and Forceram ceramic (b) of planar plate-impact and pulse-shaped plate-impact configurations for an impact speed around 800m/s.

In a second stage, 3D-printed flyer plates were considered to explore the loading ramp generated by the wavy plyer plate considering different manufacturing processes. One of them is the 3D filament printing. The wavy flyer plate built by this technology was tested under plate impact and the result was compared to the previous experiments. The results show that 3D printed buffer tend to induce a longer rising time that manufactured one. Moreover 3D printed steel offers more possibility for the flyer plate geometry so more complex flyer plate shape could be developed in the future.

Conclusion

The present experimental work aims to provide a first experimental validation of the use wavy-machined plate as flyer plate for plate impact test in view of generating smooth rising edge. After careful selection of steel to be used as material of both flyer plate and buffer plate, plate impact tests with wavy-machined flyer plate were conducted. The velocity profile measured on the target rear face confirms that this technology can provide a pulse-shaping effect due to the "wavy-shape". This effect leads to a smooth loading pulse applied to the sample with a much longer rising time compared the one observed in planar plate-impact. This loading pulse should offer the possibility to perform a Lagrangian analysis of data in which the sample's axial stress-axial strain response might be obtained based on two measurements of particle velocity on the rear face of two ceramic tiles of different thickness but both put in contact with the buffer. An experimental validation of this possibility constitutes the next step of this experimental work.

References :

[1]   J.L. Zinszner, B. Erzar, P. Forquin. (2017) Shockless characterization of ceramics. In: Casem D., Lamberson L., Kimberley J. (eds) Dynamic Behavior of Materials, Volume 1, pp 229-236, DOI: /10.1007/978-3-319-41132-3_32. Book series: Proceedings of the Society for Experimental Mechanics Series, Springer.

[2]   J.L. Zinszner, B. Erzar, P. Forquin. (2018) Shockless Characterization of Ceramics Using High-Pulsed Power Technologies, DOI: 10.1002/9781119579311.ch12, In book: Dynamic Damage and Fragmentation. Edited by Lambert D., Pasiliao C., Erzar B., Revil-Baudard B., Cazacu O., Civil engineering and Geomechanics series, Wiley.

[3]   P. Forquin, J.-L. Zinszner. (2017) A pulse-shaping technique to investigate the behaviour of brittle materials subjected to plate-impact tests. Phil. Trans. R. Soc. A 20160333. DOI: 10.1098/rsta.2016.0333.

A novel shear device for testing mineral-bonded composites under high strain-rates

Ahmed Tawfik*[†], Cesare Signorini[†], Viktor Mechtcherine[†]

[†]*Institute of Construction Materials, Technische Universität Dresden, 01062 Dresden, Germany*

Keywords: Split-Hopkinson tension bar, Impact shear, SHCC, Shear device, DIC, Confinement

1. Introduction

Mineral-bonded composites such as strain-hardening cement-based composites (SHCC) represent promising class of materials for improving the resistance of concrete structures against highly dynamic loading regimes. Under tensile loading, their behaviour features high pre-peak tensile ductility and strain capacity of up to 5%. Behaviour of SHCC have been extensively studied under tension, but is still scarcely investigated under shear loads, especially in dynamic regimes. Development of direct shear experimental setups has always been a challenging task given the several parameters influencing failure behaviour, e.g. specimen and notches geometry, shear span length, confinement level, etc. Furthermore, inducing shear stresses into the specimen and achieving a governing shear sliding failure mode (II) is required. The complexity becomes even higher when dynamic shear setups are required, as the influence of structural inertia on the apparent response of the tested specimen becomes considerable and should be accounted for. In addition to that, achieving a uniform stress state at high strain-rates is a complicated task even for impact tension experiments.

2. Shear device in a Split-Hopkinson tension bar

A novel mechanical shear testing device has been developed by the authors to enable shear testing of mineral-bonded cementitious composites at different strain-rate levels. The shear device consists of two metal adapters that accommodate a rectangular prismatic double-shear specimen [1]. The device allows dynamic shear testing by integrating it into a gravitational Split-Hopkinson Tension Bar (SHTB), where each metal adapter is connected, through a threaded connection, to the input or the transmitter bar. The development process of the shear device consisted of both geometrical development and material optimization of each adapter, such that the influence of the device on the wave propagation, in the SHTB, is limited and quantified. For shear testing at quasi-static regimes, the shear device could be integrated to any universal hydraulic testing machine. The concept of the shear device is based on the well-known Punch Through Shear (PTS) configuration, where the only difference here is that the shear specimen is punched/pushed from its sides and fixed from the middle and not the opposite, as in usual PTS loading configuration. One important feature of the developed device is that it allows optical monitoring of the fracture process of the specimen throughout the static or dynamic experiment. This is carried out through recording of the two shear zones, where cracks are expected to develop and failure to occur, with the help of 3D-stereo camera systems. This allowed accurate derivations of the specimens' displacements and modes of failure through further processing and analysing of the acquired frames by Digital Image Correlation (DIC).

3. Shear experimental results

Mortar and SHCC specimens were tested, in both quasi-static and impact regimes, using the manufactured shear device, where several parameters influencing the shear behaviour and mode of fracture of the specimen, such as confinement, shear span length (a), and notches positions, geometry, and depth, were investigated.

Experimental results showed that shear specimens tested with no confinement failed with a dominant tensile failure (mode I), while when confinement was applied, a dominant shear fracture (mode II) was obtained. In the latter case, small tension cracks formed at the locations of the maximum principle tensile stresses, but were prevented to grow further. Confinement was applied by gluing the specimen to the shear device at all common interfaces, which prevented any rotations or lateral dilation of the shear specimen during the experiment, clearly favouring the required mode II fracture. With respect to the 20 mm depth of the shear specimen, the notches depth influenced the mode of failure as well. Specimens with small notches depths, 3 mm, resulted in a compressive failure. Meanwhile, specimens with deeper notches, 7 mm, resulted in a shear sliding failure which makes it more reliable in assessing the shear parameters of the material tested. Two shear span lengths (a) were tested; 5 mm and 2 mm. The smaller shear span resulted, indeed, in a smaller shear span-to-depth ratio (a/d) fostering a favourable shear sliding failure and vertical shear cracks. By comparing the shear behaviour of the mortar and SHCC specimens, no difference in the apparent maximum force between the two materials was detected. The only difference was in the post-peak behaviour, at which the presence of fibres in SHCC specimens contributed to a relatively more ductile failure than mortar specimens. A dynamic increase factor (DIF) of around 1.5 was obtained for mortar and SHCC. Such DIF is much influenced by structural inertia due to the acceleration of the massive metal adapters along with the broken sides of the specimen. This problem is currently being investigated using FEM.

4. Shear device optimization

Although the developed shear device resulted in the required direct shear mode of fracture, the relatively big mass of the adapters influenced the wave propagation in the SHTB such that stress equilibrium was not achieved. This also hindered the ability to apply the one-dimensional wave propagation theory. Furthermore, applying confinement through gluing the specimen to the device does not enable measuring the level of confinement being applied. Accordingly, the shear device was further optimized such that its mass was reduced so its influence on the wave propagation significantly decreased. An appropriate pulse shaping technique was selected and along with the optimized shear device, a uniform stress state (stress equilibrium) was attained. The optimized shear device was threaded to accommodate mechanical screws which could be used to apply confinement to the shear specimen by the means of local forces applied perpendicularly to the longitudinal axis of the shear specimen. The amount of confinement is defined by the torque level applied to the mechanical screws. 1 mm thick metal plates are glued to the specimen, at the locations where the screws apply the load, so that any local damage is avoided.

Quasi-static and impact shear experiments on SHCC specimens were conducted using the optimized shear device. Results from impact experiments confirmed that the influence on the wave propagation was clearly reduced using the optimized shear device, by comparing the waves on both input and transmitter bars, where a state of stress equilibrium was attained. This was also supported by the increased rise time of the input wave induced due to rubber pulse shapers. Furthermore, results from both quasi-static and impact experiments showed that the failure mode depended on the amount of compressive force applied by the mechanical screws. Low applied compressive forces resulted in a governing tensile/bending failure, while a relatively higher compressive forces resulted in a compressive fracture. A shear fracture mode was reached by applying an optimum level of confining forces. Such fracture modes were illustrated by DIC analysis. Fig. 1 illustrates the optimized shear device in the SHTB.

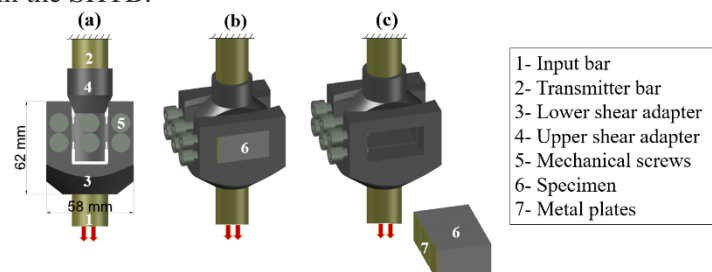**Figure 1 : Optimized shear device integrated between the SHTB bars (a) in 2D, (b) in 3D, and (c) along with the shear specimen.**

[1]   A. Tawfik, I. Curosu, G. Alsous, and V. Mechtcherine. 2022. A testing setup for investigating quasi-ductile and strain-hardening, cement-based composites (SHCC) under impact shear loading. *Int. J. Impact Eng.***167***,104280.(* doi.org/10.1016/j.ijimpeng.2022.104280*)*

Modern Direct-Impact Hopkinson Bar testing

Georg C. Ganzenmüller[*] and Puneeth Jakkula

Albert-Ludwigs-Universität Freiburg, Sustainable Systems Engineering, INATECH, Emmy-Noether Str. 2, 79110 Freiburg, Germany

Keywords: Hopkinson Bar, low impedance materials, dynamic equilibrium

Abstract:
We describe the implementation of a direct-impact Hopkinson bar, suitable for investigating the evolution
Author for correspondence georg.ganzenmueller@inatech.uni-freiburg.de. the force equilibrium in low-impedance materials. This compact design makes extensive use of off-the-shelf components. With polycarbonate as the bar material, a long pulse duration of 2.6 ms is achieved for an overall length of only 5 m, allowing to compress comparatively large specimens to high strains. In contrast to existing setups, both striker and output bar are instrumented with strain gauges to monitor force equilibrium. The absence of an input bar allows to monitor force equilibrium more accurately. The measuring principle is applied to low-density polyurethane foams, where it is demonstrated that unexpected compaction behaviour under dynamic loading can be explained by absence of dynamic equilibrium. This result could not have been reached using conventional Hopkinson Bar setups due to insufficient accuracy of dynamic equilibrium measurement.

1. Introduction

Dynamic testing of soft materials with low-density and little stiffness has traditionally been challenging [1]. The root of the problem causing the difficulty is that dynamic equilibrium of force is required for accurate force measurements during the experiment. This means that the stress state measured on either side of the specimen during uni-axial loading must be equal if the measurement is going to be representative of the bulk material behaviour. Naturally, during impact loading of a specimen emanating from one side only, the stress state requires a certain time to propagate through the specimen and establish dynamic equilibrium. This time depends on the specimen's dimensions, and its elastic wave speed, c_0. Additionally, the ratio of acoustic impedances, $z = \varrho c_0$, where ϱ is the mass density, between the specimen and its mechanical boundaries plays a role, as elastic wave transmission and reflection effects depend on this ratio [2]

Here, we are concerned with a modification of the split Hopkinson pressure bar (SHPB) [3], where the specimen is sandwiched between two slender bars. In the predominately used configuration of this setup due to Kolsky [4], a third bar, the so-called striker, impacts the first bar, which is termed the input bar. An elastic wave is created due to the impact and propagates via the input bar through the specimen, and into the output bar. Impedance differences between bar material, typically a metal, and the specimen, cause wave amplitude changes and effect compression of the specimen. The stress state in the input and output bars are inferred from strain gauge measurements, assuming a constant Young's modulus. From the stress in the bars, the forces acting on the specimen are calculated.

This approach has proven extremely successful for the dynamic characterization for metallic materials. However, it is limited in applicability to low-impedance materials for two reasons: the small force amplitude due to low specimen strength is challenging to resolve accurately on the comparatively stiff metallic bars, and the large impedance mismatch between specimen and bar material necessitates long equilibration times before accurate force readings can be obtained.

The approach presented here is based on a direct-impact Hopkinson bar. Here, no separate striker is required as the input bar itself is accelerated towards the specimen and serves as the striker. We also employ polymer bars but show that the choice of polycarbonate, together with short distances between strain gauges and specimen/bar interface, leads to negligible errors in the force measurement due to wave attenuation and dispersion. Additionally, the absence of a dedicated striker means that two nearly identical waves travel into the input and output bars. Thus, measurement of the evolution of dynamic force equilibrium becomes more accurate because wave superposition between the incident and reflected wave, as present in the classic SHPB, does not pose a problem. We note that we are not the first to pursue the general idea of a direct-impact Hopkinson bar using a striker that is instrumented with a strain gauge: Govender and Curry [5] presented this layout before with polymer bars. Hiermaier and Meenken [6] employed a metal input bar but introduced the idea of using piezoelectric foil gauges on both sides of the specimen to enhance force resolution in a direct impact configuration.

For demonstration purposes, we investigate polyurethane (PUR) foams with different densities in the range of 80 -- 240 kg/m³. We intentionally consider specimens with a length of 20 mm, which is far too long by SHPB standards, as this length implies that significant time is required to reach equilibrium. Therefore, we do not study a pure material behaviour, but a structural effect. For foams, it can be argued that these are structured materials for any size of specimen. Therefore, measured mechanical properties will depend on the size of the specimen and hence cannot straightforwardly be extrapolated to full-scale objects. Our specimens exhibit the peculiar behaviour of saturation of dynamic strength increase at high rates of strain, ~500 /s, or even negative strain rate sensitivity in case of the lowest density. The direct-impact Hopkinson bar presented here is well suited to investigate this phenomenon as it features a long pulse duration. Additionally, the high force sensitivity allows the development of dynamic force equilibrium to be accurately studied, or even whether it is achieved. We link the observed features in the force signals to an analysis of strain rate distribution over the specimen. This approach indicates that the apparent negative strain rate sensitivity is accompanied by a structural collapse front.

References:
1. Song, B.; Chen, W. 2005. Split Hopkinson Pressure Bar Techniques for Characterizing Soft Materials. *Latin American Journal of Solids and Structures* **2**, 113–152
2. Meyers, M.A. 1994 Dynamic Behavior of Materials. *John Wiley & Sons*.
3. Hopkinson, B. X. 1914. A Method of Measuring the Pressure Produced in the Detonation of High, Explosives or by the Impact of Bullets. *Philosophical Transactions of the Royal Society of London. Series A.* **213**, 437–456
4. Kolsky, H. 1949. An Investigation of the Mechanical Properties of Materials at Very High Rates of Loading. *Proc. Phys. Soc. B.* **62**, 676–700
5. Govender, R.A.; Curry, R.J. 2016. The "Open" Hopkinson Pressure Bar: Towards Addressing Force Equilibrium in Specimens with Non-Uniform Deformation. *Journal of Dynamic Behavior of Materials* **2**, 43–49
6. Hiermaier, S.; Meenken, T. 2010. Characterization of Low-Impedance Materials at Elevated Strain Rates. *The Journal of Strain Analysis for Engineering Design.* **45**, 401–409

High strain rate multi-axial loading of DP780 for CrachFEM material modeling

Pundan K Singh*[1,2], Abhishek Raj[1], Rahul K Verma[1], Lakshmana C Rao[2]

[1]*Research and Develoopment Division, Tata Steel Ltd, Jamshedpur 831001, Jamshedpur (India)*
[2]*Department of Applied Mechanics, Indian Institute of Technology, 600036, Madras (India)*

Keywords: ductile fracture, shear fracture, crash, CrachFEM, DP780, high strain rate

Abstract

Correct prediction of failure during crash loading scenario in a simulation is important to evaluate formed part and performance both at component and vehicle level. However, the situation of fracture has become complicated due to the progressive use of high strength grades since they fracture with or without any localized necking. This requires a comprehensive experimental program to characterize the material for equivalent plastic strain at fracture at specimen level. Initial work is aimed at characterizing DP780 (1.8mm) at quasistatic and then at high strain rate (up to 500/s) at different stress states. Resulting fracture limit curves which is a plot between equivalent fracture strain and stress triaxiality could be used for fracture parameter determination. In this work, CrachFEM material model is used, and its parameters are calibrated and thereafter model is utilized for force-deflection correlation with fracture strain prediction for individual experiment. It is envisaged that this work will lead to the understanding of fracture model when high strain rate loading is used.

Introduction

The failure in sheet metal could be due to sheet instability, shear fracture and ductile fracture. In sheet metal forming, instability [1] could be considered as one of failure mode and in crash loading situation shear and ductile fracture could be predominant [2,3]. However, in general the failure could depend on material, stress state, strain state, strain rate, manufacturing process and pre-strain conditions as well. There is a continued interest in development of experimental methodology in which strain to fracture under constant stress loading could be determined. The stress state is related to three invariant of the stress tensor and is commonly expressed in terms of triaxiality and Lode angle parameter [3,4]. The most common stress states useful in evaluation of crash performance are shear, tensile, plane strain and equibiaxial. Intermediate stress triaxialities could also be done, however it needs special specimen and separate experimental arrangement. In this work, shear, tensile and plane strain stress state are achieved using flat sheet standard specimen loaded until fracture at various strain rates. The equibiaxial state of stress is achieved by dome stretching deformation.

Material & Experimental Methodology

DP780 steel grade of 1.80mm thickness is characterized for determining fracture strain under constant stress state loading in a servo-hydraulic equipment Zwick HTM5020 except equibiaxial test for which only quasistatic test was possible using forming press. For all the tests i.e., shear, uniaxial tensile test, plane strain

test and equibiaxial test relevant flat sheet specimen were used, and the full field deformation is captured using DIC. Each test is repeated three times and an average fracture strain is determined by processing the failure images. The CrachFEM material model parameters are calibrated using non-linear least squares optimization by minimizing the error between experiment and analytical expression of shear and ductile fracture. The fitting between experimental data and phenomenological CrachFEM material model is shown in Figure 1.
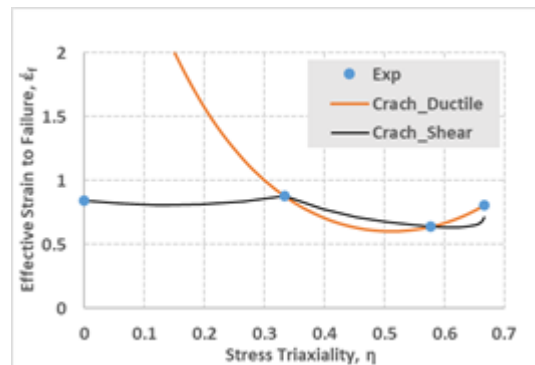

Figure 1 : Effective strain to failure vs stress triaxiality plot

Conclusions

This work highlights the experimental methodology and CrachFEM material model calibration of DP780(1.8mm) under quasistatic multiaxial loading. Further high strain rate experiments shall be conducted with simulation and correlation of individual experiments. It will shed light on effect of rate loading on fracture and further could be understood if inclusion of rate dependent fracture is influencing the component level crash performance. The following shall be attempted to complete this work:

- Fracture characterization at high strain rate at different stress state.
- Simulation and correlation with individual fracture experiment.
- Possible component crash test using the same fracture model
- Direction for future work.

References

1. P K Singh et. al. 2017. Forming limit diagram generation with reduced experiments and modelling for different grades of automotive sheet steel using CrachLab, *The J of Strain Analysis for Engg Design*, 52(5), 298-309
2. Gese H. et. al. 2004. CrachFEM – A Comprehensive Failure Model for Metallic Structures in Sheet Metal Forming and Crash Simulation, Europam October 11th to 13th, France.
3. C C Roth et. al. 2016. Ductile fracture experiments with locally proportional loading histories*, IJP*, Volume 79, Pages 328-354
4. T Wierzbicki et. al. 2005. Calibration and evaluation of seven fracture models*, IJMS*, Volume 47, Issues 4–5, 719-743

Advanced numerical methods for the characterization of materials loaded under extreme conditions

R. Arturo Rubio R. [*†], **Guilherme C. Soares**[†], **Mikko Hokka**[†]

Faculty of Engineering and Natural Sciences, Tampere University, Finland
Keywords: Inverse methods, Numerical optimization, Ti6Al4V alloy, DIC, IRT.

Abstract: This work presents a set of examples of how the combination of numerical methods and advance experimental techniques can narrow the discrepancies between physical systems and numerical models. A description of an inverse approach for the calibration of the Johnson–Cook model with damage for the Ti6Al4V alloy is provided and discussed in more detail. The experimental data used for the model calibration include full-field strain and temperature measurements of specimens tested at high strain rate. The full field strain and temperature data were obtained by digital image correlation and infrared thermography, respectively. A finite element model was constructed to reproduce the experimental conditions of the mechanical tests and an optimization algorithm was used to minimize the discrepancies between the measured and numerically computed displacement fields. The full field measurements were treated and repaired using machine learning algorithms to enrich the quality of the information provided to the model.

1. Introduction

The increase of the computational power of modern computers allows the development of numerical models of complex systems, which provide powerful tools for better understanding of the physics behind them. Such models require experimental evidence to ensure the close correlation between physical and numerical features. One example of this is the use multiaxial fatigue data to calibrate fatigue models in order to improve their sensitivity to stress triaxiality. Some material features can be measured directly or estimated from experimental measurements like those obtained with Electron Back Scatter Diffraction (EBSD) which provide information about the mesostructure of the material. Such features can be explicitly imported in Finite Element (FE) models to create synthetic microstructures for further study of mechanical processes at microscale level. As an example, the generation of synthetic microstructures have been used in the study of damage propagation in granite by electric excitation of piezoelectric phases dispersed in the structure [1].

The image processing techniques can provide accurate full-field measurements (FFM) of different features like strain and temperature at material points of a visible surface. The FFM techniques such as Digital Image Correlation (DIC) and Infrared Thermography (IRT) have been widely used to characterize the mechanical behaviour of materials showing heterogeneous evolution of strain and temperature fields. Such information can be imported into numerical models to narrow the differences between virtual and real systems by means of inverse methods (IM). The combinations of FFM and IM enhance the sensitivity of models to various aspects, such as mechanical triaxiality and changes of temperature due to adiabatic heating. Several authors have combined IM, and Finite Element (FE) simulations to calibrate constitutive plasticity models using DIC strain measurements of nonhomogeneous deformation states [2, 3]. These calibration approaches rely on two main parts: firstly, a numerical model containing all the phenomena occurring in the experiments. Secondly, an optimization algorithm that iteratively tries different combinations of the material parameters to minimize the deviation between FFM and numerically computed fields.

The plastic flow in metals leads to transformation of mechanical work into heat, which may be conducted out of the material when sufficient time is given. However, dynamic loadings lead to the accumulation of heat in the material causing temperature rise. Thus, the strain fields are necessary but insufficient to fully describe the mechanical behaviour of the metals under dynamic conditions since the temperature field of the material changes alongside the deformation process. At least to our current knowledge, there is no previous investigations in which DIC and IRT have been simultaneously used within IM approaches to calibrate plasticity models. This work presents a calibration approach to find suitable parameters of the Johnson–Cook model with damage for the Ti6Al4V alloy using synchronized FFM of strain and temperature.

2. Summary of the calibration approach

The calibration approach relies on FFM of strain and temperature of the Ti6Al4V alloy. All the experimental evidence used in this work was obtained by the IMPACT research group from Tampere University using the framework presented by Soares and Hokka [4]. The information fed to the models included DIC and IRT measurements of the Ti6Al4V alloy tested at different strain rates and temperatures. Two different data sets are considered in this approach: first, a set of experiments performed at low strain rate and low temperature to identify strain hardening behaviour of the material at reference conditions. Second, a set of experiments performed at high strain rate and within a wide range of temperatures to identify the temperature, strain rate and damage dependences of the model. An FE model was built in ABAQUS to reproduce the split Hopkinson tension bar test results to compare the model performance with the full-field displacement measurements during the calibration process. The workflow of the calibration approach consists of three main stages:

1. The experimental data was pre-treated in order to allow direct comparison between FFM data and the numerical predictions. A surface of analysis was defined within the FFM data set, and a homologous surface was defined within the FE model. The nodes within the surface of analysis of the FE model were used as reference grid to interpolate the FFM displacement data. This way the numerically predicted fields and the experimental evidence can be directly compared at material point level. A machine learning model was trained using the valid DIC and IRT measurements to repair all possible invalid readings at the analysis surface.

2. Calibration of strain hardening behaviour at reference conditions using homogeneous deformation data was carried out to reduce the size of the parameter space in the calibration process.

3. Identification of initial approximations for the temperature and strain rate dependences of the model using the measured yield stress at different strain rates and temperatures. This step allowed to start the calibration process close to the final solution, enhancing the quality of the results and reducing computational time.

4. Calibration of the temperature and strain rate dependencies of the model by minimization of the deviation between the measurements and the numerically predicted displacement fields.

The described approach estimates stresses in the samples at material point level using tests with heterogeneous deformation patterns which occur during necking. In contrast to usual calibration techniques where the information after necking is discarded, the present methodology uses the information at necking to enhance the estimation of the JCM parameters. Some preliminary results are shown in this presentation

References:

1. A. Rubio et al. 2022. Piezoelectric excitation of quartz in granite for improved drillability. In *Eurock*, Helsinki.

2. S. Cooreman et al. 2008. Identification of Mechanical Material Behavior Through Inverse Modeling and DIC. *Exp. Mech*. 48. 421-433.(10.1007/s11340-007-9094-0).

3. D. Lecompte et al. 2006. Identification of yield locus parameters of metals using inverse modeling and full field information. In *7th National congress on theoretical and applied mechanics*, Belgium.

4. G. Soares, M. Hokka. 2022. Synchronized Full-Field Strain and Temperature Measurements of Commercially Pure Titanium under Tension at Elevated Temperatures and High Strain Rates. *Metals,* 12,25. (10.3390/met12010025)

Identification of the dynamic tensile strength and fracture energy of five geomaterials subjected to spalling tests

M. Sapay[1], P. Forquin[1,1]

"Univ. Grenoble Alpes, CNRS, Grenoble INP*, 3SR, F-38000 Grenoble, France"

Keywords: Tensile strength; Spalling test; Fracture Energy; Concrete; Ultra-high-speed imaging; Virtual Fields Method

Abstract: The dynamic tensile testing method based on the spalling technique has been widely adopted as the most popular technique for obtaining the tensile material response of concrete and rock-like materials at strain rates ranging from 40 to about 200 s^{-1}. However, most of the experimental data available in the literature have been treated with processing methods based on the assumption that the material behaves linearly elastic up-to the peak stress and that failure occurs instantaneously causing the so-called velocity rebound. During the past seven years a novel processing technique has proposed based on the use of high-speed imaging and the virtual fields method (VFM). In this method, the level of stress is determined from the acceleration field obtained from full-field measurements. This method has been widely used to determine the dynamic tensile strength and fracture energy of dry common concrete. In the present paper, this technique is employed to characterize and identify the dynamic tensile properties of 5 other materials. The experimental data are compared to the results obtained from traditional processing methods. The interest to apply the VFM method to these materials is discussed as function of the microstructure and dynamic response of the tested geomaterials.

1. Introduction (Time New Roman 12) (18pt before, 12pt after)

Concrete is one of the most used building materials in civil engineering. Over the past decade, concrete and rock materials have been increasingly tested under high strain stress in order to meet the various safety requirements of concrete structures in different scenarios of accident or attack [Riedel and Forquin, 2013] or in the field of industrial processes (civil engineering applications, impact drilling in the mining industry). Under such extreme loads, the geomaterial is successively subjected to high stress rate tensile load (typical strain-rates of a few hundred 1 s-1) that produce tensile damage characterized by a high density of oriented cracks [Forquin and Erzar, 2010; Forquin and Hild, 2010]. Several experimental devices have been used in the past to characterize their response under tensile loading. On the one hand, Split Hopkinson Bar (SHB) devices were used in tensile test [Weerheijm and van Doormal, 2007] or Brazilian dynamic tests (diametric compression of a disc) [Tedesco et al, 1993]. In this configuration, the quasi-static balance of the concrete sample is assumed (equality of contact forces at sample-output bar and sample-input bar interfaces). However, to achieve this mechanical equilibrium, the loading-rate must be greatly reduced by using, for example, pulse shaping techniques [Frew et al., 2005]. Finally, these techniques are still insufficient to characterize the tensile strength of rock-like materials at stress rates greater than 10 s-1 [Forquin et al, 2013].
The tensile strength of geomaterials can be studied at higher strain-rates through spalling tests. In these tests, a short projectile [Klepaczko and Brara, 2001; Erzar and Forquin, 2010] or a small pyrotechnic charge [Weerheijm and van Doormal, 2007] is used to produce a small compression pulse that propagates through the Hopkinson bar and through the sample. It reflects as a tensile load in the sample leading to its tensile failure. This technique was developed by Klepaczko and Brara [2001] and improved by Erzar and Forquin [2010] using a projectile optimized to homogenize the tensile stress field in a large part of the sample (Figure 1). Several techniques were proposed to determine the tensile strength of the sample. The Novikov formula relies on the assumption of a linear elastic behavior up to failure [Forquin et al, 2013; Forquin and Lukić, 2018]. To

*Author for correspondence (xxxx@yyyz.zz.zz).

†Present   address

Department, Institution, Address, City, Code, Country

make the hypothesis more flexible, Pierron and Forquin [2012] proposed to the acceleration field and the virtual fields method to deduce the axial stress in any sample cross-section [Pierron and Grédiac, 2012]. This photomechanical technique was used to characterize the tensile strength, the Young's modulus, the stress-strain response [Forquin et al, 2013; Forquin and Lukić, 2018] and the fracture energy of concrete [Lukić et al, 2018].

In order to extract local strain and cross-sectional axial stress information over the sample surface, full-field optical measurements and the virtual fields method (VFM) are used. With the use of ultra-high-speed camera, the in-plane displacement fields of a sample surface are obtained using the grid method. The local Stress-FOD response of each observed dynamic fracture zone can be obtained, as well as the fracture opening speed (FOV) and specific fracture energy associated with each fracture.

In the present paper, both techniques are compared in the case of 5 concrete and rock materials. The difference is explained considering the non-linear pre-peak behavior of each material. Finally, the validity of conventional data processing is discussed.
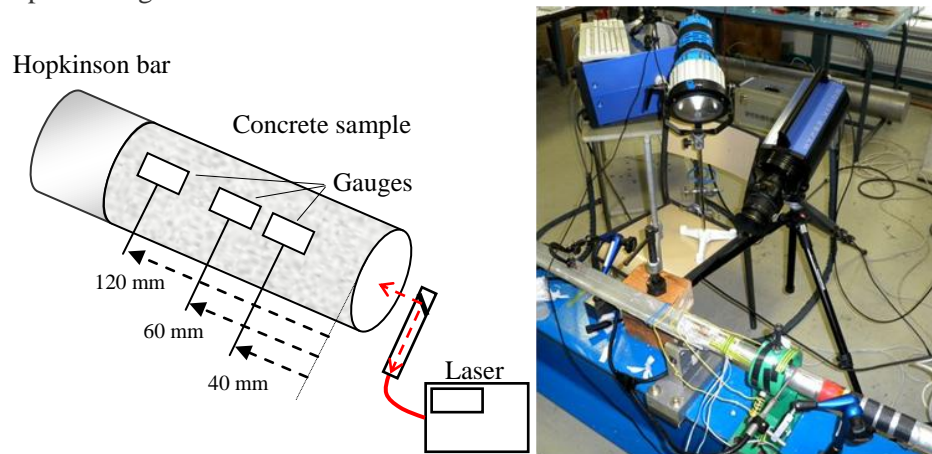

Figure 1: Spalling testing technic.

Tested materials
In the framework of this study, the dynamic strength and fracture energy of five brittle materials (R30A7 common concrete, High strength concrete and an Ultra-high-Performance concrete) as shown in Table 1 are compared .

Composition		Dry R30A7	Wet R30A7	HSC	Ductal®
Cement	[kg/m³]	263			730
Silica fume	[kg/m³]	-			235
Crushed quartz grains	[kg/m³]	-			220
Sand	[kg/m³]	838			885
Superplasticizer	[kg/m³]	-			10
Water	[l/m³]	169			160
Steel fibers	[vol. %]	-			2%
W/(C+SF)		0.64			0.17
Mechanical Properties					
Density [kg/m³]					2396
Young's Modulus [GPa]					55
Quasi-static Comp. strength [MPa]					200

Table 1. Material composition and mechanical properties of R30A7 common concrete, of high strength concrete and an ultra-high-performance concrete.

References:

1. [Riedel and Forquin, 2013] Riedel, W., and P. Forquin. "Modelling the response of concrete structures to dynamic loading." Understanding the Tensile Properties of Concrete. Woodhead Publishing, 2013. 125-142e.

2. [Forquin and Erzar, 2010] Forquin, P., and B. Erzar. "Dynamic fragmentation process in concrete under impact and spalling tests." International Journal of Fracture 163.1 (2010): 193-215.

3. [Forquin and Hild, 2010] Forquin, Pascal, and François Hild. "A probabilistic damage model of the dynamic fragmentation process in brittle materials." Advances in applied mechanics 44 (2010): 1-72.

4. [Weerheijm and van Doormal, 2007] Weerheijm, J., and J. C. A. M. Van Doormaal. "Tensile failure of concrete at high loading rates: new test data on strength and fracture energy from instrumented spalling tests." International Journal of Impact Engineering 34.3 (2007): 609-626.

5. [Tedesco et al, 1993] Tedesco, Joseph W., and C. Allen Ross. "Experimental and numerical analysis of high strain rate splitting-tensile tests." Materials Journal 90.2 (1993): 162-169.

6. [Frew et al., 2005] Frew, D. J., M. J. Forrestal, and W. Chen. "Pulse shaping techniques for testing elastic-plastic materials with a split Hopkinson pressure bar." Experimental mechanics 45.2 (2005): 186-195.

7. [Forquin et al, 2013] Forquin, Pascal, and L. Sallier. "A testing technique to characterise the shear behaviour of concrete at high strain-rates." Dynamic Behavior of Materials, Volume 1. Springer, New York, NY, 2013. 531-536.

8. [Klepaczko and Brara, 2001] Klepaczko, J. R., and A. Brara. "An experimental method for dynamic tensile testing of concrete by spalling." International journal of impact engineering 25.4 (2001): 387-409.

9. [Erzar and Forquin, 2010] Erzar, Benjamin, and Pascal Forquin. "An experimental method to determine the tensile strength of concrete at high rates of strain." Experimental Mechanics 50.7 (2010): 941-955.

10. [Weerheijm and van Doormal, 2007] Weerheijm, J., and J. C. A. M. Van Doormaal. "Tensile failure of concrete at high loading rates: new test data on strength and fracture energy from instrumented spalling tests." International Journal of Impact Engineering 34.3 (2007): 609-626.

11. [Forquin and Lukić, 2018] Forquin, Pascal, and Bratislav Lukić. "On the processing of spalling experiments. Part I: identification of the dynamic tensile strength of concrete." Journal of Dynamic Behavior of Materials 4.1 (2018): 34-55.

12. [Pierron and Forquin 2012] Pierron, F., and P. Forquin. "Ultra-high-speed full-field deformation measurements on concrete spalling specimens and stiffness identification with the virtual fields method." Strain 48.5 (2012): 388-405.

13. [Pierron and Grédiac, 2012] Pierron, Fabrice, and Michel Grédiac. The virtual fields method: extracting constitutive mechanical parameters from full-field deformation measurements. Springer Science & Business Media, 2012.

14. [Lukić et al, 2018] Lukić, Bratislav B., Dominique Saletti, and Pascal Forquin. "On the processing of spalling experiments. Part II: identification of concrete fracture energy in dynamic tension." Journal of Dynamic Behavior of Materials 4.1 (2018): 56-73.

Numerical simulations of the dynamic behavior of porous alumina ceramics

Joane Meynard[a,*], Antonio Cosculluela[a], Pierre Pradel[a]

[a] CEA CESTA, 15 avenue des Sablières CS60001, 33116 Le Barp Cedex, France

Keywords: Alumina ceramics, Porosity, Dynamic loading, DFH model, Finite-element simulations

Abstract: Highly dense ceramic materials such as alumina are commonly used in shielding solutions. Indeed, they present interesting properties such as low density, high hardness and compression strength as well as a low traction strength (1). Moreover, they exhibit a high ability to absorb energy when put under dynamic loading.

To improve protective systems, materials with higher energy mitigation ability are required. Porosity is a well-known microstructural parameter, which can decrease density while increase material damping (2). However, increasing the porosity also induces a loss of mechanical strength in the material (3), making it difficult to evaluate the impact of this parameter on the ceramic ability to mitigate energy. To evaluate the performance of such materials, the influence of porosity on dynamic mechanical properties of alumina ceramics is investigated through experiments and simulations.

Four grades of alumina ceramics were manufactured by the French enterprise Galtenco Solutions using a gel-casting process with different pore populations. To do that, the sintering conditions and the ratio of porogen agent used in the process were tuned to reach the porosity ratio specification (from 0% to 60%). Figure 1 shows characteristic scanning electron microscopy (SEM) observations of two grades of the studied alumina ceramics (4).

a)   b)

Figure 1: Characteristic SEM observations of two grades of the studied alumina ceramics –a) A-Grade (porosity ratio near 0%) and b) B-Grade (porosity ratio of about 60%)

The microstructures of the studied alumina grades are very different in terms of porosity ratio, pore size and spatial distribution. The A-Grade alumina has very few pores (with a characteristic diameter of about 1 μm) whereas the B-Grade sample shows two populations of spherical porosity with different characteristic diameters: about 1 μm for the first one and about 15 μm for the second one. Due to the significant difference in microstructures, differences in their mechanical responses under dynamic loadings are also expected.

For ceramics, the energy mitigation ability is directly linked to the dynamic multi-fragmentation behavior under dynamic loading. Predicting the impact response of these ceramics is thus critical for the design of protective systems. The DFH (Denoual-Forquin-Hild) (5, 6) anisotropic tensile damage model is used to model the dynamic behavior of the studied porous ceramics. This micro-mechanical modelling approach describes the damage mechanism occurring in brittle materials when loaded at high strain rates. It is based on the description of crack initiation induced by tensile stresses occurring from critical defaults present in the

---

*Author for correspondence (joane.meynard@cea.fr).

†Present address: CEA CESTA, 15 avenue des Sablières CS60001, 33116 Le Barp Cedex, France

material and crack propagation leading to multiple fragmentation. This model has been used in the literature to model the behavior of highly dense ceramics such as alumina, with good agreement with experiments (7). Moreover, as this model relies on physical input-parameters, it seems to be a good candidate to estimate the impact of porosity on the dynamic response of the studied materials. To do so, two explicit codes are used (in order to perform a code comparison): the Hesione hydrocode developed at the CEA and the Abaqus/Explicit code.

First, a preliminary study of this model is performed by fitting the numerical simulations from (7) of a shockless spalling test made on a high-pulsed power generator equipment. Results with the two codes show good estimation of the first moments of the fragmentation (about 1 µs), thus the estimation of the spall strength is identical with both codes. However, different fragmentation behaviors are observed at longer times. Further investigations highlight the fact that the DFH model is a probabilistic model as it uses a statistical approach for the description of the fragmentation process, which can explain the observed differences between the two codes. Therefore, a methodology is proposed to take into account the probabilistic aspect of the model on its results. A sensibility analysis on the DFH input parameters is conducted to estimate the critical parameters that need to be characterized with controlled precisions.

Secondly, the porous alumina ceramics manufactured for this work are characterized by several dynamic tests with uniaxial stress or uniaxial strain conditions (4) in order to cover a wide range of strain rates up to 10^6 s^{-1} and each test is simulated. Comparison between simulations and experiments makes it possible to evaluate the accuracy of the DFH model to describe the behavior of very porous alumina ceramics. Good agreement between simulations and experiments for each grade of alumina ceramics is obtained by identifying the critical input parameters. The impact of porosity on the mechanical response of theses ceramics is evaluated by determining the relationships between each DFH parameter and the porosity.

References:
1. Wachtman JB, Cannon W R, Matthewson MJ. 2009. Mechanical properties of ceramics, *John Wiley & Sons*, 2nd edition. (doi: 10.1002/9780470451519)

2. Panteliou SD, Zonios K, Chondrou IT, Fernandes HR, Agathopoulos S, Ferreira JMF. 2009. Damping associated with porosity in alumina. *Int. J. Mech. Mater. Des.* **5(2)**, 167-174. (doi: 10.1007/s10999-008-9092-0)

3. Ryshkewitch E. 1953. Compression strength of porous sintered alumina and zirconia: 9th communication to ceramography. *J. Am. Ceram. Soc.* **36(2)**, 65-68. (doi: 10.1111/j.1151-2916.1953.tb12837.x)

4. Henry Q, Kopp JB, Le Barbenchon L, Cosculluela A, Viot P. 2023. Effects of microstructure on mechanical behavior of multiscale porous alumina stressed up to high strain rates. In DYMAT Winter School 2023, Aussois, France.

5. Denoual C, Hild F. 2000. A damage model for the dynamic fragmentation of brittle solids. *Comput. Math. Appl. Mech. Eng.* **183**, 247-253. (doi: 10.1016/S0045-7825(99)00221-2)

6. Forquin P, Hild F. 2010. A probabilistic damage model of the dynamic fragmentation process in brittle materials. *Adv. Appl. Mech.* **44**, 1-72. (doi: 10.1016/S0065-2156(10)44001-6)

7. Zinszner JL, Forquin P, Rossiquet G. 2015. Experimental and numerical analysis of the dynamic fragmentation in a SiC ceramic under impact. *Int. J. Impact Eng.* **76**, 9-19. (doi: 10.1016/j.ijimpeng.2014.07.007)

An experimental and modelling investigation of Al 6061-T6 response under intense impulsive X-ray radiation

R. Beuton, P. Maury, J.M. Chevalier, E. Buzaud†

CEA CESTA, 15 ave des sablières CS 60001, 33116 Le Barp Cedex, France

Keywords: Shock, X-ray, laser, plasma, energy deposit

Abstract: Exposed intense impulsive X-ray radiation, materials may be subjected to the rise and propagation of potentially damaging high amplitude shock waves. Those phenomena are investigated experimentally by the exposure of an Al 6061-T6 specimen subjected to a high radiant energy x-ray source recently developed on the Laser Mega Joule (LMJ). The shock wave is observed through the measurement of the specimen back face velocity. The x-ray energy deposit through the specimen thickness, the sudden temperature rise on the front side and the resulting shock wave propagation are modelled, and the resulting calculated back face velocity is confronted to the measurement.

1. Introduction

Shock waves may be imparted to solid materials through different mechanisms implying energy transmission across a surface: solid impact, blast waves, laser impacts are well-documented examples of those mechanisms.

However, a shock wave may also emerge from an interaction with electromagnetic waves. Irradiating materials impulsively by means of a flux of elementary penetrating particles is another way to induce shock waves. This could be achieved with a source of massive particles (protons, neutrons, electrons) or high energy mass less particles like photons (UV, x-rays or gamma radiations). The radiation-matter interactions are governed by diffusion-absorption reactions, the depth at which those interactions will happen is a statistical function of the particle energy. The higher the particle energy, the higher the probability to increase the depth of penetration before interacting with the material barrier. Hence, energy from UV photons will typically be deposited on the surface of a given barrier, while gamma photons may essentially cross the barrier with limited energy deposit.

This study is considering the aggression of an Al6061-T6 disk exposed to a single radiant photon source produced from the interaction of a high intensity laser source with a volume of xenon gas enclosed in a cylindrical cavity.

2. The radiant x-ray source

The laser target is an epoxy cylinder of 3 mm height, 3.5 mm diameter and 50 µm thickness. This pipe cavity if filled with xenon gas at a nominal 1.2 atm. pressure. The pipe is vertically placed at the centre of the LMJ experiment chamber and exposed to the simultaneous irradiation from 32 LMJ beams symmetrically focussed to the centre of the target, through the top and bottom sections. Each beam is producing a 351 nm light impulse of 3 ns duration [2].

The 89.9 kJ total laser energy delivered to the pipe is sufficient to produce L-shell x-ray emission from the heated xenon plasma, at around 4.5 keV [1].

The radiant source is characterized in terms of spectrum and time-resolved power [1] by means of different spectrometers observing the radiant source from different polar and azimuthal angles. Along the equatorial

plane of the experience chamber, the radiation is filtered by the epoxy cavity itself, hence attenuating the UV photons component of the spectrum more efficiently than on the top and bottom laser entrance holes.

3. Experimental configuration

The 30 mm diameter 0.5 mm thick Al6061-T6 specimen is placed vertically, at a distance of 70 mm from the centre of the LMJ chamber. It is centred along the equatorial plane so as to take advantage of the maximal UV photons filtration. Back face velocity is measured at the centre of the specimen, through a 8 mm thick PMMA window. Measurement is performed with two complementary techniques, one base on heterodyne interferometry, the other based on Visar interferometry.

4. Numerical simulation

The numerical simulation is a three-step process. First, based on the spectrometers measurement and geometric considerations, the spectrum and time-resolved x-ray power are reconstructed on the front face of the specimen. Then a radiation transport code is used to calculate the adiabatic heating gradient through the Al 6061-T6 specimen thickness resulting from the total x-ray deposit. In a third step, a 1D hydrocode is used to model the subsequent thermal shock: the multiphase equation of state of aluminium calculates the pressure field resulting from the quasi-instantaneous temperature rise, and propagates this pressure pulse as a shock wave unloading inward towards front free surface on one side, and outward towards the back face on the other side. The resulting back face material velocity calculated at the interface with the PMMA window appears in excellent correlation with the measurement.

5. Conclusions

An experimental method has been developed to submit solid materials to intense impulsive x-ray radiations. A first experiment has been performed on an Al 6061-T6 sample, the shock wave generated and propagated through the specimen has been characterized by means of material velocity measurement. A 1 dimensional computational model has been developed and successfully correlated to the measurement. This validation study opens the door to the design and evaluation of future protective barriers against intense x-ray radiations.

References:
1. M. Primout, L. Jacquet, L. Lecherbourg et al., 2022, First High radiant energy xenon-pipe-based x-ray source on LMJ, Phys. Plasmas 29, 073302;
2. J.-L. Miquel and E. Prene 2019, LMJ & PETAL status and program overview, *Nucl. Fusion* 59 032005.

Laser-shock dynamic loading of innovative materials for beam intercepting devices of particle accelerators

Alberto Morena, Lorenzo Peroni, Martina Scapin

Department of Mechanical and Aerospace Engineering, Politecnico di Torino, Corso Duca degli Abruzzi 24, Turin, 10129, Italy

Keywords: laser-shock, beam intercepting devices, particle accelerators, shockwave, spallation

Abstract

The urge of increasing the energies stored in modern particle accelerators is highlighting the safety issues of these large machines. In particular, the accidental scenarios of one or more particle bunches deflecting from their trajectory must be considered. Indeed, the impacted structures should be able to withstand high stresses at high strainrates in order to protect the expensive equipment installed behind them. As a matter of fact, the European project ARIES with its Work Package 17 was mainly focused at developing and investigating the behaviour of innovative advanced materials engineered for beam intercepting devices (BID), such as collimators, dumps and absorber blocks. In this challenging context an experimental campaign, named P219, was performed with the aim of testing graphitic materials for BID applications while subjected to high-power laser shocks. The tests were conducted at the Petawatt High-Energy Laser for Heavy Ion Experiments (PHELIX) laser facility at GSI research centre in Darmstadt, Germany.

The upcoming years will be crucial for the development of the equipment of the future particle accelerators, like the upgrade project of the CERN Large Hadron Collider (LHC), identified as High-Luminosity LHC (HL-LHC), or the Future Circular Collider (FCC). All these projects are united by the need of structures made of new materials able to cope with the severe thermo-mechanical conditions caused by the quasi-instantaneous energy deposition of a particle bunch impact. Nonetheless, these materials should also meet the operational requirements of particle accelerators, namely high electrical conductivity and ultra-high vacuum compatibility. Thus far some of the BIDs installed in the LHC were made of Carbon-fiber Carbon (CFC) and isotropic polycrystalline graphite, however these materials are expected not to meet the requirements for the HL-LHC upgrade. For this reason, the graphite-matrix composites reinforced with Molybdenum carbides (MoGr) were already installed in the LHC but are still under examination for the HL-LHC and numerous other materials are still under development such as Chromium carbide graphite (CrGr), Copper Graphite (CuGr) and Copper Diamond (CuCD).

In the framework of the ARIES project an extensive experimental campaign was performed at the PHELIX laser facility. Several specimens made of different materials and coatings were impacted by high energy laser shocks with the aim of characterizing their thermo-mechanical properties.
Indeed, when a high-intensity laser beam irradiates the surface of a component, it leads to a quasi-instantaneous heating causing the matter to change state from solid to plasma. Therefore, the produced plasma tends to expand inducing pressures up to several gigapascal on the surroundings. If the pressure field is sufficiently intense, it can generate a shockwave able to travel through the entire thickness of the hit component. When the disturbance reaches a free surface it gets reflected and starts travelling backwards as a tensile wave. The generated tensile wave can be high enough to critically damage the component, eventually

leading to its fracture which is generally referred to as spall fracture.

Before the beginning of the P219 campaign, the thicknesses of the target samples were opportunely designed by means of hydrodynamic simulations to investigate various damage regimes. The laser-matter interaction, the successive shockwave travelling and breakout were taken into account and the simulation procedure was tuned by means of previous similar experiments on graphite.

The methodology applied during the testing was to keep the intensity of the laser as constant as possible and to vary the thicknesses of the specimens in order to obtain different stresses on the back surface and so different spallation conditions. Hence, the specimens were thin discs with a diameter of 10 mm and thickness from 0.75 mm to 3.5 mm. The PHELIX energy was set to a range from 50 to 60 J, the pulse was a 1.5 ns square pulse with a wavelength of 527 nm and the focal spot obtained by phase plates was of 1 mm in diameter. As a result, the obtained laser intensity varied in the range of 3.4 to 5.9 TW/cm^2. Altogether the shot targets were 46 and the tested materials were isotropic graphite, CFC, MoGr, CrGr, CuGr and CuCD. The anisotropic materials were tested in both preferential directions, e.g., the in-plane (IP) and the through plane (TP), which means that they were shot respectively perpendicularly to the graphite basal planes and parallel to the graphite basal planes.

Some of the aforementioned specimens were also coated by a functional thin film of Molybdenum or Copper. The coating is actually adopted on the LHC collimators aiming at enhancing the electrical conductivity of these components.

During the experimental campaign online diagnostics were adopted to measure the back surface velocity and to investigate the damage mechanisms.

In this sense a Photonic Doppler Velocimetry system (PDV) was focused on the back surface of the specimen. Its purpose was to measure the speed of the back free surface and of the potential debris detached from the target. However, the PDV temporal resolution was limited to 55 ns and different techniques to enhance the reflectivity of the surfaces had to be applied, such as fine polishing and flash coatings of few micrometres. Indeed, also a meticulous adjustment of the alignment of the PDV system was necessary.

With the aim of capturing images of the damage on the back surface and of the debris ejection, shadowgraphy was applied. The setup was composed of diode enlightenment system and a high-speed camera. The camera was set to record with 26.6 µm/pixel as resolution at framerates ranging from 186 kfps to 580 kfps. The exact timing of the image capture was recorded by means of an oscilloscope.

Since the PDV system is very influenced by the focal distance, the camera images analysis is fundamental to determine the average speed of the debris.

The irradiated specimens were collected and will be examined by means of scanning electron microscopy and tomography: the post-mortem analysis of the targets will be able to give indispensable insights about the size and position of the crater or of the subsurface cracks left by the spallation.

The shape and the size of the ejected debris will be also evaluated, since the debris were collected thanks to a PMMA plate placed at 12 mm from the back surface.

In conclusion, thanks to the P219 experimental campaign, the behaviour of innovative materials for BID applications under high shock loading will be evaluated. In fact, from the collected data, the spallation stress can be evaluated as well as the time of travelling of the shockwave in the material. The gathered information will also serve as a benchmark for the hydrodynamic simulations concerning the laser-matter interaction, the shockwave propagation and the materials failure.

Finite element simulations of dynamic compression of bulk metallic glasses at elevated temperatures using split hopkinson pressure bar setup

Arun Kamble and Parag Tandaiya

Department of Mechanical Engineering, Indian Institute of Technology, Bombay, Mumbai-400076, INDIA

Keywords: BMGs, Constitutive model, Shear band, SHPB, Finite element analysis, Dynamic compression.

Abstract

The dynamic compression of Vitreloy-1 and $Zr_{64.13}Cu_{15.75}Ni_{10.12}Al_{10}$ Bulk Metallic Glasses (BMGs) at elevated temperatures is numerically simulated in this work using a split hopkinson pressure bar (SHPB) setup in the Abaqus/Explicit finite element analysis software. The objective of the present study is to develop and validate a constitutive model and simulation methodology that can predict the high strain rate response of BMGs at elevated temperatures. Therefore, a constitutive model for both the BMGs accounting for the effects of high strain rate and temperature have been developed and numerically implemented by writing user material subroutine. The methodology for modelling SHPB setup in Abaqus from the published literature for aluminium specimens has been reproduced and applied to the BMG specimens. The Vitreloy-1 exhibits rate insensitive response under dynamic loading at both room and elevated temperatures. The failure stress decreases with increasing temperature in the $Zr_{64.13}Cu_{15.75}Ni_{10.12}Al_{10}$ BMG. A satisfactory agreement between the yield strength and shear band morphology predicted by the present simulations and observed in experimental work by other researchers validates the constitutive model and simulation methodology. The current findings are an important step toward developing a material model for BMGs that is applicable at high strain rates and elevated temperatures.

Constitutive model and simulation methodology

Anand and Su [1] proposed a finite deformation Mohr-Coulomb-based isotropic elastic-viscoplastic constitutive model to represent the mechanical response of BMGs. This model, however, does not account for the coupled effects of strain rate and temperature. As a result, we added the strain rate and temperature effects to the cohesion term of Anand and Su model. The user material subroutine VUMAT was used to numerically implement this modified Anand and Su model in Abaqus/Explicit software. The modified Anand and Su model is then used to simulate the dynamic compression behaviour of BMGs at elevated temperatures using the SHPB setup. The SHPB experiments on Vitreloy-1 and $Zr_{64.13}Cu_{15.75}Ni_{10.12}Al_{10}$ BMG reported in the work of Lu et al.[2] and Liu et al.[3], respectively, are numerically simulated using Abaqus. The strain rate coefficients and temperature parameters of Vitreloy-1 and $Zr_{64.13}Cu_{15.75}Ni_{10.12}Al_{10}$ BMG which correspond to the modified Anand and Su model, are calibrated using experimental work by Lu et al.[2] and Liu et al.[3], respectively. The methodology of modeling SHPB setup in Abaqus given by Iwamoto and Yokoyama (2012) for aluminium specimens has been reproduced and used. The CAX4R axisymmetric elements are used to model the BMG specimens. CAX6M elements were used to model the striker, pressure bars, and pulse shaper. The general contact algorithm available in Abaqus/Explicit is used at contact surfaces.

Results and Discussions

Using SHPB experiments at strain rates of 250 s^{-1} and 1000 s^{-1}, Lu et al. [2] discovered the dynamic stress-strain curves for the Vitreloy-1 BMG over a wide temperature range. Finite element simulations in

Abaqus were carried out using the same SHPB setup, temperature range, and strain rate as used by Lu et al.[2]. The reflected and transmitted signal from the incident and transmitter bar, respectively were used to compute stress-strain curves numerically. Figure 1 depicts the experimental and simulation (FEA) stress-strain curves of Vitreloy-1. The yield strength predicted by present simulations of dynamic compression of Vitreloy-1 for various temperatures are in good agreement with experimental results. Simulations with increasing temperature and a strain rate of 1000 s^{-1} accurately captured the yield strength decrease observed in experiments [2]. Liu et al.[3] obtained the dynamic behavior of a $Zr_{64.13}Cu_{15.75}Ni_{10.12}Al_{10}$ BMG at elevated temperatures (from 423 to 683 K) and high strain rates (from 5000 to 10000 s^{-1}) using SHPB setup. The finite element simulations using same setup are carried out. The simulation results of maximum principal logarithmic plastic strain (SDV24) and temperature distribution (SDV32) contour plots at initial temperature, T = 573 K and $\dot{\epsilon}$ = 4200 s^{-1} are shown in Figure 2. The yield strength predicted by present dynamic compression simulations of $Zr_{64.13}Cu_{15.75}Ni_{10.12}Al_{10}$ BMG at strain rate of 4200 s^{-1} is in close agreement with experimental data. The finite element simulations correctly captured the formation of shear bands (SDV24) and ductile damage within shear bands, which is similar to the failure observed in the experiments.
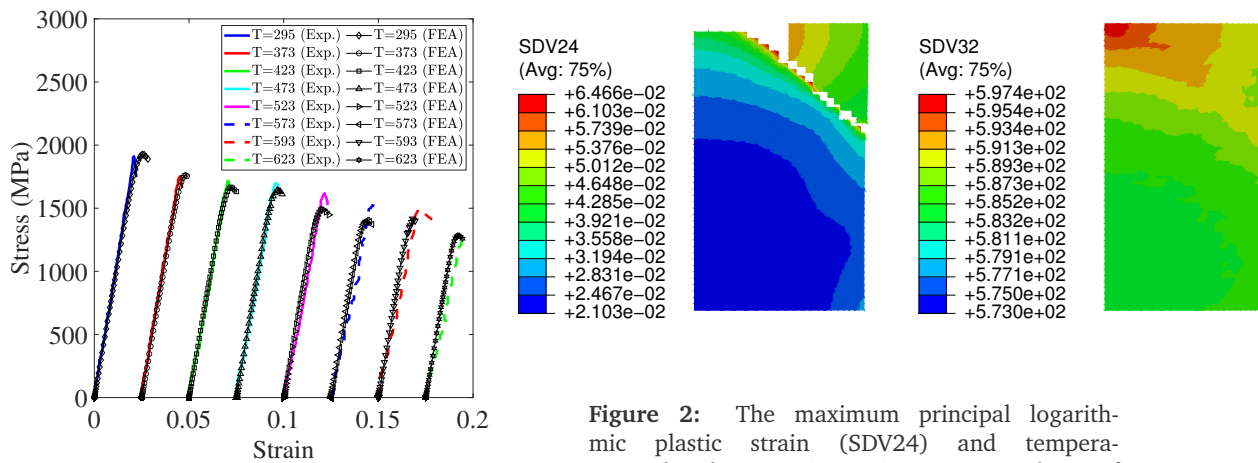
Figure 1: Stress-strain curves of Vitreloy-1 BMG specimens at various temperatures ($\dot{\epsilon}$ = 1000 s^{-1})

Figure 2: The maximum principal logarithmic plastic strain (SDV24) and temperature distribution (SDV32) contour plots of $Zr_{64.13}Cu_{15.75}Ni_{10.12}Al_{10}$ BMG specimen for initial temperature, T = 573 K and $\dot{\epsilon}$ = 4200 s^{-1}.

Conclusion

The modified Anand and Su model, which includes strain rate and temperature effects, can be used to simulate BMG specimens during impact and machining events at high strain rates and temperatures.

References

1. L Anand and C Su. 2005. A theory for amorphous viscoplastic materials undergoing finite deformations, with application to metallic glasses. *Journal of the Mechanics and Physics of Solids*, **53.6**, 1362–1396. (https://doi.org/10.1016/j.jmps.2004.12.006)
2. Jun Lu, Guruswami Ravichandran, and William L Johnson. 2003. Deformation behavior of the $Zr_{41.2}Ti_{13.8}Cu_{12.5}Ni_{10}Be_{22.5}$ bulk metallic glass over a wide range of strain-rates and temperatures. *Acta materialia*, **51.12**, 3429– 3443. (https://doi.org/10.1016/S1359-6454(03)00164-2)
3. WD Liu and Kai-Xin Liu. 2010. Mechanical behavior of a Zr-based metallic glass at elevated temperature under high strain rate. *Journal of Applied Physics*, **108.3**, 033511. (https://doi.org/10.1063/1.3467779)

Optimization Strategy for an Unit Cell towards programming the Strain Rate Sensitivity into Lattice Structures

Sankalp Patil[1,2,*]**, Georg. C. Ganzenmüller**[1,2]**, Klaus Hoschke**[1]** and Stefan Hiermaier**[1,2]

[1]*Fraunhofer Institute for High-Speed Dynamics, Ernst-Mach-Institute, EMI, 79104 Freiburg im Breisgau, Germany*
[2]*Institute for Sustainable Systems Engineering, Albert-Ludwigs Universität Freiburg, 79110 Freiburg im Breisgau, Germany*

Keywords: Programmable Strain Rate Sensitivity, Metal Additive Manufacturing, Design Optimization, Friction.

Abstract

This work will present an optimization strategy for the friction unit cell that paves a way to program the strain rate sensitivity into metallic lattice structures. The new design incorporates a friction mechanism that brings along its own time scale to couple with the time scale of loading. The geometrical parameters of the unit cell are dominant to exploit the friction properties. The parametrization technique along with an optimization strategy to maximize the energy dissipation will be demonstrated.

Summary

The design freedom within the metal additive manufacturing allows to devise materials or structures specifically tailored for crash and impact applications. However, the base materials developed for metallic additive manufacturing intrinsically possess weak strain rate sensitivity. There is a need for practical technique in the case of metallic lattice structures that induce pronounced strain rate sensitivity similar to that in the case of glassy polymers [1]. The time dependent behaviour of metallic lattice structures has been characterized by many authors in order to assess the energy absorbing and dissipative capabilities [3] [4] [5]. However, the attempts made to design a strain rate dependent lattice structure or unit cell are limited or not existing in the case of metals. S. Janbaz et al. [6] have designed a strain-rate dependent mechanical metamaterial by laterally attaching two beams with different levels of strain rate dependencies, i.e. hyperelastic and visco-hyperelastic thus acting as a single beam. The direction in which the beam buckles is governed by the velocity of loading thus having a controlled response. However, the technique is introduced and illustrated with polymers. Here, we deviate from the path of employing complicated material mixes to introduce pronounced strain rate sensitivity into metallic lattice structures. Instead, a mechanism at the mesoscale that brings in its own time scale is necessary. This work introduces the design methodology of the unit cell by considering friction as a time dependent mechanism [2] at the mesoscale and thereby investigates the resulting time-dependent phenomena. This work presents the parametrization technique and optimization strategy of the unit cell in order to exploit the frictional properties.

The Fig. 1 shows a 2D auxetic unit cell with an added friction mechanism. It is designed with the fundamental idea of redirecting the vertical compressive load into the horizontal direction, such that the central stems are pressed against each other, creating contact pressure. Therefore the friction force is affected by the axial compression. The magnitude of the friction force can be controlled by the geometry of the curved beams. Their thickness, t and bending radii, R are the dominant parameters to achieve this task. As in Fig. 1, the unit cell design frames to be a close representation of the classical viscoelastic model. Here, the curved beams represent the spring signifying stiffness and the linear frictional struts within auxetic cell represent the dashpot signifying damping behaviour of the structure.
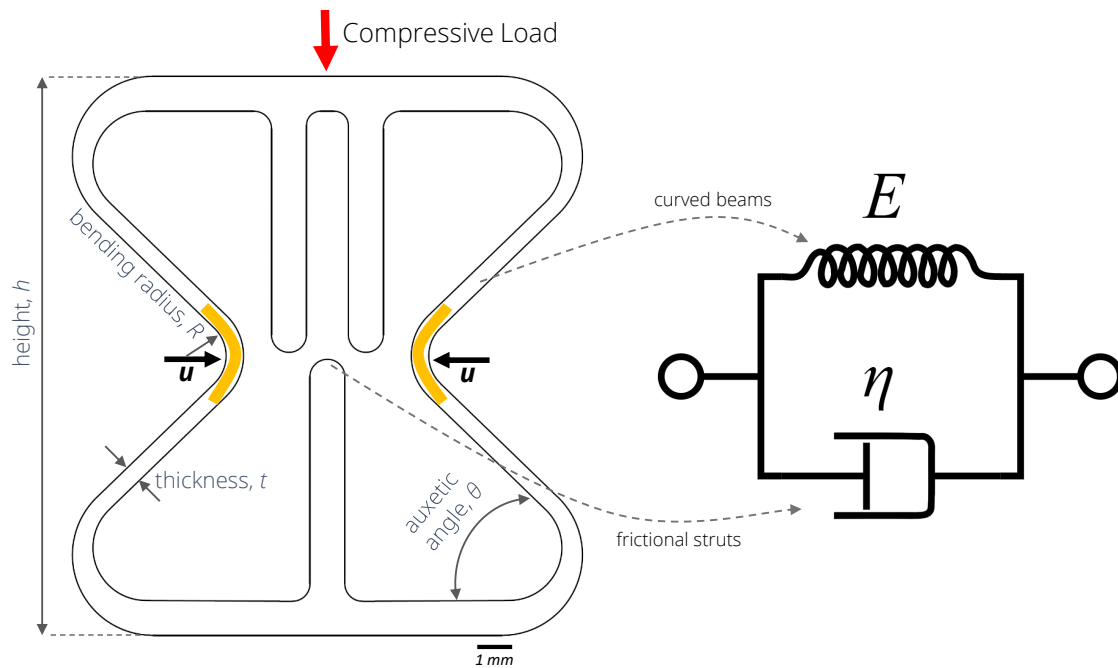
Figure 1: Unit cell design along with the representation of its key geometrical features. The design strategy redirects the vertical compressive load into displacement of the curved beams in horizontal direction, u. The curved beams and the linear frictional struts of the unit cell respectively represent the spring and dashpot of the classical viscoelastic model.

For maximum energy dissipation, the optimal parameter space of the unit cell geometry is desirable. This is important for the maximum exploitation of the proportionality regime of the Coulomb friction, i.e., a constant ratio of normal force and friction force. This work will present the parametrized unit cell and thereby put forward an optimization procedure to maximize the energy absorption and dissipation within the system. The optimal parameter space is equally important to enhance the elastic deformation within the structure.

References

1. Ganzenmüller GC, Patil S, Maurer M, Sauer M, Jung M, Hiermaier S. Sep 2019. A Simple Glassy Polymer Model. Journal of Dynamic Behavior of Materials, 5(3):331343.
2. Oestringer LJ, Proppe C. 2019. On the calculation of a dry friction coefficient. PAMM
3. Tancogne-Dejean T, Spierings AB, Mohr D. Sep 2016. Additively-manufactured metallic micro-lattice materials for high specific energy absorption under static and dynamic loading. Acta Materialia116, 14-28.
4. Fíla T, Koudelka P, Falta J, Zlámal P, Rada V, Adorna M, et al. Feb 2021. Dynamic impact testing of cellular solids and lattice structures: Application of two-sided direct impact Hopkinson bar. International Journal of Impact Engineering148:103767
5. Neuhäuserová M, Fíla T, Koudelka P, Falta J, Rada V, leichrt J, et al. Aug 2021. Compressive Behaviour of Additively Manufactured Periodical Re-Entrant Tetrakaidecahedral Lattices at Low and High Strain-Rates. Metals11(8), 1196.
6. Janbaz S, Narooei K, Manen Tv, Zadpoor AA. 2020. Strain ratedependent mechanical metamaterials. Science Advances
7. Garland AP, Adstedt KM, Casias ZJ,White BC, Mook WM, Kaehr B, et al. Oct 2020. Coulombic friction in metamaterials to dissipate mechanical energy. Extreme Mechanics Letters 40, 100847.

Synchrotron X-Ray Diffraction for Investigating High Strain Rate Material Behavior

Matti Isakov[†], Veera Langi[†], Lalit Pun[†], Guilherme Soares[†], and Mikko Hokka[*†]

Tampere University, Materials Science and Environmental Engineering, Impact Laboratory
Keywords: Strain induced phase transformations, high strain rate, synchrotron, diffraction

Abstract: Stability of austenite in steels is highly important as it has a strong influence in the strain hardening behaviour of the alloy. The softer austenite can readily transform to much harder martensite bellow certain temperatures or during plastic deformation. The latter is especially interesting as the phase transformation also significantly improves the ductility and energy absorption capability of the steel. Unfortunately, the phase transformation rate is significantly lower at high strain rates due to adiabatic heating and the direct effects of strain rate on the kinetics of the phase transformation. Ultra-brilliant X-ray radiation available at modern synchrotron facilities offers possibilities to study the changes in the material structure using X-ray diffraction under dynamic loading. Recently, we have carried out measurements that demonstrate the capabilities of the technique at strain rates up to 10 s^{-1}. In this work we discuss the possibilities and limitations of the method and show examples of the recent measurements.

1. Introduction

The microstructure of the steels containing metastable austenite can change dramatically during plastic deformation. The austenitic phase can change to much harder martensite, and this phase transformation leads to higher strain hardening capability. At high strain rates, the phase transformation rate is considerably lower and because of this the alloys typically have low or even negative strain rate sensitivity [1]. In the past, the microstructure evolution of the steels has been investigated by various ex-situ methods such as electron microscopy and different diffraction methods. However, these experiments routinely require that the mechanical loading is interrupted when the microstructure is being examined, which leads to the inevitable fact that the thermomechanical history of the deforming specimen is not similar to a continuously deforming sample. The heat generated by the plastic work is transferred to the surroundings of the specimen when the mechanical loading is interrupted. Therefore, such experiments do not replicate the exact deformation history at high strain rates. Recently, some attempts have been made to utilize synchrotron radiation for in-situ characterization of the high strain rate deformation [2]. In these experiments a bulk specimen is deformed at a high rate, while the X-ray beam passes through the specimen allowing the transmission diffraction pattern to be examined from the opposite side. In the literature there are attempts for such measurements at strain rates up to 1000 s^{-1}. These experiments rely on imaging a scintillator plate with a high speed camera and analyzing the intensities and directions of the diffracted beams from the obtained optical images. While this method is fast and allows investigations of very high strain rate deformation, the use of the scintillator and a high speed camera are semi-qualitative measures of the diffracted intensities. Therefore, in our work we have focused on an alternative method at intermediate strain rates but at higher resolution. In this paper we present the capabilities and limitations of these new measurements and show examples how the method can be used for characterization of material structure during high strain rate deformation.

*Author for correspondence (mikko.hokka@tuni.fi).
†Present address: Present address: Tampere University, POB 589, 33014 Tampere, Finland

2. Experimental

For the mechanical loading of the specimens, we have designed and procured a high-speed miniature universal load frame (Psylotech µTS) that can be mounted on the hexapod sample manipulator at the DanMAX line. The load frame is equipped with two actuators allowing double strain rates compared to single actuator systems, and the symmetric loading of both ends of the specimen allows the center point of the specimen to be imaged with X-Ray without any need to reposition (or rotate) the specimen. The beam energy of 35 keV has strong transmission through 0.5 mm thick steel specimens, and the Pilatus 3X 2M detector allows frame rates up to 250 Hz, which gives approximately 2.5 diffraction images per a percent of deformation at the strain rate of 1 s^{-1}. The deformation of the specimen was observed with optical cameras and DIC was used to compute the strains on the surface. For the future experiments, we can also include a thermal camera or a pyrometer to track the temperature of the specimen during adiabatic deformation.

3. Conclusions

The results demonstrate that the synchronization between all the actions, i.e., mechanical loading of the specimen and the acquisition of the optical and X-Ray images are well synchronized. The measurement is capable of resolving the phase fractions of the studied steels in-situ during the deformation of the specimen at very high angular and intensity resolution. Finally, the measurement also provides new information on the atomic level stress-strain distribution during the macroscopic loading of the specimen. This measurement facilitates detailed analysis on the effects of strain rate on mechanically induced phase transformations, as exemplified by the novel results of a strain rate jump experiment carried out on a metastable austenitic stainless steel. The discussion followed by the presentation is expected to give new insights on how the methodology could be developed, and to discover new possible applications for the newly developed method.

References (Time New Roman 11, bolt):
1. Isakov M., Hiermaier S., Kuokkala V.-T., 2015, Effect of Strain Rate on the Martensitic Transformation During Plastic Deformation of an Austenitic Stainless Steel *Metall. Mater. Trans. A.* 46A, 2352-2355.
2. Finfrock, C, Ellyson B., Becker, C. et al. (2022). Resolving the Martensitic Transformation in Q&P steels in-situ at dynamic strain rates using synchrotron X-ray diffraction. *Metall. Mater. Trans. A.* https://doi.org/10.1007/s11661-022-06788-x

Visualizing Microstructure Effects on Shock Wave Propagation, Temperature Rise, and Phase Chain Utilizing Laser Array Raman Spectroscopy

A. Dhiman, T. Dillard[†], V. Tomar[*]

School of Aeronautics and Astronautics,
Purdue University, West Lafayette, Indiana, 47906, USA

Keywords: Shock wave, *In-situ* dynamic stress, mechanical Raman spectroscopy, Photon Doppler Velocimetry

*Author for correspondence (tomar@purdue.edu).
†Presenter
Aeronautics and Astronautics, Purdue University, 701 W Stadium Ave, West Lafayette, IN, 47907, USA

Abstract:

Quantifying phase change of materials during shock compression offers valuable insight when modelling temperature rise and reaction mechanisms within energetic materials. However, quantifying phase change within heterogeneous materials during shock compression is greatly limited by current diagnostic techniques. Previously, time-gated Raman Spectroscopy has been used for chemical analysis at the nanosecond time scale; however, these analyses were limited to a small domain or single point of measurement. In this work, we present a unique setup where measurements of Raman spectra can be observed at multiple points simultaneously across a microstructure using a laser array method. This technique was used to quantify the effect of friction and shock confinement occurring at the interface between two energetic crystals. The Shock-induced temperature distribution and phase-field were measured as a function of proximity between the energetic particles. The results show a correlation between temperature rise and melting of energetic material as a function of microstructure variation.

Introduction:

Understanding shock behaviour within a material is crucial to proper design and material choices in a wide array of applications such as space suits, satellites, and aircraft. In these applications, even the smallest objects moving at hypersonic velocities can cause massive damage. As such, these applications require the development of composites and materials capable of dissipating high-energy impact. The introduction of stress inside these materials induces a change in Raman shift which can be directly correlated to the equivalent stress [7; 8; 11; 12]. The in-situ measurement of the Raman shift during shock impact as a function of time can then be used to predict stress during the shock propagation and residual stress after the impact.

To allow researchers and scientists to observe high energy impacts across complex microstructures, in this work we have utilized time-gated mechanical Raman Spectroscopy. Because this is the only laboratory method of directly measuring the local stress inside materials at nanosecond time-scale, it has been developed as a robust technique for stress measurement under quasi-static [1;4;6] and shock impact conditions [5;10;9]

Methods:

The impacts were performed on HTPB samples fabricated using a mixture of R-45M liquid polybutadiene (Firefox Enterprise Inc.) and isophorone diiso-icyanate (IPDI) at an OH index ratio of 1.05. These materials were stirred manually and a vacuum was applied for 30 minutes to remove trapped air. The mixture was poured into molds with a depth of 1 mm. Finally, the samples were cured at 60° C in a convection oven for 7 days. In this work, a Princeton Instruments Raman spectrometer combined with an

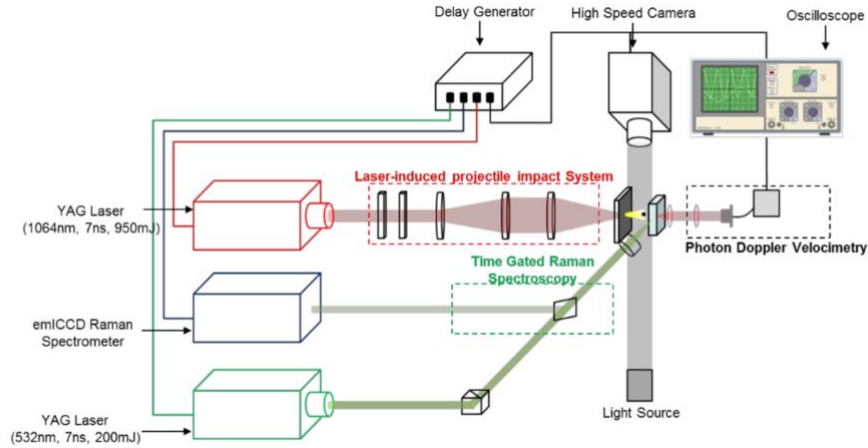emICCD (PI-MAX, ~500 picosecond resolution) was used to record the Raman spectra under shock impact.

Figure 1: Schematic of Particle Launch System and Time gated Mechanical Raman Spectroscopy

Figure 1[13] displays the schematic of the laser-induced particle system where 250μm Zirconia particles were accelerated by high energy expansions of plasma induced by laser ablation via 1064 nm pulse laser. The particle was accelerated for 500μm before hitting the Hydroxyl-terminated polybutadiene sample where sample deformation was recorded using a high-speed camera at a 0.9MHz frame rate. The system was integrated with photon Doppler velocimetry (PDV) to obtain nanosecond resolved information of impact velocity and local deformation speed at the area of impact within the sample.

Discussion:
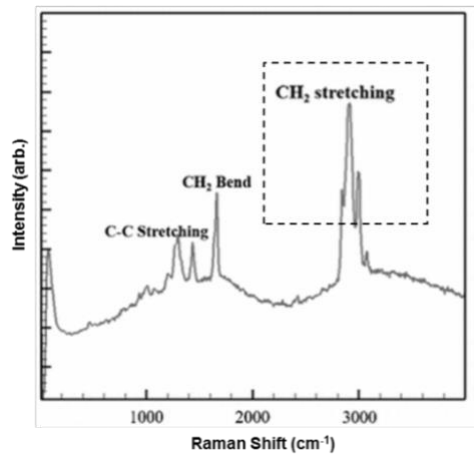
Figure 2: Raman spectrum for Hydroxyl- terminated polybutadiene

This work utilizes the observable change in Raman Shift to correlate stress within the Hydroxyl-Terminated polybutadiene caused by shock impacts. The Raman shift corresponding to CH2 stretching as shown in Figure 2[13] was analysed using fitting of three Gaussian peaks and change was observed for peaks around 2915 cm^{-1} with arrival of shock and aftershock. The max peak shift observed with the arrival of shock lasted less than 100nm followed by an exponential decay after the shock. The max peak shift was calibrated with an analytical solution for 1D longitudinal stress propagation inside a rod using equation 1[2; 3] where ρ is the ambient density, U_s is the shock velocity, and U_{p_max} is the maximum particle velocity.

$$\sigma_{max} = \rho U_s u_{p\_max} \tag{1}$$

Conclusion: Utilizing a 532nm laser array with Raman spectroscopy in combination with photon doppler velocimetry, Shock patterns and stress evolutions across interfaces were observed via change in Raman shift. This particular technique provides the ability to study shock as it interacts with interfaces within complex material structures. With this technique shock waves were observed to exponentially decay after impact.

References
1. Gan, M., Samvedi, V., & Tomar, V. Raman spectroscopy-based investigation of thermal conductivity of stressed silicon Microcantilevers. Journal of Thermophysics and Heat Transfer, 29(4), 845-857 (2014). doi: https://doi.org/10.2514/1.T4491

2. Akhondizadeh, M. Analytical solution of the longitudinal wave propagation due to the single impact. Journal of Low Frequency Noise Vibration and Active Control, 37(4), 849-858 (2018). doi: 10.1177/1461348418793122

3. Millett, J. C. F., Bourne, N. K., & Akhavan, J. The response of hydroxy-terminated polybutadiene to one- dimensional shock loading. Journal of Applied Physics, 95(9), 4722-4727 (2004). doi: 10.1063/1.1689758

4. Gan, M., & Tomar, V. An in situ platform for the investigation of Raman shift in micro-scale silicon structures as a function of mechanical stress and temperature increase. Review of scientific Instruments, 85(1), 013902 (2014). doi: https://doi.org/10.1063/1.4861201

5. Hebert, P., Bouyer, V., Rideau, J., Doucet, M., & Terzulli, L. P. Raman Spectroscopy Study of Laser- Shocked Tatb- Based Explosives. Shock Compression of Condensed Matter - 2011, Pts 1 and 2, 1426 (2012). doi: 10.1063/1.3686587

6. Prakash, C., Gunduz, I. E., Oskay, C., & Tomar, V. Effect of interface chemistry and strain rate on particle-matrix delamination in an energetic material. Engineering Fracture Mechanics, 191, 46-64 (2018). doi: https://doi.org/10.1016/j.engfracmech.2018.01.010

7. Verma, D., & Tomar, V. Interface Mechanical Strength and Elastic Constants Calculations via Nano Impact and Nanomechanical Raman Spectroscopy. Fracture, Fatigue, Failure and Damage Evolution, Vol 7, 1-5 (2018). doi: 10.1007/978-3-319-62831-8_1

8. Prakash, C., Olokun, A., Gunduz, I. E., & Tomar, V. (2019). Interface Mechanical Properties in Energetic Materials Using Nanoscale Impact Experiment and Nanomechanical Raman Spectroscopy Nano-Energetic Materials (pp. 275-290): Springer.

9. Tang, C., Song, Y. F., Liu, X. S., Zhu, X. J., Liu, W. L., Yang, Q. X., . . . Yang, Y. Q. Characterization of laser- driven shock compression by time-resolved Raman spectroscopy. Physica Scripta, 94(1) (2019). doi: Artn 01540110.1088/1402-4806.Aaee1e

10. Rastogi, V., Chaurasia, S., Rao, U., Sijoy, C. D., Mishra, V., Kumar, M., . . . Deo, M. N. Time-resolved Raman spectroscopy of polystyrene under laser driven shock compression. Journal of Raman spectroscopy, 48(7), 1007- 1012 (2017). doi: 10.1002/jrs.5166

11. Zhang, Y., Wang, H., & Tomar, V. Visualizing Stress and Temperature Distribution During Elevated Temperature Deformation of IN-617 Using Nanomechanical Raman Spectroscopy. Jom, 70(4), 464-468 (2018). doi: 10.1007/s11837-017-2710-2

12. Zhang, Y., Prakash, C., & Tomar, V. (2019). In-situ Crack Tip Stress Measurement at High Temperature in IN-617 Using Combined Nano-Indentation and Nano-Mechanical Raman Spectroscopy Fracture, Fatigue, Failure and Damage Evolution, Volume 6 (pp. 51-56): Spring

13. Dhiman, A., Dillard, T., & Tomar, V.(2022). Visualizing Shock Induced Thermo-Mechanical Change at Bi-crystal Interface Using Laser Array Based Nano-second Raman Spectral Imaging. (Submitted)

12. Zhang, Y., Prakash, C., & Tomar, V. (2019). In-situ Crack Tip Stress Measurement at High Temperature in IN-617 Using Combined Nano-Indentation and Nano-Mechanical Raman Spectroscopy Fracture, Fatigue, Failure and Damage Evolution, Volume 6 (pp. 51-56): Spring

Effect of carbon nanotube interlayers on the low velocity impact damage resistance of CFRP composites

Karthik Ram Ramakrishnan[1*], Zhifang Zhang[2]

1Bristol Composites Institute, University of Bristol, BS8 1TL, United Kingdom

2Research Center for Wind Engineering and Engineering Vibration, Guangzhou University, Guangzhou, 510006, China

Abstract: Carbon nanotubes have emerged as promising nano-scale reinforcement for improving the mechanical properties of composites. A new technique for introducing the nano-reinforcements in the composite is the use of thin CNT films as interleaves between composite layers. In this article, the impact resistance of carbon fibre reinforced composite (CFRP) with CNT interlayers are investigated experimentally using drop tower impact testing. High speed imaging was used to observe the initiation of damage in the composite. The study shows that the addition of CNT interleaves is an effective way to improve impact damage resistance.

1. Introduction

The latest generation of advanced FRP composites with nano-scale reinforcements such as carbon nanotubes (CNT), carbon nano fibres (CNF), graphene or nanoclay are expected to find increasing use in aerospace applications in the following years [1]. These multi-scale or hierarchical composites provide improved structural properties such as excellent delamination resistance and in-plane mechanical properties in addition to non-structural properties such as improved thermal and electrical conductivity, electromagnetic shielding, self-sensing behaviour, etc [2]. A substantial amount of research on nano-reinforcements has been directed towards improving the impact damage resistance of composites. Several researchers [3–7] have studied the effect of CNTs embedded in the matrix on the impact damage resistance of carbon fibre composites. An alternative approach is stacking films, fabrics or veils containing the nanoparticle in-between CFRP layers during the lamination process of the composite structures [8–12]. The CNT film is a thin macro-assembly of a large number of individual CNTs. The use of CNT porous sheets called Bucky papers (BP) which are impregnated during the first stages of the curing is versatile technique that can be used for other nanomaterials. The use of CNT films and bucky papers for introducing the nanophase has the advantage that it can promote the adoption of nanotechnology in industrial environment through integration with existing manufacturing processes and infrastructure. In this paper, the low velocity impact damage resistance of CFRP composites with CNT film interlayers is investigated using drop tower impact testing. Two configurations of the interleaved CNT films, namely two plies (CNT2) and four plies (CNT4) are compared to the reference case of CFRP composite with no CNT film interlayers (CNT0).

2. Methodology

The low velocity impact tests are typically conducted using falling weight impact testing machine or drop tower and the force, displacement and velocity histories are measured [24]. In the present study, the impact

tests were conducted using an Instron® CEAST 9250 drop tower setup. Square plates of 70 mm length were clamped between two steel plates with a hole of internal diameter 40 mm. A hemispherical steel impactor of 20 mm diameter was used for the impact tests. The mass of the impactor carriage was 6.15 kgs. Photron SA-Z high-speed camera was used to acquire images of the lower surface of the target at a frame rate of 20000 fps and resolution of 1024 x 1024 pixels. A mirror was placed at a 45°angle under the test area as shown in Fig. 1 (c) allowing the camera to capture the reflected image of the lower surface. LaVision image splitter was used to obtain stereo images of the sample. A speckle pattern was painted on to the surface of the composite target. Stereo DIC analysis was performed on the images to measure the full-field displacement of the target surface. The drop tower is equipped with pneumatic rebound catcher system to arrest the impactor after the initial impact and to avoid repeated loads on the target.
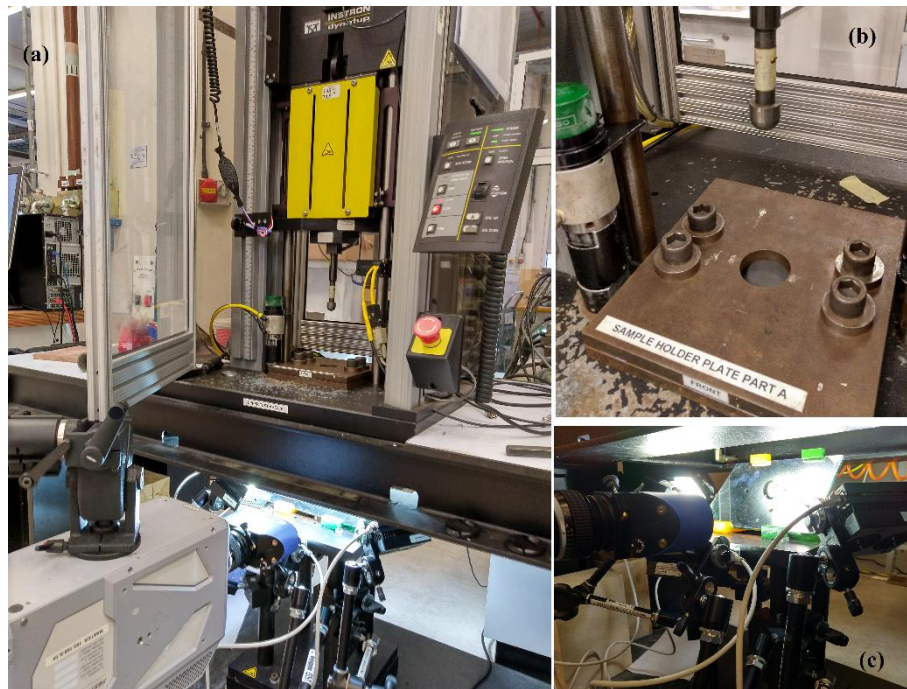
Figure 1: Drop tower impact test setup

References:

[1]   Kostopoulos V, Masouras A, Baltopoulos A. A critical review of nanotechnologies for composite aerospace structures. CEAS Sp J 2017;9:35–57. https://doi.org/10.1007/s12567-016-0123-7.

[2]   Saghafi H, Fotouhi M, Minak G. Improvement of the Impact Properties of Composite Laminates by Means of Nano-Modification of the Matrix—A Review. Appl Sci 2018;8:2406. https://doi.org/10.3390/app8122406.

[3]   Kostopoulos V, Baltopoulos A, Karapappas P, Vavouliotis A, Paipetis A. Impact and after-impact properties of carbon fibre reinforced composites enhanced with multi-wall carbon nanotubes. Compos Sci Technol 2010;70:553–63. https://doi.org/10.1016/j.compscitech.2009.11.023.

[4]   Kara M, Muhammed K, Caner A, Avc A. Impact behavior of carbon fi ber / epoxy composite tubes reinforced with multi-walled carbon nanotubes at cryogenic environment. Compos Part B Eng 2018;145:145–54. https://doi.org/10.1016/j.compositesb.2018.03.027.

[5]   Soliman EM, Sheyka MP, Reda M. Low-velocity impact of thin woven carbon fabric composites incorporating multi-walled carbon nanotubes. Int J Impact Eng 2012;47:39–47. https://doi.org/10.1016/j.ijimpeng.2012.03.002.

[6]   Mahdi TH, Islam ME, Hosur M V., Jeelani S. Low-velocity impact performance of carbon fiber-reinforced plastics modified with carbon nanotube, nanoclay and hybrid nanoparticles. J Reinf Plast Compos 2017;36:696–713. https://doi.org/10.1177/0731684417693429.

[7]   Moumen A El, Tarfaoui M, Hassoon O. Experimental Study and Numerical Modelling of Low Velocity Impact on Laminated Composite Reinforced with Thin Film Made of Carbon Nanotubes 2018:309–20. https://doi.org/10.1007/s10443-017-9622-8.

[8]   Wang S, Downes R, Young C, Haldane D, Hao A, Liang R, et al. Carbon Fiber/Carbon Nanotube Buckypaper Interply Hybrid Composites: Manufacturing Process and Tensile Properties. Adv Eng Mater 2015;17:1442–53. https://doi.org/10.1002/adem.201500034.

[9]   Li T, Li M, Gu Y, Wang S, Li Q, Zhang Z. Mechanical enhancement effect of the interlayer hybrid CNT fi lm / carbon fi ber / epoxy composite 2018;166:176–82. https://doi.org/10.1016/j.compscitech.2018.02.007.

[10]   Cheng X, Liu L, Feng X, Shen L, Wu Z. Low Temperature-Based Flexural Properties of Carbon Fiber / Epoxy Composite Laminates Incorporated with Carbon Nanotube Sheets 2019;1900247:1–10. https://doi.org/10.1002/mame.201900247.

[11]   Marriam I, Xu F, Tebyetekerwa M, Gao Y, Liu W, Liu X. Synergistic e ff ect of CNT fi lms impregnated with CNT modi fi ed epoxy solution towards boosted interfacial bonding and functional properties of the composites 2018;110:1–10. https://doi.org/10.1016/j.compositesa.2018.04.011.

[12]   Ou Y, Gonzalez C, Vilatela J. Understanding interlaminar toughening of unidirectional CFRP laminates with carbon nanotube veils. Compos Part B 2020;201. https://doi.org/10.1016/j.compositesb.2020.108372.

Enhance crashworthiness of 3D printed cellular materials

Utzeri M.[†*1] **Scapin M.**[2] **Sasso M.**[1] **Peroni L.**[2]

[1]*Polytechnic University of Marche, Department of Industrial Engineering and Mathematical Sciences, 12 Breccie Bianche, Ancona 60131, Italy*
[2]*Polytechnic of Turin, Department of Mechanical and Aerospace Engineering, 24 Corso Duca degli Abruzzi, Turin, 10129, Italy*
Keywords: Cellular material, Additive Manufacturing, Crashworthiness, Polymer

Abstract: Cellular materials are the subject of much attention due to their excellent mechanical properties. They should be applied in energy absorbers or structural components with an optimised mass distribution. In this work, 3D printed Gyroid structures with different densities were considered. Two types of additive manufacturing technologies and materials were analysed: Fused Filament Fabrication of nylon reinforced with short carbon fibres and Digital Light Processing of photo-reactive liquid resin. Compression tests were performed under quasi-static and dynamic loading conditions and the results were compared in terms of specific energy absorption. Moreover, the Gyroid structures were coated in order to enhance their crashworthiness properties.

Summary

Two Additive Manufacturing technologies were used to prepare the samples. Fused Filament Fabrication (FFF) technique was adopted for samples made of PA reinforced by short carbon fibers; Masked Stereolithography (MSLA) technique was adopted for samples made of photo-reactive liquid resin. The raw resin is a commercial high-quality resin named Premium Tough, Liqcreate product. The resin has crystal-clear transparency and a peculiar mechanical property as high toughness and large strain to failure.

The TPMS structures were designed by means of Topology software. The nTopology software can generate a wide range of architecture and cellular materials. Among them, the Gyroid structure was chosen.

In order to measure the effective structures mechanical properties, the cubic volume of 30 mm side was filled with 8-unit cells. This arrangement 2x2x2 guarantees a great compromise in terms of maximum size can be tested and boundary condition effects on the unit cell behaviour. The scaffolds of unit cells are reported in Figure 1(a). The wall thickness was changed in order to manage the density: for each structure, two different wall thicknesses were considered achieving relative density equal to 15%, 20%.
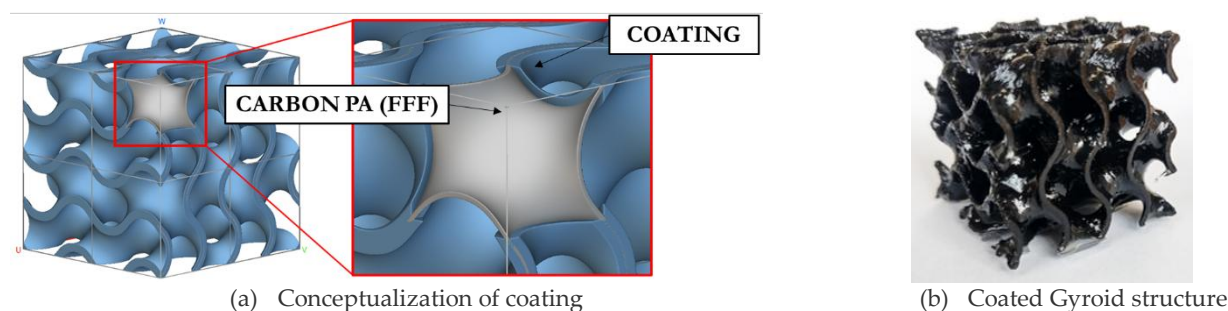

(a) Conceptualization of coating   (b) Coated Gyroid structure

Figure 1: Coating.

Furthermore, the 3D printed Gyroid structures were coated with a gelcoat based on epoxy resin, Prochima

product, as shown in Figure 1(b). The coated structure increases the relative density of the base structure by 2%. Quasi-static and medium strain-rate compression tests were performed by an electrodynamic testing machine (Electroforce3500 - TA Instruments), available at DYNLab laboratory at Politecnico di Torino. The tests were conducted at a nominal strain-rate of 10^{-3} and 3×10^1 s^{-1}. The medium strain-rate tests were recorded with a high speed camera (Photron AX50). Thanks to the high epoxy resin toughness, the TPMS structures can be compressed without reaching explosive failure. Both Gyroid structures show the common linear stage after the yielding point. This post-yielding behaviour can be similar to a plateau when the relative density is low. When the relative density increases, the post-yielding slope becomes more and more relevant. Both TPMS structures show a specific strain where a first failure occurs during the plastic region. After these points, the stresses drop down without reaching zero and the densification phase begins. This kind of stress-strain curve is preferable when high specific absorption energy (SEA) is required on industrial applications.
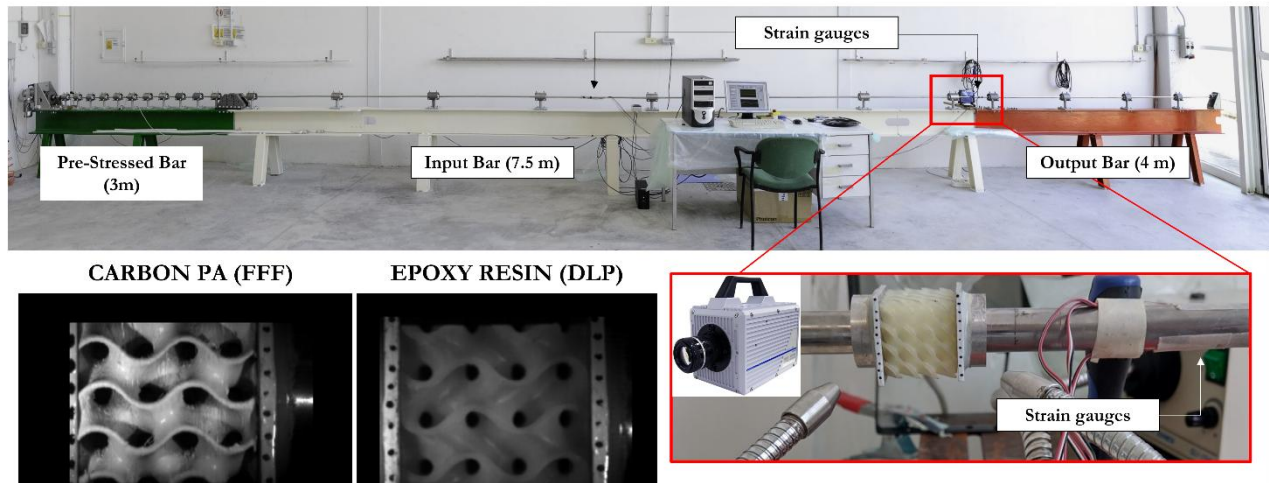
Figure 2: Split Hopkinson Pressure Bar

Dynamic tests were performed by a Split Hopkinson bar, available at the lab of Polytechnic University of Marche in Figure 2, which is a direct tension-compression Hopkinson bar made of three aligned bars, named pre-stresses (3m), input (7.5m) and output bar (4m). Each test was recorded by a Photron® SA4 at 100 kfps. The compressive behaviour was determined by multistage compressive waves because of the high deformation need. The strain signal was obtained by image analysis. The specimen equilibrium was checked considering the input, transmitted, and reflected waves. So, the higher strain rate achieved was 150 1/s. The stress was determined by the transmitted wave on the output bar. The signals are showed in Figure. 3.
The stress strain curve was obtained filtering the raw data stress-strain measured as Figure 4 shows.
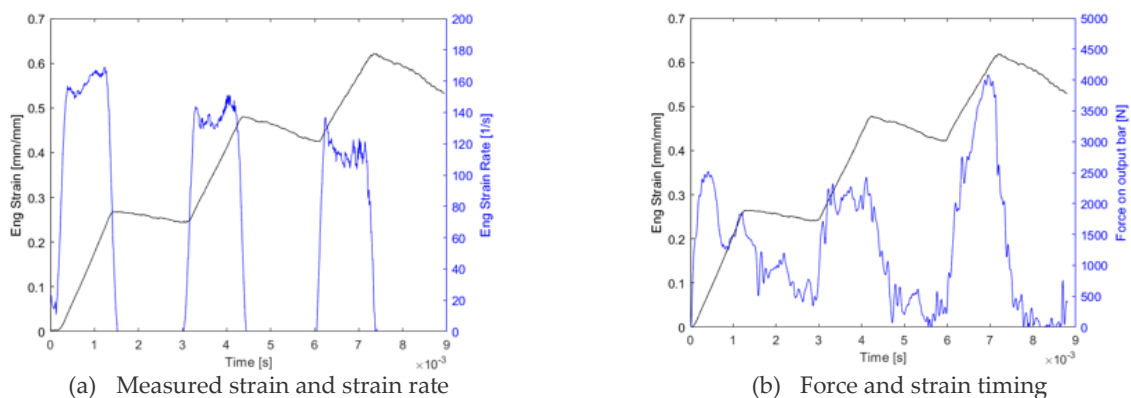

(a) Measured strain and strain rate   (b) Force and strain timing

Figure 3: Signals of multi-stage compression

The experimental results showed a dependence of the engineering stress-strain curves on the relative density. In addition, both materials are very sensitive to strain-rate variations, significantly increasing its resistance under dynamic conditions. The yielding point of the Gyroid structure with 15% and 20% relative density reaches about four times the yielding point under quasi-static loading. However, the strain rate sensibility leads to brittle behaviour of the epoxy resin thus the TPMS structures are no longer able to withstand higher deformations. However, the Carbon-PA does not become brittle as the epoxy resin under dynamic loading.

The Gyroid structures made by Carbon-PA are able to withstand high deformation and absorb energy during the impact. Indeed, they show a relevant plastic phase after the yielding point. Moreover, the TPMS structure made by MSLA shows a relevant fragmentation during the compression phase.
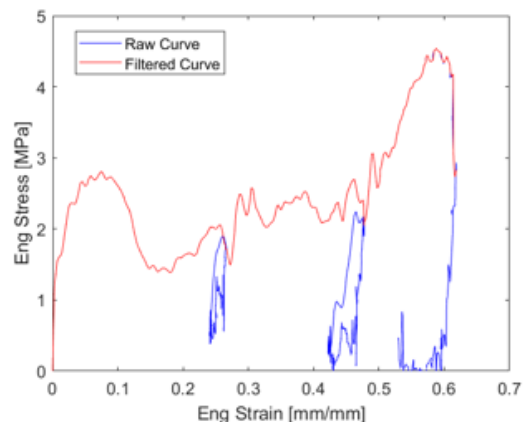

Figure 4: Post-processing of stress-strain curve

A laboratory-scale instrumented hammer for intermediate strain rate testing: Application to hot forging of nickel-based superalloys

J. Agirre[1], J. Mendiguren[1], B. Erice[1,2], N. Otegi[1], L. Galdos[1]

[1] *Department of Mechanics and Industrial Production, Mondragon Unibertsitatea, Loramendi 4, 20500 Mondragon, Spain*
[2] *IKERBASQUE, Basque Foundation for Science, Bilbao, Spain*

Keywords: Forging, plasticity, intermediate rate testing, nickel-based superalloys

Abstract: Hammer forging is a widely employed manufacturing process in which the initial billet, that usually has a simple geometry, is plastically deformed in one or more operations to produce parts with complex final geometries. It is frequently employed to produce components for the automotive, the aeronautical or the oil and gas industries where high strength and ductility products are required, as it is cost effective for large series production [1]. The main characteristic of the forging hammers is the large deformation speeds achieved when forming the material. The strain rate that the material undergoes during hammer forging operations typically ranges from 10 up to 300 s^{-1}, while in the case of mechanical or hydraulic press forging it does not exceed 30 s^{-1} [2].

Mechanical testing within this strain rate range using hydraulic universal testing machines equipped with conventional load cells becomes extremely challenging due to their limited stroke velocities and the difficulties to acquire smooth load measurements. Split Hopkinson Pressure Bar (SHPB) systems could be used for intermediate rate testing but they have certain limitations at this strain rate range (< 300s^{-1}) [3]. For that reason, an automated laboratory-scale hammer was developed and validated, which was equipped with a heating system (Figure 1). This novel thermomechanical tester was employed to experimentally characterise the flow behaviour and microstructural evolution of Inconel 625 nickel-based superalloy under hot hammer forging conditions, combining both intermediate strain rates (≈300 s^{-1}) and high temperatures (>1,000ºC) (Figure 2).
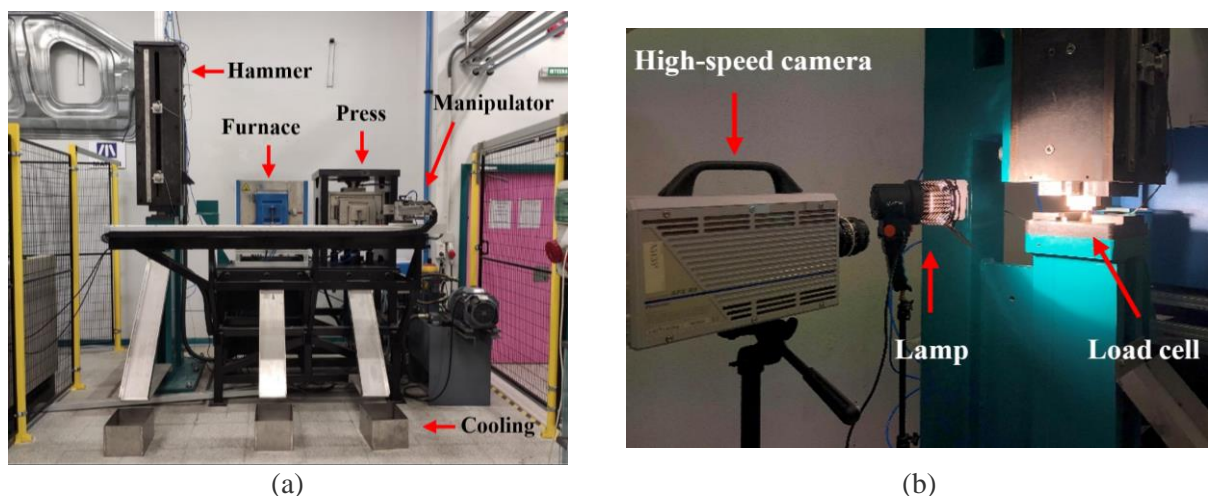
(a)   (b)

Figure 1: a) Laboratory-scale instrumented forging hammer. b) Close-up of the experimental setup that includes a high-speed digital camera.

*Author for correspondence (jagirreb@mondragon.edu).
†Present address: Department of Mechanics and Industrial Production, Mondragon Unibertsitatea, Loramendi 4, 20500 Mondragon, Spain

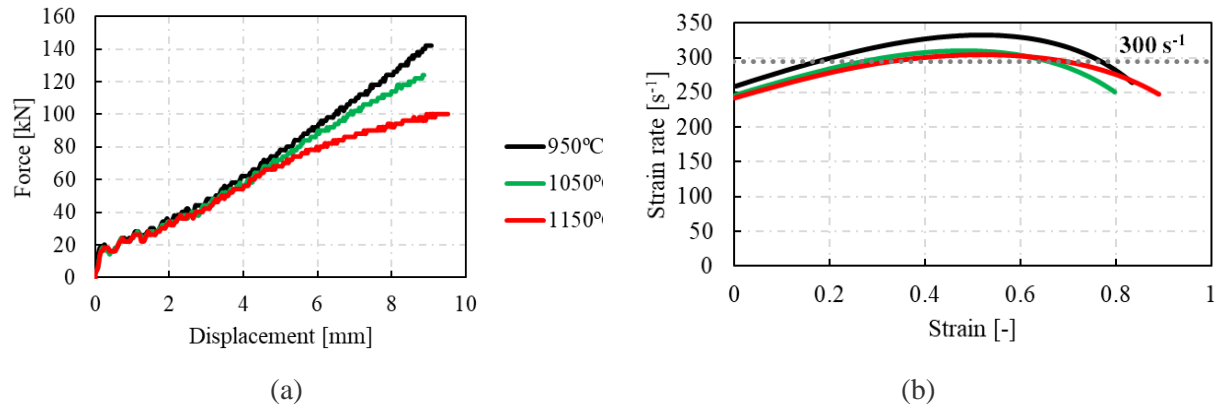(a)   (b)

Figure 2: a) Experimental force-displacement curves of Inconel 625 obtained from uniaxial compression tests performed at the instrumented hammer at 950ºC, 1,050ºC and 1,150ºC. b) Strain rate evolution during the tests.

References:

[1]   T. Altan and G. Ngaile, *ASM Cold and Hot Forging*. 2005.

[2]   Y. V. R. K. Prasad, K. P. Rao, and S. Sasidhara, *Hot Working Guide - A Compendium of Processing Maps*, 2nd ed. 2015.

[3]   G. Gary and D. Mohr, "Modified Kolsky Formulas for an Increased Measurement Duration of SHPB Systems," *Exp. Mech.*, vol. 53, no. 4, pp. 713–717, 2013.

Mechanical characterisation and constitutive modelling of single layer UHMWPE composite: application to low-velocity impact loading

T. Poulet*,[1,2,3,4], A. Bracq[1], Y. Demarty[1], P. Respaud[2], J. Beugels[2], B. Bennani[4], N. Bahlouli[3], F. Lauro[4]

[1] *French-German research institute of Saint-Louis, 5 rue du Général Cassagnou, 68300 Saint-Louis, France*
[2] *Tencate Advanced Armour France, 50 Route du Louvier, 38270 Primarette, France*
[3] *ICUBE Laboratory, UNISTRA, 2 rue Boussingault, 67000 Strasbourg, France*
[4] *LAMIH Laboratory, UPHF, 180 rue Joseph-Louis Lagrange, 59300 Famars, France*

Keywords: UHMWPE, mechanical testing, digital image correlation, finite element analysis, drop tower impact testing

Abstract: Ultra-High Molecular Weight Polyethylene (UHMWPE) fibre composites are commonly used in bulletproof vests as a result of their high tensile stiffness and strength, as well as a low density. The characterisation of the material's mechanical behaviour is necessary in order to accurately model a ballistic impact and its complex failure mechanisms. In-plane tensile properties of the composite are determined at the layer scale over a wide range of strain rate using various testing apparatus and the digital image correlation technique. An orthotropic material model with strain rate sensitivity available in LS-DYNA® is chosen to describe the composite behaviour. Drop tower impact experiments are performed to assess the proposed material model.

1. Introduction

UHMWPE based composites are one of the most advanced materials used in bulletproof vests thanks to a high tensile stiffness and strength as well as a low density. For ballistic impact modelling purposes using finite element (FE) tools, the mechanical characterisation of the material is mandatory. Testing conditions in terms of loading modes and strain rates have to match the ones occurring during a ballistic impact event [1]. The composite is often considered at the layer scale in numerical models [1-3]. Therefore, the mechanical characterisation should be conducted at the same scale [4]. The aim of the study is twofold. Firstly, a commercially available UHMWPE fibres reinforced composite is characterised over a wide range of strain rate and loading directions. Secondly, a constitutive material model is chosen and associated model parameters are identified. For material model assessment, drop tower impact experiments are developed and performed.

2. Materials and methods

In this work, the Dyneema® HB210 UHMWPE fibre composite is studied. This material is made of a polyurethane matrix and SK99 fibres. The mechanical characterisation is carried out on one layer of the material, composed of four plies in [0°, 90°, 0°, 90°] configuration, with an average thickness of about 160 µm. The in-plane tensile mechanical behaviour of the composite is characterised in both quasi-static and dynamic conditions, covering strain rates ranging from 10^{-4} to 100 s^{-1}. In order to investigate the strain rate influence, various experimental methods for the universal press, drop tower, and split Hopkinson tensile bars were developed. Two loading directions were considered. For the first one, the samples were positioned perpendicularly relative to the fibres, as for the second one the fibres were diagonal to the loading axis. Combined with the previously mentioned numerical scale considerations, structural effects are minimised due

---

to the low thickness of the samples. Therefore, the high degree of scattering in the material properties at 0° of the fibres, [4], could be avoided, together with the problematic influence of thickness discussed in [5]. Puncture impact experiments were conducted using a drop tower apparatus at an initial velocity of 4 m/s. A circular sample of 100 mm in diameter was impacted by a rigid 10 mm hemispherical indenter. An orthotropic material model with strain rate sensitivity, available in LS-DYNA, was chosen to describe the composite material behaviour. This model considers 8-node hexahedral solid elements.

3. Results and discussion

To measure local strains and to examine strain homogeneity, digital image correlation has been systematically used during experiments. An almost linear stress-strain response is obtained, shown in Figure 1, similar to the observations in [4]. Moreover, it can be observed on the figure that the responses obtained in HB210 present a higher modulus and strength compared to the previous grade HB26. This is due to the increase of mechanical properties of the latest fibre (SK99) compared to the older one used in HB26 (SK76), as shown in literature. Figure 2 shows the force-time histories obtained after repeated impact tests using a drop tower system. Sample slipping was avoided and the repeatability of measurements and failure mechanisms ensure that such tests can be used to validate the material model identified using in-plane characterisation tests.
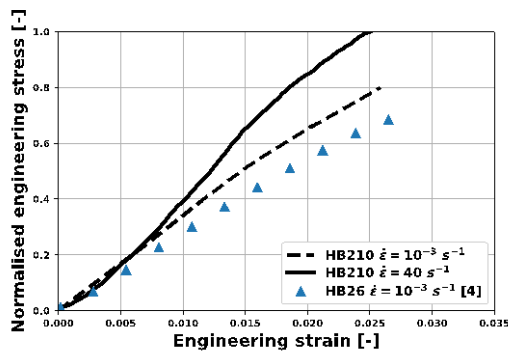
Figure 1: Comparison of stress-strain curves at 0° of HB26 and 210 at two strain rates.
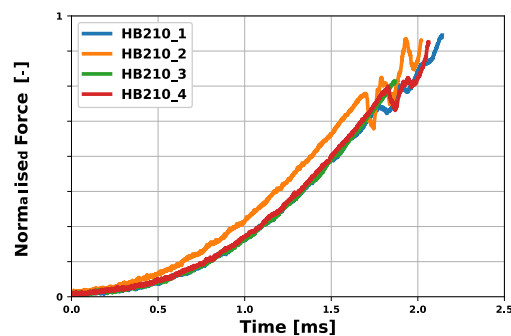
Figure 2. Force-time histories during puncture impact tests at an initial velocity of 4 m/s on a circular HB210 sample.

References:
1. Hazzard, M. K., Trask, R. S., Heisserer U., Van Der Kamp, M., and Hallet, S. R. 2018. Finite element modelling of Dyneema® composites: From quasi-static rates to ballistic impact. *Compos. Part A Appl. Sci.* **115**, 31-45. (https://doi.org/10.1016/j.compositesa.2018.09.005)
2. Lässig, T., Nguyen, L., May, M., Riedel, W., Heisserer, U., van der Werff, H., and Hiermaier, S. 2015. A non-linear orthotropic hydrocode model for ultra-high molecular weight polyethylene in impact simulations. *Int. J. Impact Eng.* **75**, 110-122. (https://doi.org/10.1016/j.ijimpeng.2014.07.004)
3. Camalet. T. 2020. Caractérisation et modélisation du comportement dynamique des matériaux constituant une structure de protection céramique-composite. Thesis, Strasbourg. (http://www.theses.fr/s164305)
4. Heisserer, U., and van der Werff, H. 2016. Strength matters: Which strength of Dyneema® fiber composites to use in hydrocode models? – A discussion. *29th International Symposium on Ballistics.*
5. Iannucci, L., Del Rosso, S., Curtis, P. T., Pope, D. J., and Duke, P. W. 2018. Understanding the Thickness Effect on the Tensile Strength Property of Dyneema®HB26 Laminates. *Materials* **11**. (https://doi.org/10.3390/ma11081431)

Response of polymer-based interpenetrating phase composites in impact loads

Agyapal Singh[a], Oraib Al-Ketan[a,b] , Nikolaos Karathanasopoulos[a,c*]

[a]New York University (NYU), Department of Engineering, Abu Dhabi Campus, UAE
[b]Core Technology Platforms (CTP), New York University Abu Dhabi, Abu Dhabi, UAE
[c]Department of Mechanical and Aerospace Engineering, Tandon School of Engineering, New York University, Brooklyn, NY, 11201, USA

Keywords: TPMS, IPC, Composites, Additive manufacturing, Drop Tower, Impact

Abstract: Nature-inspired architected materials premise effective property combinations that are well beyond the limits of classical engineering materials. The current study expands the study of architected, single phase and interpenetrating phase composites (IPC) with regular periodic inner phase reinforcements in the dynamic loading range. In particular, sheet-based IWP and Fisher-Koch TPMS lattice architectures with reinforcement phase contents of 20, 25 and 30% are investigated under static and dynamic loadings. To that scope, static and impact drop tower tests with different testing speeds as low as 0.5, and up to 6.5 m/s are performed, resulting in strain rates ranging from $\dot{\varepsilon} = 10^{-3}\ s^{-1}$ up to $\dot{\varepsilon} = 5000\ s^{-1}$. For the specimen manufacturing, VeroPureWhite was used as the reinforcement phase and TangoBlackPlus as the matrix, constituting the soft rubbery material of the interpenetrating phase (Fig. 1) The impact of the strain rate on the effective plateau stress and overall energy absorption of the metamaterial specimens is quantified. Differences in-between the IWP and Fisher-Koch based architectures are observed, while strain rate and density dependent differences are quantified. It is shown that IPC designs can absorb up to nearly three times the energy of their corresponding single phase counterparts, with the exact difference to depend on the strain rate. The study provides evidence that TPMS-based interpenetrating phase composite structures are excellent energy absorption candidate materials not only for static, but also for high strain-rate loading applications.
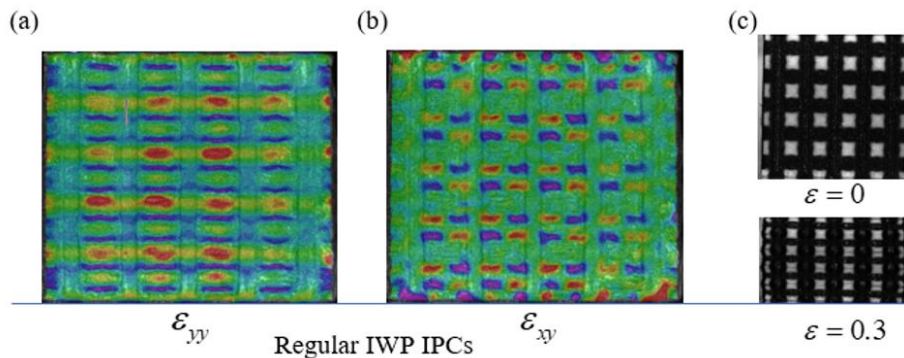
Figure 1: *Digital image correlation (DIC) normal (ε_{yy}) and shear (ε_{xy}) strain fields for regular IWP IPC designs along with the deformed state under static testing in (c).*

Acknowledgments

Treviso, Italy.

Dynamic characterisation of two spinel ceramics

Jean-Luc Zinszner[a], Christophe Coureau[b], David Lebaillif[c]

[a]CEA, DAM, Gramat, FR-46500 Gramat, France
[b]Solcera, FR-27000 Evreux, France
[c]Nexter Systems, FR-78022 Versailles Cedex, France

Abstract:

Since the sixties, ceramics are commonly used for designing high performance armours. Indeed, they present very high compressive strengths combined with low densities. However, the maximum tensile strength that the material can withstand is generally lower by one order of magnitude in comparison with their compressive strength. This relatively low tensile strength combined with the brittle behaviour of ceramics leads to a fragmentation of the target during a ballistic impact. Thus, the knowledge of the dynamic tensile and dynamic compressive behaviour of these materials is essential if one wants to simulate the ballistic response of the material.

In this study, two spinel ceramics used for the design of transparent armours and having different microstructures are characterised under dynamic compressive and dynamic tensile loadings. For performing the tests, a high-pulsed power generator allowing to generate a ramp loading is used. A strong influence of the material's microstructure on its dynamic behaviour is observed. The spinel having the finest microstructure indeed presents a Hugoniot elastic limit two time greater than the other spinel. Strong differences are also observed in terms of spall stresses and strain-rate sensitivities.

Introduction

Advanced ceramic materials are well known for a wide range of applications, such as electrical insulators, semiconductors or biomedical implants. Another application is their use as protective materials in the front face of bi-layered armour configurations. Indeed, with their outstanding hardness and compressive strengths, they allow to shatter the projectile during impact. Moreover, ceramics also present a low density, which is generally more than the half of steel density, allowing a significant weight benefit in comparison to monolithic steel plate armours. However, due to their relatively low tensile strength (in comparison with their compressive strength) and their brittle behaviour, a fragmentation of the ceramics is also observed during an impact. Thus, in order to numerically simulate the impact of a projectile against a bi-layered armour with ceramics in front plate, one has to well characterise the dynamic behaviour of the ceramic.

For the design of transparent armours, spinels appear as very interesting materials. Indeed, they present a low producing cost in comparison with sapphires and they are more resistant than glass materials. In this study, the dynamic compressive behaviour and the dynamic tensile behaviour of two transparent spinel ceramics are characterised. The two spinels are provided by two different companies. The first spinel, called US Spinel, is provided by the american company Coorstek. This spinel presents a coarse grain microstructure, with a mean grain size about 100µm. The second spinel, provided by the French company Solcera and called FR Spinel, presents a finer microstrusture with a grain size less than 10µm.

Methods and results

The dynamic characterisations are performed by using the GEPI machine [1], located in CEA Gramat. The GEPI machine is based on High Pulsed Power (HPP) technologies. This generator applies the strip line concept: two aluminium plane electrodes, separated by dielectric foils and locally connected by a short circuit are subjected to an intense current focused on the load region. In those experiments, the current reaches a maximum intensity of 3.3 MA in nearly 0.5μs. The association of current and magnetic field produces Lorentz forces applied on the internal face of the electrodes. This pressure pulse then propagates through the electrodes and through the specimens.

The use of this kind of generator gives many advantages in comparison to plate impact experiments that are generally performed for dynamic characterisations. For the characterisation of the dynamic compressive behaviour, the symmetry of the GEPI configuration and the isentropic loading applied to the materials allows performing a lagrangian analysis [2]. This method allows determining the whole loading path of the material whereas only one point on this loading path can be obtained after one plate impact experiment. After calculating the axial stress with the lagrangian analysis, the knowing of the equation of state of the material allows accessing to the evolution of the deviatoric stress. Strong differences in terms of Hugoniot Elastic Limit (HEL) and in terms of deviatoric stress between the two spinel grades. The FR Spinel grade presents a HEL about 14.5GPa whereas the US Spinel grade exhibits a HEL about 7.8 GPa. The maximum deviatoric stress that the material can sustain is also two times greater for the FR Spinel grade (Figure 1a).
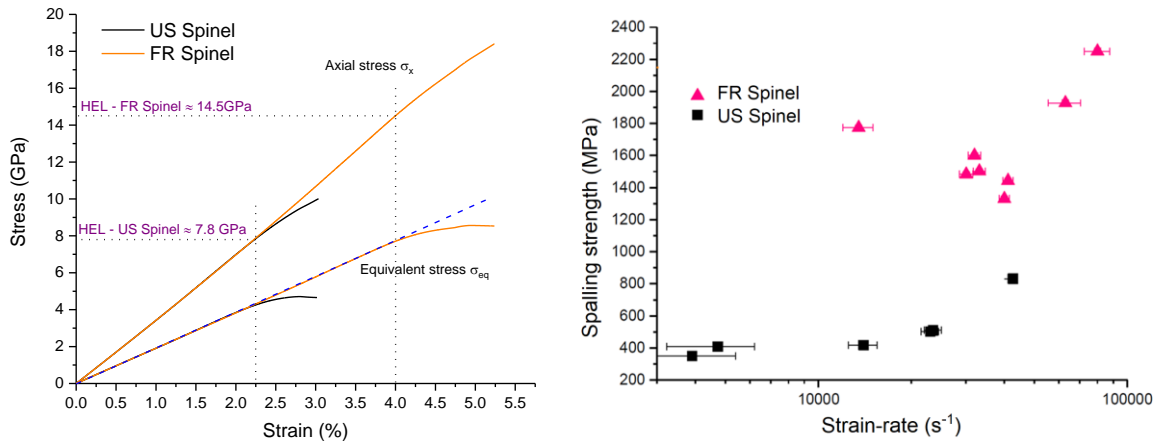

Figure 1: a- Comparison between the dynamic compressive behaviour of the US Spinel and the FR Spinel grades; b- strain-rate sensitivities of the dynamic tensile strengths of the two spinel grades.

The GEPI machine also gives advantages for characterizing the dynamic tensile behaviour of materials. Indeed, in comparison with plate impact experiments where a shock loading is applied, the use of HPP generator allows generating a ramp loading. This ramp loading allows then calculating the strain-rate at failure. Several spalling experiments were performed on each spinel grade for determining the strain-rate sensitivities. It appears that the FR Spinel grade exhibit tensile strengths considerably greater than the US Spinel grade whatever the strain-rate. On some experiments, 4 velocity measurements were performed on the rear face of the samples. The comparison between the velocity signals allowed to demonstrate that the FR spinel exhibit a probabilistic behaviour at strain-rates up to 30,000 s^{-1}. At 50,000 s^{-1}, a deterministic behaviour is observed. This probabilistic/deterministic transition of the tensile failure of ceramics was explained and discussed by Hild, Denoual Forquin and Brajer [3].

Conclusions

In this study, two transparent spinel ceramics were characterised under dynamic compressive and dynamic tensile loadings by using a high pulsed-power generator. The use of this kind of generator gives many advantages for the dynamic characterisation of materials in comparison with plate impact experiments that are commonly performed. Strong differences were observed between the two spinel grades whatever the loading.

Under dynamic compression, the FR spinel grade presents a Hugoniot Elastic Limit about two times the one of the US spinel grade. Under dynamic tension, the FR spinel grade also exhibit spall stresses more than 2 times the ones of the US spinel grade whatever the strain-rate at failure. Spalling experiments with 4 velocity measurements performed on the samples allowed to demonstrate a probabilistic behaviour of the tensile failure of the FR spinel at strain-rates up to 30,000 s^{-1}.

References
1. C. Mangeant, F. Lassalle, P. L'Eplattenier, P.L. Héreil, D. Bergues, G. Avrillaud. 2001. Syrinx project: compact pulse-current generators devoted to material study under isentropic compression loading. *PPPS-2001 Pulsed Power Plasma Science 2001* (10.1109/PPPS.2001.1002040)

2. J. Cagnoux, P. Chartagnac, P.L. Héreil, M. Perez. 1987. Lagrangian analysis. Modern tool of the dynamics of solids. *Annales de Physique* **12**, page range. (10.1051/ANPHYS:01987001205045100)

3. F. Hild, C. Denoual, P. Forquin, X. Brajet. 2003. On the probabilistic–deterministic transition involved in a fragmentation process of brittle materials. *Computers and Structures* **81**, 1241-1253. (10.1016/S0045-7949(03)00039-7)

Multiaxial rate dependent behavior of Titanium alloys

Govind Gour, Yuan Xu, Julian Reed, Nik Petrinic, Antonio Pellegrino*

Department of Engineering Science, University of Oxford, Oxfordshire, Parks Road, OX1 3PJ, United Kingdom

Keywords: High strain rate, Titanium alloys, Digital image correlation, multi-axial loading

Abstract: The determination of the mechanical response of titanium alloys to multiaxial loading is of paramount importance for aerospace manufacturing application. The present research aims to investigate the influence of combined loading (tension-torsion) on the mechanical response of Ti6Al4V alloy. A distinct specimen geometry comprising four flat dog bone ligaments circumferentially arranged around the axis of the sample is used for tension, torsion and tension-torsion combined loading conditions. The low rate experiments were performed using a Zwick-250 screw driven machine. The high strain rate experimental campaign is conducted using an in-house built novel Tension-Torsion Hopkinson bar equipped with multiple high speed cameras.

Introduction

Generally, in any fan blade off or bird strike impact event, it is very likely that material experiences a combination of the stresses. Depending on the nature of the impact, the developed stresses could be any combination of normal and shear. For instance, aircraft frame, jet engine fan containments, joint replacement systems, high pressure compressors, and certain components in the landing gear typically undergo combined loading situations on a regular basis due to the nature of the complex working conditions [1-4]. Chen et al. [5] conducted an experimental study on pure titanium under various combinations of the tension and torsion loading at low rate. The outcome focused on the microstructure and fracture morphology of the tested specimens therefore the results did not report any stress-strain curves. In another attempt, Randall and Campbell [6] applied combined tension/torsion loading on pure titanium over a limited range of moderate strain rates using a biaxial hydraulic testing machine. It is clear that understanding the influence of multiaxial loading on titanium alloys is crucial to improve the material and the design of components. So far, the dataset and knowledge on the mechanical response of titanium alloys under combined loading is very limited due difficulties in laboratory experimentation and instrumentation.

In this investigation, a novel specimen geometry featuring four flat dog-bones circumferentially arranged is selected. Each dog-bone has a gauge length of 1 mm, width of 1.5 mm and thickness of 0.75 mm. The quasi-static tension, torsional and combined experiments are conducted using a Zwick-250 screw driven universal machine, as shown in **Figure 1** (a). Four cameras (iDs UEye USB 3.0) were synchronised and placed in front of each ligament to video-record the macroscopic deformation mechanism and to capture the failure initiation on the surface of the specimens. A fine grey-scale speckle pattern was applied to the surface of the specimen to acquire full-field tensile and shear displacement by means of digital image correlation (DIC) analysis of the high-resolution video footage. The applied force and torque were recorded via the respective resistive load cells, while the history of the axial and shear strain within the gauge section of the specimen were measured from DIC using the commercial software GOM ARAMIS. **Figure 1** (b) presents the quasi-static response of a ligament type specimen under tension, torsion and tension-torsion loading conditions. The stress state under combined loading (tension-torsion) is defined by the bi-axial loading ratio β, of tangent equal to the ratio between the tensile stress σ and the shear stress τ

multiplied by √3. A wide range of bi-axial ratio enables to characterise the mechanical response of materials during tension dominated and shear dominated combined loading conditions.
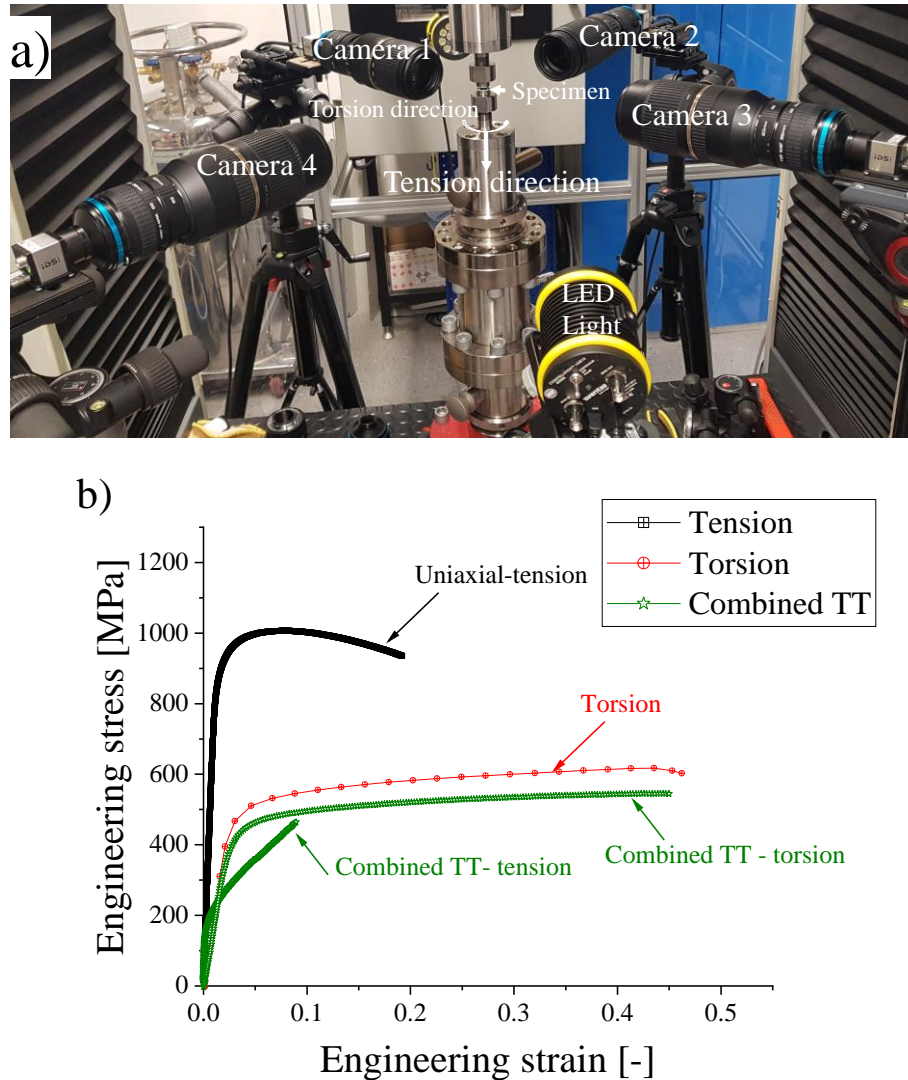

Figure 1: a) experimental setup for quasi-static testing of tension-torsion loading conditions, b) quasi-static stress-strain responses of the material subjected to uniaxial tension, torsion and combined tension-torsion loading.

High strain rate combined loading experiments were carried out using an in-house developed Tension-Torsion Split Hopkinson Bar apparatus (TTHB) [7] allowing for the direct population of the high rate failure and yield surfaces from experimental data. This, enables a better understanding of materials during deformation and failure at high strain rate and motivates the development of novel constitutive models

References

1. Boyer, R.R., *An overview on the use of titanium in the aerospace industry.* Materials Science and Engineering: A, 1996. **213**(1-2): p. 103-114.
2. Shalaby, H., et al., *Failure of titanium condenser tube.* Engineering Failure Analysis, 2011. **18**(8): p. 1990-1997.
3. Chen, Q. and G.A. Thouas, *Metallic implant biomaterials.* Materials Science and Engineering: R: Reports, 2015. **87**: p. 1-57.
4. Ma, T.-H., et al., *Comparison of multiaxial low cycle fatigue behavior of CP-Ti under strain-controlled mode at different multiaxial strain ratios.* International Journal of Fatigue, 2020. **140**: p. 105818.

5.	Chen, H., et al., *Experimental study on pure titanium subjected to different combined tension and torsion deformation processes.* Materials Science and Engineering: A, 2017. **680**: p. 278-290.
6.	Randall, M., *Dynamic properties of materials under combined stresses.* 1972, University of Oxford.
7.	Xu, Y., et al., *Experimental analysis of the multiaxial failure stress locus of commercially pure titanium at low and high rates of strain.* International Journal of Impact Engineering, 2022. **170**: p. 104341.

Analysis of damage and deformation processes in hailstones under impact loading: dynamic testing and numerical simulation

P. Forquin[a]

[a]*Univ. Grenoble Alpes, CNRS, Grenoble INP, 3SR Lab., pascal.forquin@univ-grenoble-alpes.fr*

Keywords: Hailstone, impact tests, dynamic fragmentation, confined compression, numerical simulation

Abstract: The abstract should be no more than 200 words and should not contain references or unexplained abbreviations or acronyms. Your abstract should be concise and informative and should read well as a standalone piece. The general scope of the article as well as the main results and conclusions should be summarised. Please also ensure that your abstract contains all likely search terms, to assist indexers (e.g. PubMed) which scan only the title and abstract of articles. If possible, it is beneficial to have all your keywords written into the abstract. (Time New Roman 11)

1. Introduction

Although the fall of very large hailstones remains relatively rare and difficult to predict, we know that they can reach a size of about 18 cm for a weight of 2.5 kg [1]. The speed of free fall and the kinetic energy increasing non-linearly with the size of the hailstone, such impacts can generate not only devastation on crops but can also induce severe damage on vehicles and on residential structures (roofs, openings windows, etc.). The risk of impact against aircraft (airplanes, helicopters, space launchers) which concerns impacts from smaller hailstones at a higher speed may also constitutes a major issue. Better knowledge of the mechanical forces generated by the impact of hailstones and the associated risks is of major importance in many areas (meteorologists, rescuers, insurers, contractors, industrialists, farmers, political decision-makers, etc.).

However, the dynamic forces generated by such impacts remain difficult to establish based on analytical of numerical calculations. Indeed, the growth of a hailstone is the result of an agglomeration of water droplets around a solid core transported at high altitude under the effect of the strong convective winds within cumuliform clouds before falling to the ground. It results in highly heterogeneous microstructure, generally in the form of multi-layers (onion-like structure) [2], that is characterized by high variability (each hailstone is unique and unlike any other). Since these microstructures are very difficult to reproduce artificially, the question arises of the representativeness of the samples tested in the laboratory and the relevance of using the mechanical parameters obtained experimentally to model the behaviour of real hailstones under impact loading.
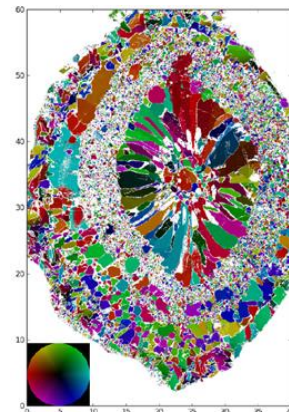

Figure 1: Microstructure of a real hailstone observed by automatic ice texture analyzer (AITA) [2].

*Author for correspondence (pascal.forquin@univ-grenoble-alpes.fr).
†Address: 3SR Lab., 1270 rue de la piscine, 38400 Saint-Martin d'Hères

2. Implemented approach

Faced with these obstacles, a strategy was implemented by the 3SR and IGE laboratories based on the development of model microstructures to study and better understand the influence of the microstructure of water-ice on its mechanical behaviour under static, dynamic and impact loading. In the framework of D. Georges' PhD thesis [3] a protocol was set for the fabrication of two microstructures with low and high porosity. These microstructures were subjected to dynamic tensile loading by the spalling method [4] and the dynamic response was compared to the prediction provided by the DFH (Denoual-Forquin-Hild) analytical model in which the fragmentation process is described [5].

In the present work, these low porosity and high porosity microstructures were first subjected to dynamic confined loading through SHPB (Split-Hopkinson Pressure Bar) quasi-oedometric compression dynamic tests. These new experimental data provided an identification of the mechanical behaviour under high confining pressure and strain-rate. Next, the same microstructures were subjected to impact loading. To do so, 40 mm diameter spheres were projected against the end of an instrumented Hopkinson bar. The dynamic loading was deduced from the strain gauges taped to the Hopkinson bar. In addition a high speed camera (Phantom V2012) was used to visualize the damage process induced in each sphere in the few microseconds following the impact (Fig. 2). Finally, the impact behaviour of each microstructure was numerically simulated with the Abaqus-explicit finite-element code taking into account the constitutive laws identified through spalling tests and dynamic quasi-oedometric compression tests. The experimental and numerical results provide a new insight of damage and deformation processes involved in hailstones under impact loading.
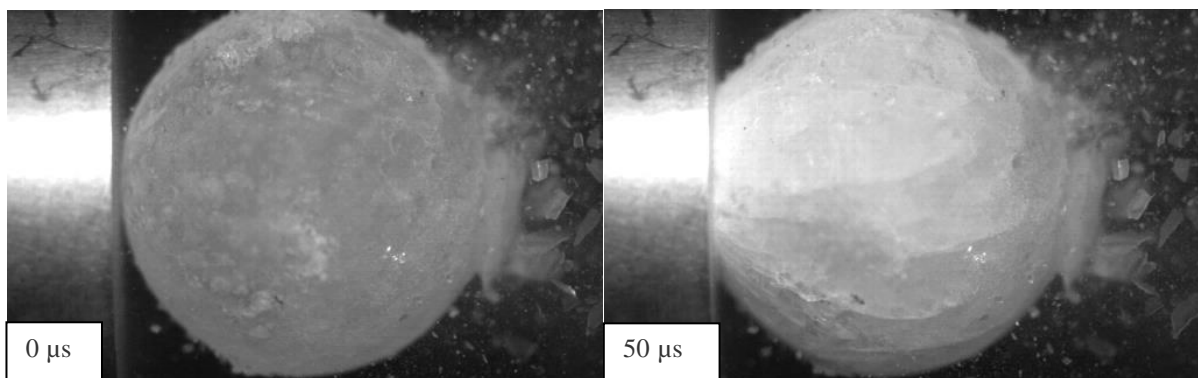

Figure 2: Ice sphere impact test (3SR Lab). Visualization of the fragmentation process with high-speed imaging.

References:

1. CA Knight, NC Knight. 2005. Very large hailstones from Aurora, Nebraska. *Bulletin of the American Meteorological Society* **86**(12), 1773–1781. DOI: 10.1175/BAMS-86-12-1773.

2. M. Montagnat, M. Bourcier, A. Philip, P. Bons, C. Bauer, P. Deconinck, P. Hereil. 2020. Characterization of the texture of large hailstones. hal-02942822.

3. D. Georges. 2020. Etude expérimentale et modélisation de la réponse mécanique de la glace polycristalline sous chargement de traction dynamique : Influence de la porosité. PhD thesis, Univ. Grenoble Alpes,.

4. D. Georges, D. Saletti, P. Forquin, M. Montagnat, P. Forquin, P. Hagenmuller. 2021. Influence of Porosity on Ice Dynamic Tensile Behavior as Assessed by Spalling Tests, *J. Dyn. Behavior Mat.*, DOI: 10.1007/s40870-021-00300-z.

5. P. Forquin, M. Blasone, D. Georges, M. Dargaud. 2021. Continuous and discrete methods based on X-ray computed-tomography to model the fragmentation process in brittle solids over a wide range of strain-rates-application to three brittle materials, *J. Mech. Physics Solids*, **152**, 104412, DOI: 10.1016/j.jmps.2021.104412

On the Mechanical Properties of Tungsten Heavy Alloys used in Kinetic Energy Impactors

Christian C. Roth[a] , Teresa Fras[a,b] and Dirk Mohr[a]*

[a]*Department of Mechanical and Process Engineering, Swiss Federal Institute of Technology (ETH), Zurich, Switzerland*
[b]*French-German Research Institute of Saint-Louis (ISL), 68301 Saint-Louis, France*

Keywords: Tungsten heavy alloy, plasticity, fracture, strain rate

Abstract: With their superior material properties at high strain rates and temperatures, tungsten alloys are widely used in tool making, machining as well as ballistic applications. In the latter, kinetic energy penetrators made from tungsten heavy alloy (WHA), so called long rods, travel at speeds >1km/s. Here, we study the material response of WHA bars with a diameter of 5mm and a length of 80mm at strain rates ranging from 0.001/s to more than 10000/s. Uniaxial compression experiments are carried out on a universal testing machine and a Split-Hopkinson Pressure bar (SHPB) at low (0.001/s), intermediate (1/s) and high (1000/s) strain rates. Taylor impact experiments performed on a single stage gas gun are used to assess the material response at very high strain rates (>>1000/s). Digital image correlation is performed on pictures obtained from optical (high speed) photography, while high speed infrared imaging is used to measure the temperature rise due to plastic work at intermediate strain rates of 1/s. Sub-sized tensile specimens extracted from the tungsten bars are tested on a novel micro-tensile testing system. The effect of the stress state on the plastic and fracture behavior is investigated with six different geometries, comprising shear (SH), central hole (CH) and notched tension with two different cut-out radii (NT6, NT20). To assess any any strength differential effect or anisotropy, uniaxial tensile (UT) experiments are performed along and transverse to the cylinder axis. Based on the experimental results, a constitutive modeling framework is developed and calibrated for Finite Element simulations. It comprises a yield surface accounting for the strength differential effect in conjunction with a strain rate and temperature dependent hardening law. To represent the strain hardening, a mixed Swift-Voce law is used. A stress state and strain rate dependent fracture initiation model is calibrated based on the results of the hybrid-numerical experimental analysis.

*Author for correspondence (dmohr@ethz.ch).
†Present address: Department of Mechanical and Process Engineering
Swiss Federal Institute of Technology (ETH), Technoparkstrasse 1,
8005 Zurich, Switzerland

RATE-DEPENDENT STRESS-STRAIN RESPONSE OF POLYPROPYLENE: ROBOT-ASSISTED TESTING AND NEURAL NETWORK MODELING

Benoit Jordan[1] and Dirk Mohr[1]*

[1]*Department of Mechanical and Process Engineering, Swiss Federal Institute of Technology (ETH), Zurich, Switzerland*

Keywords: Automated testing; neural network hardening model; polypropylene; rate-dependent

Abstract: - The temperature and strain rate dependent tensile response of polypropylene is described using a neural-network based hardening model. A hybrid modeling approach is taken by combining mechanism-based and data-based modeling. The "big data" required for machine learning is generated using a custom-made robot-assisted testing system. The core of this talk presents the findings reported in [1].
Large deformation experiments are performed on flat tensile specimens with a shallow notch covering temperatures ranging from 20 to 80°C, and strain rates ranging from 10-3 to 10-1/s. Without making any a priori assumptions on the specific mathematical form, the function relating the stress to the viscous strain, the viscous strain rate and temperature is identified using machine learning. In particular, a back propagation algorithm is employed to identify a suitable neural network function based on the results from more than 40 experiments. The neural network model is employed in series with a temperature-dependent spring to describe the stress-strain response of polypropylene. The resulting constitutive equations are solved numerically to demonstrate that the identified model is capable to predict the experimentally-observed stress-strain response for strains of up to 0.6.

References:

1. B. Jordan, M. B. Gorji, D. Mohr. 2020. Neural network model describing the temperature- and rate-dependent stress-strain response of polypropylene. International Journal of Plasticity. 135. (https://doi.org/10.1016/j.ijplas.2020.102811)

*Author for correspondence: Dirk Mohr (dmohr@ethz.ch).
†Present address: *Department of Mechanical and Process Engineering, Swiss Federal Institute of Technology (ETH), Zurich, Switzerland*

NEURAL NETWORK MODEL DESCRIBING THE RESPONSE OF TUBULAR STRUCTURES SUBJECT TO IMPACT LOADING

Emmanouil Sakaridis and Dirk Mohr*

**Department of Mechanical and Process Engineering,
Swiss Federal Institute of Technology (ETH), Zurich, Switzerland**

*Corresponding author. E-mail address: dmohr@ethz.ch

ABSTRACT- This presentation discusses the machine-learning based prediction of the force-displacement response of structures subject to impact loading and follows the developments reported in [1]. To enable the use of machine learning, an extensive dataset of force-time curves is generated, using detailed finite element models of box structures of different geometries that are impacted at different velocities. A neural network model is designed to predict the force as a function of the geometry, impact velocity and time. The hyper-parameters of the fully-connected network are determined first and the performance of the resulting tuned model is evaluated on a separate test set. The evaluation reveals a non-random error distribution which can be correlated with the physical properties of the structural collapse. A comparison of the surrogate model errors with deviations resulting from geometric imperfections indicate that the proposed machine learning based approach is capable of predicting the crushing response with a level of accuracy comparable to the errors that would be caused by a minor change in geometric imperfection.

[1] Emmanouil Sakaridis, Nikolaos Karathanasopoulos, Dirk Mohr, Machine-learning based prediction of crash response of tubular structures, International Journal of Impact Engineering (2022), https://doi.org/10.1016/j.ijimpeng.2022.104240.

Dynamic indentation response of Lithium-ion batteries: Experiments and Modeling

Thomas Tancogne-Dejean[1,†], Vincent Grolleau[1,2], and Dirk Mohr[1]*

[1]Department of Mechanical and Process Engineering,
Swiss Federal Institute of Technology (ETH), Zurich, Switzerland
[2]Univ. Bretagne Sud, IRDL, UMR CNRS 6027, F-56100 Lorient, France

Abstract: Lithium-ion cells can undergo thermal runaway when subjected to large deformation loading leading to fire and the release of toxic fumes. This poses a strong safety concern for electric vehicles from e-bikes and e-scooters to electric cars during crash. The crashworthiness of electric vehicles therefore relies on the accurate understanding and modeling of the large deformation response of lithium-ion cells over a large range of strain rates and loading conditions. In the present study, an extensive experimental campaign is performed on several lithium-ion cell types (pouch and prismatic) subjected to out-of-plane indentation. Speeds ranging from a few millimeters per minute are obtained on universal testing machines, while Split Hopkinson Pressure Bars and catapult are used for loading up to ten meters per second. The experiments reveal a large strain rate sensitivity, with the displacement at the onset of short circuit strongly decreasing with increasing speed. Furthermore, a non-monotonic relationship for the maximum force is observed. Overall, the energy absorbed by lithium-ion cells decreases from low to high strain rates. Based on the experimental observations, a phenomenological strain-rate dependent hardening response is proposed. Together with a Deshpande-Fleck yield locus, the calibrated model is able to accurately reproduce the experimental data and is further validated.

* *Corresponding author. E-mail address:* *dmohr@ethz.ch.*
Present address: Department of Mechanical and Process Engineering, Swiss Federal Institute of Technology (ETH), Zurich, Switzerland

Neural Network Based Temperature And Strain Rate Dependent Plasticity And Fracture Modelling

Xueyang Li*, Christian C. Roth and Dirk Mohr

Swiss Federal Institute of Technology (ETH), Zurich, Switzerland

Keywords: Dynamic Testing, Rate- and Temperature Dependency, Machine Learning, Ductile Fracture

Abstract: The accurate description of the strain rate and temperature dependent response of metals is a perpetual quest in crash-worthiness and forming applications. In the present study, more than 120 fracture experiments are performed to better understand the combined effects of stress state, strain rate and temperature on the onset of ductile fracture for an Aluminum Alloy AA7075-T6. The experimental campaign covers strain rates ranging from 0.001/s to 1000/s, and temperatures ranging from 20°C to 360°C. A YLD2000-3D yield surface combined with a neural network based hardening law is chosen to accurately describe the large deformation plasticity response of the material. The constitutive model is implemented in a user material subroutine for FE simulation. To enhance the numerical stability in the return-mapping algorithm, a counterexample regularization technique is employed to guarantee a positive strain rate sensitivity. Subsequently, loading paths to fracture are extracted, which feature evolving stress triaxiality, Lode angle parameter, strain rate and temperature histories. As a main contribution, a neural network parameterized Hosford-Coulomb fracture model is proposed and trained using the actual loading path histories. The accuracy of the proposed fracture model is validated against the experimental onset of fracture, obtaining a mean absolute error of 0.08 on the terminal damage.

*Author for correspondence (lixue@ethz.ch).
†Present address: Technoparkstrasse 1, 8005 Zürich, Switzerland

Static and dynamic in-plane torsion testing of sheet metal

Xavier Colon[a,b], Vincent Grolleau[a,b]*, Bertrand Galpin[b,c], Christian C. Roth[a] and Dirk Mohr[a]

a) Department of Mechanical and Process Engineering, Swiss Federal Institute of Technology (ETH), Zurich, Switzerland
b) IRDL,Univ. Bretagne Sud, CNRS UMR 6027, F-56100 Lorient, France
c) Ecoles Saint-Cyr Coetquidan, CREC, F-56380 Guer, France

Keywords: torsion, finite strain, simple shear, strain hardening, strain rate

Abstract: Knowledge of the evolution of a material's yield surface and its anisotropic plastic flow from experiments is critical when choosing a constitutive model.

Recently, an enhanced in-plane torsion experiment was developed that allows the observation of the entire gage section of a grooved disc-shaped (sheet) specimen with a single optical camera for digital image correlation measurements.

Here, an extension of this setup is proposed to perform torsion experiments at high strain rates. The specimens are clamped on their outer circumference, while the inner circumference is loaded by a Hopkinson torsion bar, using a specially designed short-time release brake. To ensure strain localization away from the clamped boundaries, a local thickness reduction in the form of a circular groove is machined. Experiments at low (0.001/s), intermediate (1/s) and high strain rates (>100/s) are performed on a wide range of engineering materials, from low strength aluminum alloys to ultra-high strength steels. The material's hardening response is obtained up to an order of magnitude larger than in uniaxial tensile tests. In addition, the evolution of the anisotropy is assessed experimentally and numerical simulations are performed to obtain more information about the materials' strain rate and temperature dependent behavior under proportional shear loading.

*Author for correspondence (vgrolleau@ethz.ch).
Present address: Department of Mechanical and Process Engineering, Swiss Federal Institute of Technology (ETH), Technoparkstrasse 1, 8005 Zurich, Switzerland

SHPB experiments on plate-lattice materials made through selective laser melting: experiments & analysis

Paul P. Meyer[1], Thomas Tancogne-Dejean[1], Xueyang Li[1], Christian C. Roth[1] and Dirk Mohr[1]*

[1]Department of Mechanical and Process Engineering, Swiss Federal Institute of Technology (ETH), Zurich, Switzerland

Keywords: plate-lattice, high strain rate, hopkinson bar system

Abstract: This presentation discusses the rate-dependent response of additively-manufactured architected materials while following the results reported in [1]. Plate-lattice structures of cubic symmetry are fabricated from stainless steel 316L through selective laser melting. To characterize their potentially rate-dependent mechanical response, compression experiments are performed on a universal testing machine and a custom-made direct impact Hopkinson bar system. The latter achieves strain rates of about 500/s with sufficiently long loading pulses. Tensile specimens are also manufactured to determine the stress-strain response of the cell wall material for strain rates ranging from 10-3 to 103/s. The results show that plate-lattices of about 20% relative density crush progressively when subject to large strain compression. Their specific energy absorption increases significantly when increasing the applied strain rate from 0.001 to 500/s. This observation is explained by the strain rate sensitivity of the base material. Good quantitative and qualitative agreement between the experiments and the simulations is observed when using a detailed finite element model of the plate structures in conjunction with a modified Johnson-Cook model of the cell material. The comparison of the simulation results for plate- and truss-lattices of the equal-density reveal a 45% increase in specific energy absorption.

References:

1. Tancogne-Dejean, T., Li, X., Diamantopoulou, M. et al. 2019. High Strain Rate Response of Additively-Manufactured Plate-Lattices: Experiments and Modeling. J. Dynamic Behavior Mater. **5**, 361–375. (https://doi.org/10.1007/s40870-019-00219-6)

*Corresponding author. E-mail address: dmohr@ethz.ch

Micro-tensile experiments of metals covering a wide range of stress-states

Thomas Beerli, Christian C. Roth, Vincent Grolleau and Dirk Mohr*

Department of Mechanical and Process Engineering, ETH Zurich, Tannenstrasse 3, 8092, Zurich, Switzerland

Keywords: Micro testing, Ductile fracture, Intermediate strain-rate, Tensile testing

Abstract: A novel micro-testing system is presented which is used to test sub-sized tensile specimens extracted from a wide range of engineering materials, ranging from aluminium extrusion to ultra-high strength steels. Overall, three specimen families with gauge section width's ranging from $0.5mm – 2mm$ are developed. Each of the families consists of five different geometries comprising shear (SH), central hole (CH) and notched tension with two different cut-out radii (NT6, NT20), which are used to investigate the effect of the stress state on the plastic and fracture response. A confocal optical measurement system is used in conjunction with a high precision stage to accurately measure the specimen dimensions prior testing. A microscopic lens with a 5MP optical camera to captures images for Digital Image Correlation. The applicability of the methodology is validated against standardized specimen geometries. Examples in the characterization of otherwise inaccessible engineering materials and structures as well as the calibration of constitutive and fracture models are shown. The static testing system can characterize viscoplastic effects at strain rates ranging from 10-4 to 1/s. To attain higher strain rates, an extension of the proposed methodology to high strain testing with miniature Hopkinson bars is also presented.

*Author for correspondence (**dmohr@ethz.ch**).

Composite materials and multi-material assemblies under dynamic stresses at high strain rates

Pr. Michel ARRIGONI

ENSTA-Bretagne, IRDL, 2 rue François Verny, 29806 Brest Cedex 09, ORCID 0000-0002-7237-3303

Keywords: high strain rate, shock wave, numerical modelling, impact, laser, velocimetry, multi-materials

Abstract (Time New Roman 11, bolt): The requirements for the service life of some high value-added structures in the aeronautics or aerospace fields, as well as for defence applications, are becoming higher and higher. The expected mechanical performances are increased to resist to severe shocks and impacts for lower and lower expected structural weigh. This antagonism gives birth to the paradigm of physical protection by advanced materials. Among these materials, composite materials remain a preferred choice but cannot be sufficient on their own in some situations involving extreme loads such as detonation waves or shock waves resulting from ballistic impacts as shown in fig 1 or hypervelocity fragments. In these cases, the dynamic behaviour must be revisited to consider the supersonicity related to shock waves propagating in the target material. This presentation aims at presenting experimental methods allowing the establishment of numerical models dedicated to this kind of events. These models are used in predictive tools of numerical modelling in order to limit the number of experiments, generally dangerous, expensive and where some key parameters cannot be easily tuned. The numerical tool also allows optimization steps. A few examples taken from the research work carried out at the Dupuy de Lôme Research Institute illustrate the modelling approach. These examples highlight the progress of the experimental and numerical methods used to study the mechanical effects of impacts and explosions.
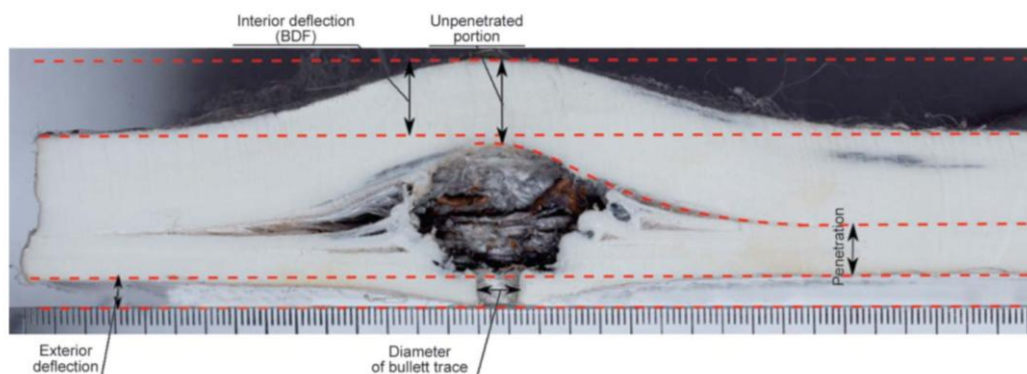
Figure 1 : Impact of a 7.62 x 39 FMJ bullet stopped in a 22 mm thick composite plate.

Author Index